UK FLUIDS 2025 LIVERPOOL

UK Fluids Conference 2025

University of Liverpool

2nd – 4th September 2025

Book of Abstracts

TOC

Table of Contents

PLEN: Plenary talks

PLEN/001: The Collaborative Computational Project for Wave Structure Interaction

Professor Deborah Greaves, School of Engineering, Computing and Mathematics, Plymouth University

Abstract: The UK is a world leader in offshore renewable energy and has committed to delivering 60 GW of offshore wind by 2030 as part of its Net Zero and energy security strategies. Achieving these ambitions requires a step change in our ability to model and predict wave–structure interaction (WSI) processes that govern the performance, safety, and sustainability of floating offshore wind turbines, coastal defences, and maritime infrastructure. Professor Deborah Greaves will outline the key areas of research in the Collaborative Computational Project for Wave Structure Interaction, together with access routes to National HPC resource on ARCHER2 through the HEC-WSI.

PLEN/002: Complex Droplet Dynamics on Nature-Inspired Liquid Repellent Surfaces

Professor Halim Kusumaatmaja, Institute for Multiscale Thermofluids, School of Engineering, University of Edinburgh, Edinburgh EH9 3FD, U.K.

Abstract: Wetting of surfaces by liquids is commonly observed in everyday life and is of paramount importance for many natural and engineering processes. In many cases, it is beneficial to design surfaces that repel liquids: these surfaces can suppress icing and surface fouling, they reduce drag and friction, and contaminants can be removed easily. Interestingly, nature provides several conceptually distinct inspirations to design liquid repellent surfaces. Many natural surfaces such as lotus leaves and duck feathers are rough. The roughness amplifies the surface hydrophobicity leading to superhydrophobic properties with very large contact angles. In contrast, on pitcher plants, a layer of liquid imbibes the surface corrugations, providing a smooth liquid surface that substantially reduces friction. In this talk, I will discuss recent works by my group and our collaborators to understand complex droplet dynamics on structured, nature-inspired liquid repellent surfaces. In particular, I will focus on three phenomena. First, I will elucidate salient mechanisms of how particles can be captured and removed by liquid droplets, which is key for designing self-cleaning surfaces. Second, I will discuss how droplet dynamics are important for suppressing icing on superhydrophobic surfaces. Third, I will explain distinctive features of droplet dynamics on uniform and patterned lubricant infused surfaces, such as lubricant cloaking and the formation of wetting ridge, and how they give rise to new wetting states, contact line pinning mechanisms, and friction scaling laws.

PLEN/003: What's New in the Flow of Polymer Solutions?

Professor Rich Kerswell, DAMTP, University of Cambridge

Abstract: The addition of a small amount of long-chain polymers to a Newtonian solvent such as water gives rise to a whole host of interesting phenomena due to the introduction of elasticity into the flow. I will briefly review these before focussing in on so-called 'elastic turbulence' which can exist in the absence of inertia (i.e. at vanishing Reynolds number) and 'elasto-inertial turbulence' which seems to need both inertia and elasticity but only 2 dimensions to exist. I will discuss recent progress made in trying to understand how these complex states come about as well as some new insight into the standard theoretical model - called the FENE-P model - for such dilute polymer flows.

PLEN/004: Current and Future Challenges for complex weapons: An Aerodynamics Perspective

Dr. Steve Lawson, Head of Aerodynamics UK, MBDA

Abstract: Complex weapons present distinctive challenges with respect to aerodynamic design, characterisation and modelling of performance. The talk will firstly provide an introduction to the range of Aerodynamic flows and current challenges that exist within our current programmes. Next, examples of collaboration are presented, including those with Academia. Finally, perspectives on future challenges for aerodynamics in the defence industry are presented and discussed.

PLEN/005: Nanoscale dynamics of thin liquid films – the UKFN Thesis Prize Award lecture

Dr. Muhammad Rizwanur Rahman, Department of Mechanical Engineering, Imperial College London, UK (now: Mechanical Engineering, Ahsanullah University of Science and Technology, Dhaka)

Abstract: Thin liquid films play pivotal roles in various natural phenomena and engineering processes. Yet, our understanding is limited by the scarcity of atomic insights. This work investigates the nanoscopic details of thin films, their rupture, and the transport of surfactants along the film surfaces. At this scale, experimental investigations are prohibitive; and conventional theoretical approaches are inadequate due to their reductive approximations.

This work employs molecular dynamics simulations which enables the examination at the most fundamental scale. The processes by which film breakup occurs are found to share similar molecular origin. Present study on the growth of rupture sites identified the limitations of continuum scale theories in explaining retraction rates for thinner films, and corrections are proposed that rectify the discrepancies. Notably, a spatio-temporal memory of rupture is identified, highlighting the concept of deterministic outcomes emerging from stochastic processes.

For the stability and rupture of these films, the transport of surfactant molecules and their subsequent distribution play crucial roles. The mechanism of such transport along the deforming surfaces of the films is investigated. This process is influenced not only by the boundary conditions, but also by the chemical nature, the molecular architecture, and solubility of the surfactant molecules. To capture this inherently molecular nature of the transport process, we include the molecular details into the existing continuum model. This establishes that the transport equation preserves substantial accuracy in capturing the underlying physics.

By uniquely confirming the applicability of the transport equation for a molecularly thin film, this study elucidates the long-debated relationship between the continuum and the nanoscale. Together, the findings from this study represent an important step in bridging the physics of fluids across scales.

PLEN/006: Active Matter meets Biophysics (and Rheology) - the Tom Duke prize lecture awarded by the Biological Physics Group UK

Professor Julia Yeomans (Department of Physics, Oxford University)

Abstract: Life defies equilibrium. Key examples are molecular motors that harness chemical energy to drive intracellular transport. Cells self-organise molecular components into intricate structures that enable them to grow, reproduce, and move. At a larger scale, collections of cells follow coordinated pathways of division, differentiation and reorganisation as a single cell develops into a mature organism. The rheology of cell collectives is complex with deformability playing a key role.

Active systems, driven by energy input at the level of individual particles, also exist out of thermodynamic equilibrium. Dense active matter shows distinctive collective behaviour: active turbulence, motile topological defects and co-ordinated flows, reminiscent of the rotation of cell clusters or the swirling patterns of a starling murmuration.

In this talk, I will discuss how the physics of active matter is offering fresh perspectives on mechanobiology and developmental biology: from expanding bacterial colonies and the rheology of active cell monolayers to chick morphogenesis.

ADV: Advanced techniques including AI, machine learning and data-driven approaches

ADV/001: FluidGPT-1: a proof-of-concept model for attention-based flow pattern generation in CFD. Presentation and future perspectives

[1*]Dapelo, Davide; [1]Bridgeman, John

[1]Department of Civil and Environmental Engineering, School of Engineering, University of Liverpool. *Presenting Author

The integration of artificial intelligence in computational fluid dynamics (CFD) remains limited, as traditional methods often fail to capture critical flow parameters like viscosity, Reynolds number, or Smagorinsky constant whenever not explicitly passed to the model. The proof-of-concept model FluidGPT-1 addresses this through architecture based on autoregressive Transformers (like in ChatGPT), merged with U-Nets (like in computer vision), in order to predict time-dependent fluid flow patterns. Unlike U-Net-only models, which rely solely on the immediate previous timestep, FluidGPT-1 harnesses transformers' attention mechanisms to capture long-term dependencies, indirectly accounting for essential but missing parameters. The model is trained on 4,081 short synthetic 2D fluid flow simulations generated with the OpenLB Lattice-Boltzmann library, employing random domain geometries, inlet/outlet configurations, and laminar flow conditions. Numerical experiments show that FluidGPT-1 generalizes effectively and accurately predicts future flow patterns without direct parameter inputs. This transformer-based approach reduces computational complexity by eliminating the need for explicit parameter encoding while retaining accuracy across diverse CFD configurations. Future perspectives are presented.

ADV/002: Improving turbulence control through explainable deep learning

[1*]Beneitez, Miguel; [2]Cremades, Andres; [3]Guastoni, Luca ; [2]Vinuesa, Ricardo

[1]Department of Mechanical and Aerospace Engineering, The University of Manchester, Manchester, M13 9PT, UK
miguel.beneitez@manchester.ac.uk.

[2]FLOW, Engineering Mechanics, KTH Royal Institute of Technology, Stockholm, SE-100 44, Sweden.

[3]School of Computation, Information and Technology, Technical University Munich, 85748 Garching, Munich, Germany.

*Presenting Author

Flow control is paramount in many industrial applications, e.g. to reduce the overall fuel consumption in airplanes or to enhance mixing in chemical reactors. Recently, it has been shown that control strategies discovered through deep reinforcement learning (DRL) can outperform traditional control techniques for turbulent flows. These control strategies typically have goals such as drag reduction but lack physical insights of the coherent structures underpinning turbulent flows.

In this talk, we integrate explainable deep learning (XDL) to objectively identify the coherent structures containing the most informative regions in the flow, with a DRL model trained to reduce them. We consider a minimal open channel of size [Lx, Ly, Lz] = [2.67, 1, 0.8] with $Re_\tau = 180$ to train a DRL model by sensing the flow field (u, v) on a plane y+ = 15. The learned control policies are evaluated in a large channel of size [Lx, Ly, Lz] = [2π, 1, π]. The XDL-based DRL discovers novel control strategies that outperform traditional methods (opposition control and classically identified coherent structures) in terms of drag reduction, as shown in Fig. 1 (left). This demonstrates that combining DRL with XDL can produce causal control strategies that precisely target the most influential features of turbulence by directly addressing the core mechanisms sustaining turbulence.

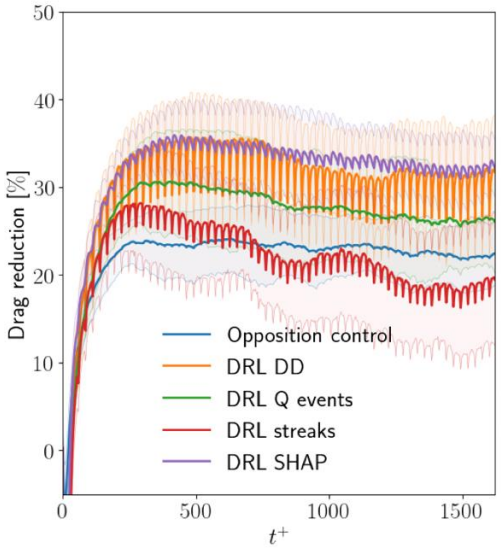

Figure 1. Reduction of the quantities of interest with respect to the uncontrolled case. Results are averaged over the 50 initial conditions used for policy evaluation. Solid lines denote mean values and shaded regions indicate one standard deviation. Colors indicate different control strategies: opposition control (blue), DRL for direct drag reduction (orange), DRL for Q- event reduction (green), DRL for streak reduction (red), and DRL for SHAP reduction (purple)

ADV/003: A Design Optimisation Framework for Laval Nozzles in Uniform Supersonic Chemical Reactors

Author: Luke Driver
Supervisors: Gregory de Boer, Nik Kapur, Dwayne Heard, Julia Lehman
Email: scldr@leeds.ac.uk

Abstract: The Interstellar media is a low temperature, low density (<100K) vacuum, comprised of gas and dust. The ISM contains upwards of 450 species which are involved in roughly 6200 gas phase reactions. Some reactions have been suggested to be pathways to complex organic molecules (COM's), potential precursors to life. Finding the reaction rate of these reactions is the key to understanding the chemical evolution of the universe. Experimentally, low temperatures are obtained by expanding an inert bath gas (Nitrogen, Argon, Helium) through a Laval nozzle, generating a supersonic, low-temperature jet where reactions are performed. Nozzles are designed using the method of characteristics (MOC), which is a way of generating a conventional nozzle geometry for a set of design conditions that produces a shock free exit flow. This assumes irrotational, inviscid flow, and hence the solution produced by this method is not accurate and provides no insight into the length of the jet or if a better nozzle geometry exists for a particular flow condition. The length of the jet and shock magnitude are critical as they determine the kinetic measurement error and what reactions can be performed; hence, chemists would like to design based on these variables. There currently exists no CFD or design framework for the CRESU method, and this project aims to develop a fully automated (black box) framework that allows chemists to perform CFD on existing nozzles to obtain high fidelity data to improve current experimental techniques, and to enhance these designs through shape optimisation which uses kriging and neural network surrogates.

ADV/004: Advanced Particle Size Characterisation in Liquid-Solid Mixtures Using Ultrasound and Physics-Guided Machine Learning

Hossein, Fria and Angeli, Panagiota

Department of Chemical Engineering, University College London, London, WC1E 7JE, United Kingdom :Contact E-mail : *f.hossein@ucl.ac.uk

This study introduces an innovative approach that combines ultrasonic spectroscopy with physics-informed machine learning (ML) for particle size distribution (PSD) analysis in solid-liquid mixing. Ultrasonic attenuation coefficient spectroscopy, coupled with inversion algorithms, was employed to characterize PSD during the dispersion of ballotini glass beads (density 2500 kg/m^3; size range from 300 to 1000 μm) suspended in a stirred vessel. The experimental setup involved a Pyrex glass cylindrical vessel with 80 mm height, 66 mm inner diameter and 2 mm wall thickness. The vessel was equipped with an impeller rotating at 571 rpm to ensure uniform mixing. Ultrasound signals spanning frequencies from 500 to 9500 kHz were transmitted through the vessel, and the attenuation of these signals was measured to obtain attenuation spectra affected by particle size and concentration. The experiments were conducted under room temperature with particles dispersed in tap water at a volume fraction of 2.15%. To enhance the accuracy of the PSD estimation, a regularized inversion approach based on physical principles was established to ensure stable solutions. Furthermore, a Random Forest machine learning model, integrated with the physical scattering equations, was trained on experimental data including ultrasound attenuation spectra alongside microscopy measurements for labeling. This physics-informed ML approach (Fig.1 left) showed remarkable accuracy, predicting PSD with errors below 1% (Fig.1 right), superior to ultrasound inversion algorithms[1] and closely matching the results from microscope imaging.

The developed method offers a cost-effective, real-time, non-intrusive solution for industrial particle size analysis and has the potential to be extended to other multiphase systems including liquid-liquid and gas-liquid ones. Overall, combining ultrasonic spectroscopy with advanced ML techniques provides a robust tool for rapid, accurate, and physically consistent particle characterization, supporting process optimization and quality control across applications in process engineering and pharmaceuticals.

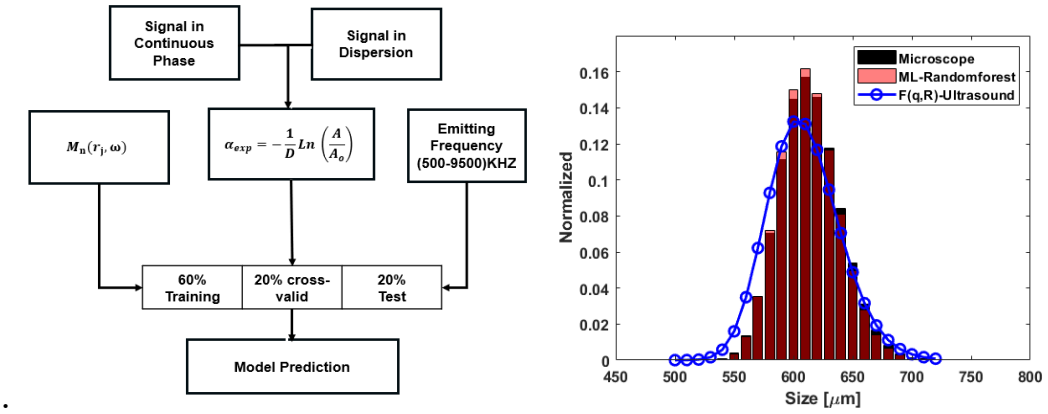

Figure 1. ***Left,*** *Schematic diagram of physics informed ML for PSD prediction.,* ***Right,*** *Particle Size Distribution (PSD): The blue line represents the inverted particle size distribution derived from ultrasound attenuation coefficients. The black bars illustrate the particle size distribution measured through microscope imaging, while the pink bars denote the predictions generated by the physics informed ML.*

We would like to acknowledge the support from the UKRI PREMIERE Programme Grant (EP/T000414/1).

[1]Hossein, F. Duan, C. Angeli, P., 2024, Advanced ultrasound techniques for studying liquid–liquid dispersions in confined impinging jets. *POF*, 36, 082011.

ADV/005: SCHEDULED TEMPORAL LOSS WEIGHTING: A STABLE STRATEGY FOR TRAINING NEURAL PDE SOLVERS

[1*]Coker, Oluwaseun; [2]Khan, Amirul; [3]Wang, He; [4]Jimack, Peter

[1] School of Computer Science, University of Leeds, Leeds, UK, LS2 9JT; scoc@leeds.ac.uk .

[2] School of Civil Engineering, University of Leeds, Leeds, UK, LS2 9JT; A.Khan@leeds.ac.uk .

[3] AI Centre, Department of Computer Science, University College London, London, UK, WC1E 6BT; he_wang@ucl.ac.uk .

[4] School of Computer Science, University of Leeds, Leeds, UK, LS2 9JT; P.K.Jimack@leeds.ac.uk .

The dynamics of fluids, as seen in weather prediction, and aerodynamic design, are typically modeled using time-dependent partial differential equations (PDEs). Accurate solutions to these PDEs are essential for optimization and control. While classical numerical methods provide reliable results, they can be computationally expensive. Machine learning offers a promising approach to alleviate this computational burden.

Neural network based PDE solvers (Neural PDE solvers) provide a robust framework for solving PDEs by directly learning solutions from data, offering a computationally efficient approach. However, training these solvers for a long-time horizon, can be difficult and costly. This challenge arises from gradient instabilities due to the accumulation of errors in autoregressive training, where predictions are fed back into the model for next predictions. While various training techniques have been proposed to enhance training stability, the optimal strategy for achieving stable and accurate long-term predictions remains an open question.

Curriculum learning, a technique that prioritizes the training of easier tasks before progressing to more complex ones, can enhance training stability for transient PDEs. Existing discrete curriculum learning strategies control the training horizon by gradually increasing the number of predicted time steps. However, this approach can lead to overfitting to early dynamics, hindering the optimization of later dynamics. To mitigate this issue, we propose a continuous curriculum learning approach, scheduled temporal loss weighting, which enables more stable and efficient training. By dynamically adjusting the weights assigned to the loss at each predicted time step during training, we can consider the entire dynamic range from the outset, while maintaining gradient stability. We validate our method on various nonlinear PDEs in fluid dynamics, demonstrating superior performance compared to discrete curriculum strategies and state-of-the-art models.

ADV/006: Machine learning based intelligent CFD surrogates for interactive design exploration of built environments)

[1*]Adia, Usamah; [2]Khan, Amirul; [3]Sleigh, Andrew; [4]Wang, He

[1]University of Leeds, Leeds, United Kingdom, scuaa@leeds.ac.uk [2]University of Leeds, Leeds, United Kingdom, A.Khan@leeds.ac.uk [3]University of Leeds, Leeds, United Kingdom, p.a.sleigh@leeds.ac.uk [4]UCL Centre of Artificial Intelligence, Department of Computer Science, University College London, London, United Kingdom he_wang@ucl.ac.uk .

Civil engineers must consider numerous factors when designing the built environment. Understanding the impact of airflow links to design properties such as thermal comfort/energy efficiency (Chow 2022). It is not feasible to use traditional CFD methods due to the high computational/time cost. Creating a machine learning (ML)-based surrogate model offers a potential solution. This work combines multiple computational and machine-learning methods to produce fast fluid dynamic surrogates. Reduced order models (ROMs) are used to minimise the required data such as functional principle component analysis (FPCA). FPCA produces eigenfunctions associated with the data, models will be trained to learn how these functions relate to other factors such as geometry. The primary goal is to develop a model capable of adapting to different geometries and producing accurate fluid flow results without the need for retraining. FPCA has been used to show that it can capture a larger amount of variation using fewer components when compared to POD, allowing flow field reconstruction with similar accuracy using a lower amount of data. FPCA has extracted the top components of the model, and a Gaussian process regressor (GPR) has been trained to predict several of these components for unknown boundary conditions, which have been used to reconstruct the flow field. The results can be seen in the following figure where POD/FPCA reconstructions have been compared to each other and the full data set. The results show that the model can predict the flow towards the inlet but struggles as the flow develops, this will require further work.

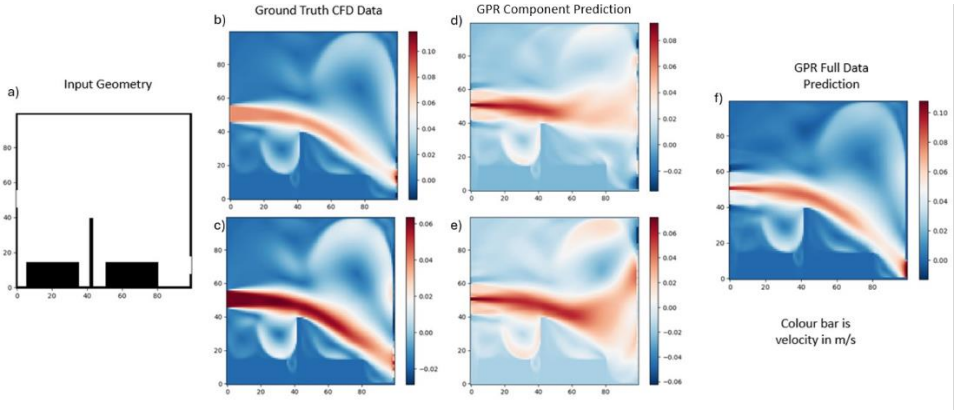

Figure 1. Contour plots comparing the flow field for an inlet position showing a) Inlet position, b) groundvtruth CFD data after POD reconstruction, c) ground truth CFD data after FPCA reconstruction, d) the GPR prediction using POD components, e) the GPR prediction using FPCA components and f) the GPR prediction for the full data set.

David H.C. Chow. Indoor environmental quality: Thermal comfort. In *Reference Module in Earth Systems and Environmental Sciences*. Elsevier, 2022.

ADV/007: Design of Dimpled Surfaces for Drag-Reduction Using Design-by-Morphing and Mixed-Variable Bayesian optimization

[1*]Nasr, Ahmed Mohamed Eisa; [2]Sheikh, Haris Moazam

[1]University of Southampton, University Road, Southampton, Hampshire, SO17 1BJ, United Kingdom, A.M.E.Nasr@soton.ac.uk. [2]University of Southampton, University Road, Southampton, Hampshire, SO17 1BJ, United Kingdom, H.M.Sheikh@soton.ac.uk. *Ahmed Mohamed Eisa Nasr

Dimples and similar drag-reducing surface features function as efficient passive flow control devices, capable of reducing aerodynamic drag by modifying turbulent boundary layers without requiring active energy input. Nonetheless, the underlying mechanisms governing the behaviour of dimples remain insufficiently understood, and realizing their full benefit demands the exploration of diverse shape configurations-often at high computational cost. To address this challenge, we propose a design optimization framework for dimpled surfaces that accommodates both geometric adaptability with computational efficiency. The dimples geometries are generated using Design-by-Morphing (DbM), a novel data-driven shape generation technique that incorporates existing topological profiles to define an expressive design space with minimal design variables (Sheikh et al., 2023). This method enables a continuous and compact design space that encompasses a diverse array of smooth dimple geometries while maintaining local feature quality.

To efficiently navigate this design space, we utilize the mixed-variable, multi-objective Bayesian optimization (MixMOBO) algorithm (Sheikh & Marcus, 2022), which identifies promising and high-performance dimple configurations with minimal LES simulations, thereby significantly reducing the computational burden compared to conventional approach. The integrated DbM–MixMOBO architecture facilitates the systematic computationally tractable exploration of drag-reducing dimple geometries. Our results demonstrate the framework's capability to identify promising and non-intuitive dimple shapes associated with substantial drag reduction, aligning with observations from previous studies (Lee et al., 2024), facilitating a deeper understanding of the underlying flow mechanism influencing dimple performance, thereby advancing the broader study of passive flow control. This approach represents a powerful new paradigm in fluid mechanics design, enabling efficient discovery of high-performance solutions under limited computational budget, paving the way for broader aerodynamic and hydrodynamic design applications.

References:

Lee, S., Sheikh, H. M., Lim, D. D., Gu, G. X., & Marcus, P. S. (2024). Bayesian-Optimized Riblet Surface Design for Turbulent Drag Reduction via Design-by- Morphing With Large Eddy Simulation. *Journal of Mechanical Design*, *146*(8). https://doi.org/10.1115/1.4064413

Sheikh, H. M., Lee, S., Wang, J., & Marcus, P. S. (2023). Airfoil optimization using Design-by-Morphing. *Journal of Computational Design and Engineering*, *10*(4), 1443–1459. https://doi.org/10.1093/jcde/qwad059

Sheikh, H. M., & Marcus, P. S. (2022). Bayesian optimization for mixed-variable, multi-objective problems. *Structural and Multidisciplinary Optimization*, *65*(11). https://doi.org/10.1007/s00158-022-03382-y

ADV/008: Low-order network modeling of an industrial thermoacoustic rig using Bayesian data assimilation

[1*]Zheng, Jingquan; [1]Yoko, Matthew; [2]Andr\'e Fischer; [2]Claus Lahiri; [1]Juniper, Matthew

[1]University of Cambridge, Department of Engineering, UK, jz567@cam.ac.uk [2]Rolls-Royce Deutschland, Dahlewitz, DE. *Presenting Author

Accurate and computationally efficient modeling of thermoacoustic instabilities is crucial for developing low-emission combustion technologies effectively. In this paper, we develop and show a low-order network model (LONM) for non-reacting and reacting flows in the SCARLET (SCaled Acoustic Rig for Low Emission Technologies) test rig and optimize model parameters in the reacting case by physics-based Bayesian inference. For the non-reacting flow, a combination of area jump and duct network elements models the complex injector, which has several axial swirlers. We model these swirlers as duct elements with effective areas derived from experiments. The network predicts the non-reacting mean flow field and acoustic field with less than 2 % and 10 % discrepancy with respect to the experimental measurements across different operating conditions, respectively. For the reacting case, we model the flame as a compact flame and derive an injector-geometry-based flame transfer function (FTF). The initial reacting model showed significant acoustic discrepancy due to the uncertain parameters within the FTF. We then assimilate experimental data to optimize the uncertain parameters of the FTF by minimizing the negative log-posterior likelihood of the parameters, given the prior assumptions and the data. After data assimilation, the network predicts the reacting mean flow field and acoustic field with a discrepancy less than 1 % and 23 %, respectively. This assimilation process reduces the acoustic model error by 37 % compared to the reacting model without assimilation. This paper shows that the LONM can accurately predict the mean flow field and acoustic response of the SCARLET rig. Furthermore, Bayesian data assimilation significantly improves the reacting model's predictive accuracy and shows the most influential parameters of the model, which enhances physical insights into the flame response with respect to the acoustic perturbation.

ADV/009: HARD CONSTRAINT PROJECTION IN A PHYSICS INFORMED NEURAL NETWORK

[1]Horne, Miranda JS*; [2]Jimack, Peter K; [3]Wang, He; [4]Khan, Amirul

[1,2,4]University of Leeds: [1]scmho@leeds.ac.uk, [2]p.k.jimack@leeds.ac.uk [4]a.khan@leeds.ac.uk. [3]University College London he_wang@ucl.ac.uk.

The field of physics informed machine learning is a growing area of research, motivated by the computational expense of traditional methods. One of the key architectures in this field is the physics informed neural network (PINN) [1], which embeds the governing equations through a regularisation in the loss function, defined by the residuals of the governing equations. The introduction of the residual term in the loss function introduces new hyperparameters to tune, while also making the optimisation more challenging [2], and only approximately satisfies the governing equations.

In this talk, we present a method for embedding these governing equations in a strict manner, following the work done by Chen et al. [3]. The hard constraint method used by Chen et al. utilises tools from linear algebra to define a projection to a hyperplane containing exact solutions to the finite difference discretisation of the governing PDEs. We extend the hard constraint projection method from a 2D linear PDE, to multiple nonlinear PDEs (including the Burgers' and Navier Stokes equations) with a variety of parameter settings and consequently provide a commentary on the strengths and weaknesses of the hard constraint projection method.

[1] M. Raissi, P. Perdikaris, and G. E. Karniadakis, “Physics-informed neural networks: A deep learning framework for solving forward and inverse problems involving nonlinear partial differential equations,” Journal of Computational Physics, vol. 378, pp. 686 – 707, 2019.

[2] A. Krishnapriyan, A. Gholami, S. Zhe, R. Kirby, and M. W. Mahoney, “Characterizing possible failure modes in physics-informed neural networks,” in Advances in Neural Information Processing Systems, M. Ranzato, A. Beygelzimer, Y. Dauphin, P. Liang, and J. W. Vaughan, Eds., vol. 34. Curran Associates, Inc., 2021, pp. 26 548– 26 560.

[3] Y. Chen, D. Huang, D. Zhang, J. Zeng, N. Wang, H. Zhang, and J. Yan, “Theory-guided hard constraint projection (HCP): A knowledge-based data-driven scientific machine learning method,” Journal of Computational Physics, vol. 445, p. 110624, 2021

ADV/010: Forecasting the evolution of three-dimensional turbulent recirculating flows from sparse sensor data

*[1]Papadakis, George; [2]Lu, Shengqi

[1]Department of Aeronautics, Imperial College London, SW7 2AZ, g.papadakis@ic.ac.uk, *presenting author

[2]Department of Aeronautics, Imperial College London, SW7 2AZ, s.lu19@ic.ac.uk

A data-driven algorithm is proposed that employs sparse data from velocity and/or scalar sensors to forecast the future evolution of three-dimensional turbulent flows. The algorithm combines time-delayed embedding together with Koopman theory and linear optimal estimation theory. It consists of 3 steps; dimensionality reduction (currently POD), construction of a linear dynamical system for current and future POD coefficients and system closure using sparse sensor measurements. In essence, the algorithm establishes a mapping from current sparse data to the future state of the dominant structures of the flow over a specified time window. The method is scalable (i.e.\ applicable to very large systems), physically interpretable, and provides sequential forecasting on a sliding time window of prespecified length. It is applied to the turbulent recirculating flow over a surface-mounted cube (with more than 10^8 degrees of freedom) and is able to forecast accurately the future evolution of the most dominant structures over a time window at least two orders of magnitude larger that the (estimated) Lyapunov time scale of the flow. Most importantly, increasing the size of the forecasting window only slightly reduces the accuracy of the estimated future states. Extensions of the method to include convolutional neural networks for more efficient dimensionality reduction and moving sensors will be also discussed.

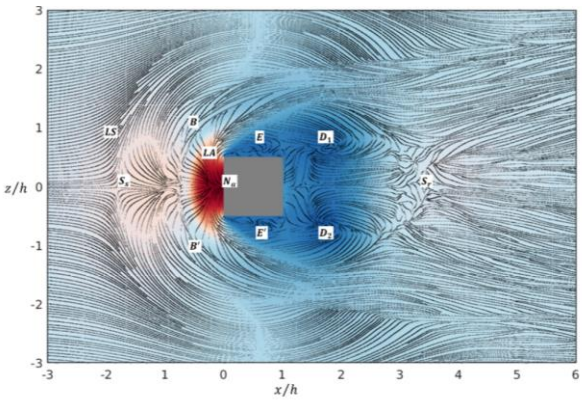

Figure 1. Time-averaged streamlines superimposed on contours of mean pressure field (xz-plane at distance 0.003h from the bottom wall).

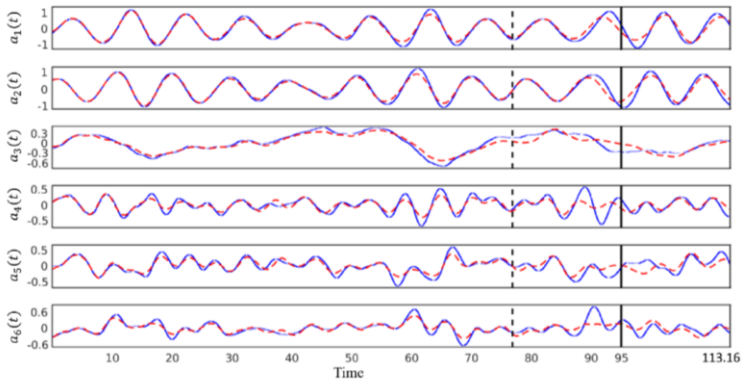

Figure 2 Forecasting of the future evolution of the POD coefficients using velocity measurements at $np = 14$ sensor points, over a time window of $q \times \Delta t = 18.16$ time units, with $m_u = 37$. Blue lines indicate DNS and red lines reconstruction/forecasting. The solid vertical line indicates the starting point of the forecasting dataset.

G. Papadakis and S. Lu (2025) arXiv:2505.05955

ADV/011: Machine Learning-Driven Optimisation of Wall-Normal Blowing for Global Net Power Saving in Turbulent Boundary Layers

[1*]Chen, Xiaonan; [2]Diessner, Mike; [3]Wilson, Kevin; [4]Whalley, Richard

[1]School of Engineering, Newcastle University, Newcastle upon Tyne, United Kingdom. [2]School of Computing, Newcastle University, Newcastle upon Tyne, United Kingdom. [3]School of Mathematics, Statistics & Physics, Newcastle University, Newcastle upon Tyne, United Kingdom. [4]School of Mechanical & Aerospace Engineering, Queen's University Belfast, Belfast, United Kingdom. *Presenting Author

In this study, low-amplitude uniform wall-normal blowing techniques were investigated experimentally in turbulent boundary layer flows and positive net power saving was successfully achieved. Building on our previous work on skin-friction drag reduction, the machine-learning framework NUBO (Newcastle University Bayesian Optimisation), designed for the efficient optimisation of expensive-to-evaluate black-box functions, was extended to maximise net power saving by balancing drag reduction benefits against actuation power costs. Experiments were conducted in a wind tunnel at freestream velocities randomly chosen between 5 m/s and 20 m/s, allowing NUBO to optimise across a range of Reynolds numbers within a single optimisation campaign, rather than requiring separate optimisations for each freestream condition. Velocity measurements near the wall were performed using a laser Doppler velocimetry (LDV) system capable of resolving velocities down to 20 microns from the wall, allowing accurate estimation of skin-friction coefficients from the mean velocity profiles within the linear sublayer. Skin friction at several streamwise locations, both under control and uncontrolled conditions, was measured using LDV to calculate the global skin-friction drag reduction. The blowing intensity was monitored using a mass flow meter, which measured the mass flow rate supplied to the blowing device, while the pressure drop across the blowing device was measured using a pressure transducer to estimate the energy consumption of the actuation system. To reduce the number of optimisation iterations, batches of four blowing conditions were evaluated for net power saving, after which NUBO proposed the subsequent batch of conditions for testing. As a result, significant global skin-friction reduction was obtained when applying uniform wall-normal blowing, as shown in Figure 1, and under certain optimised blowing conditions, positive net power saving was achieved by balancing the energy costs of actuation with the aerodynamic benefits of drag reduction. Furthermore, the most optimal uniform wall-normal blowing intensity corresponding to maximum net power saving was rapidly identified by NUBO for each randomly chosen freestream velocity after relatively few iterations, demonstrating the strong potential of combining active flow control techniques with machine-learning-driven optimisation to enhance aerodynamic performance and energy efficiency.

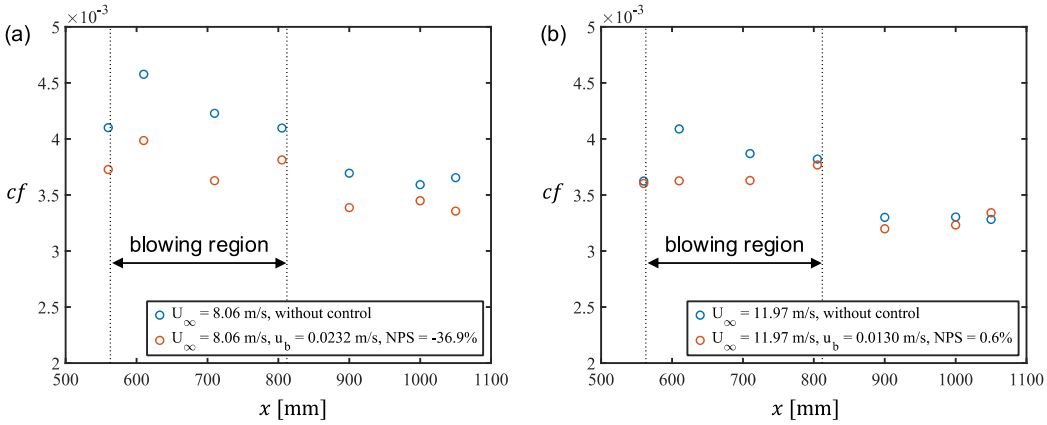

Figure 1. Distribution of skin-friction coefficients along the streamwise direction. (a) Significant global drag reduction achieved, but with negative net power saving; (b) Smaller global drag reduction achieved, but with positive net power saving. These results highlight the importance of balancing drag reduction benefits against the energy costs of actuation.

ADV/012: Scaling convolutional layers for generative models of plasma turbulence

[1,2*]Williams, Josh; [1,3]Castagna, Jony

[1]STFC Hartree Centre, Daresbury Laboratory, Warrington, UK. [2] josh.williams@stfc.ac.uk. [3] jony.castagna@stfc.ac.uk. *Presenting Author

Simulating plasma turbulence in the edge region of tokamak fusion reactors is challenging due to lack of RANS and LES models able to capture the strong inverse cascade of energy injected at small scales by the magnetized particles. Previously, we have used generative adversarial networks (GANs) to reconstruct DNS plasma flowfields in large eddy simulations (Castagna, et al., 2024). However, when training large GANs on high resolution images, the model and its activations no longer fit on a single GPU. To overcome GPU memory limitations for training GANs on high resolution flowfields, we aim to leverage spatial parallelism through the Livermore Big Artificial Neural Network (LBANN) framework (Dryden, et al., 2019). This essentially performs domain-decomposition for the convolutional layers in a GAN, allowing one image to be spread across several GPUs. Increasing the number of spatial decompositions (or 'shards') from one GPU to two and then four GPUs gave a strong scaling efficiency 67.5% on one node (4 GPUs), similar to Dryden, et al. (2019). We then found a weak efficiency of 70% with four shards and 128 data-parallel ranks (512 GPUs total). GPU memory was reduced by a factor of 3.4 when using 4 shards. Alongside performance results, we will demonstrate the GAN's ability to reconstruct DNS flow fields given filtered DNS data.

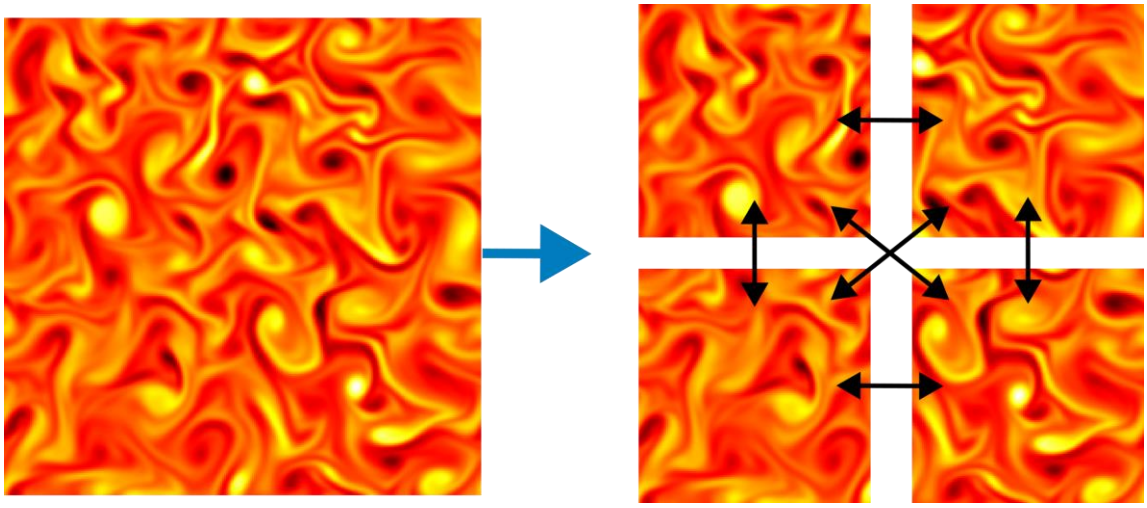

Figure 1. Schematic of the parallelisation process for a two-dimensional plasma vorticity flowfield. We perform a halo-exchange across GPU internal and external periodic boundaries at each convolutional layer (forward and backward pass).

Castagna, J., Schiavello, F., Zanisi, L., and Williams, J., StyleGAN as an AI deconvolution operator for large eddy simulations of turbulent plasma equations in BOUT++, *Physics of Plasmas*, Vol. 31, No. 3, 2024.

Dryden, N., Maruyama, N., Benson, T., Moon, T., Snir, M., and Van Essen, B., "Improving strong-scaling of CNN training by exploiting finer grained parallelism," *2019 IEEE International Parallel and Distributed Processing Symposium (IPDPS)*, IEEE, 2019, pp. 210–220

ADV/013: Diffuse-domain periodic Navier-Stokes solver for 4D flow-MRI reconstruction

[1*]Cheetham, Thomas W., [1]Kontogiannis, Alexandros and [1]Juniper, Matthew P.

[1]Department of Engineering, University of Cambridge, Trumpington Street, Cambridge CB2 1PZ, UK *tc563@cam.ac.uk

We solve a pulsatile boundary value Navier-Stokes problem using a diffuse-domain finite element method to handle complex geometries. The periodic nature of the flow is exploited using a harmonic balance approach to express the forward problem as a set of coupled problems at collocation points in the time domain. The pressure and velocity fields are solved at all collocation points simultaneously using a Schur complement approach with a Krylov subspace method and a block-circulant preconditioner. Matrix-free methods within the Deal.ii library are leveraged to reduce memory requirements and efficiently invert sub-matrices using h-adaptive geometric multigrid algorithms. Current work in progress is to use this periodic forward solver to assimilate 4D flow-MRI data. A general inverse periodic Navier-Stokes problem is solved, using a Bayesian framework with prior Gaussian random fields for regularisation. The most likely model parameters are inferred by maximising the posterior probability to find the MAP estimator using adjoint-accelerated gradient-based methods. By solving this inverse problem we segment the flow-MRI scan and reconstruct the velocity field from low SNR data whilst uncovering hidden flow quantities such as the wall shear stress and pressure drop.

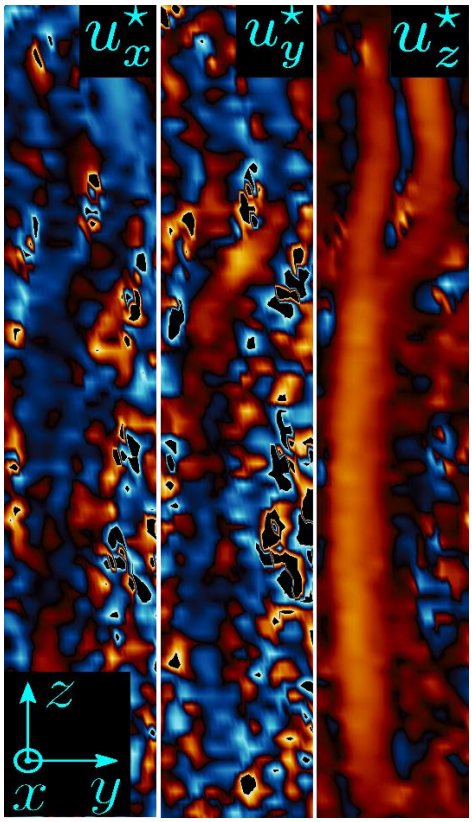

Figure 1. In-vivo 4D flow MRI measurements of the velocity field within a patient's Carotid artery. Data courtesy of Prof. Martin Graves, Cambridge University Hospitals.

ADV/014: DATA-DRIVEN IDENTIFICATION OF FLOW STRUCTURE IN FREE_SURFACE TURBULENT CHANNEL FLOW OVER SQUARE BARS

[1*]Jalalabadi, Razieh, [2]Guseva, Anna

[1]Civil, Environmental and Geomatic Engineering, University College London, Gower Street, London WC1E 6BT, United Kingdom.
[2]Laboratory for Astrophysics Research and Instrumentation (LIRA), The Paris Observatory, France *Presenting Author

In this work, Proper Orthogonal Decomposition (POD) and Dynamic Mode Decomposition (DMD) are used to identify the dominant flow structures in free-surface turbulent channel flow over rough bed. Spanwise-aligned square bars attached to the wall are considered as roughness (Jalalabadi *et al.*, 2021). The bar spacings correspond to transitional and k-type roughness; in the former a stable vortex is formed between bars while in the later a recirculation zone is generated at the downstream of the bar that extends to a reattachment point and a standing wave is developed over the water surface (Jalalabadi *et al.*, 2022). A large Dataset generated by large-eddy simulations are used to extract flow patterns. Using POD approach, it is revealed that the first 16 modes contain 99% of the total energy in flow over both bars spacing. The dominant modes were calculated using DMD with different truncation numbers but the same number, 16, showed the most physically meaningful results (Yang *et al.*, 2022). The first two dynamic modes extracted using POD and DMD are shown in Figure 1. In flow over k-type (larger) bar spacing, the interaction of the bulk flow with the standing wave at the water surface is seen in both POD and DMD modes while the effects of recirculation zone are clearly seen in the DMD ones as well. In flow over transitional (smaller) bar spacing, DMD results show a periodic structure. Such structure is only seen in the second dominant mode in the POD results. The non-orthogonality of modes and consideration of frequencies in extracting dominant structures in DMD approach can lead to the differences between POD and DMD results.

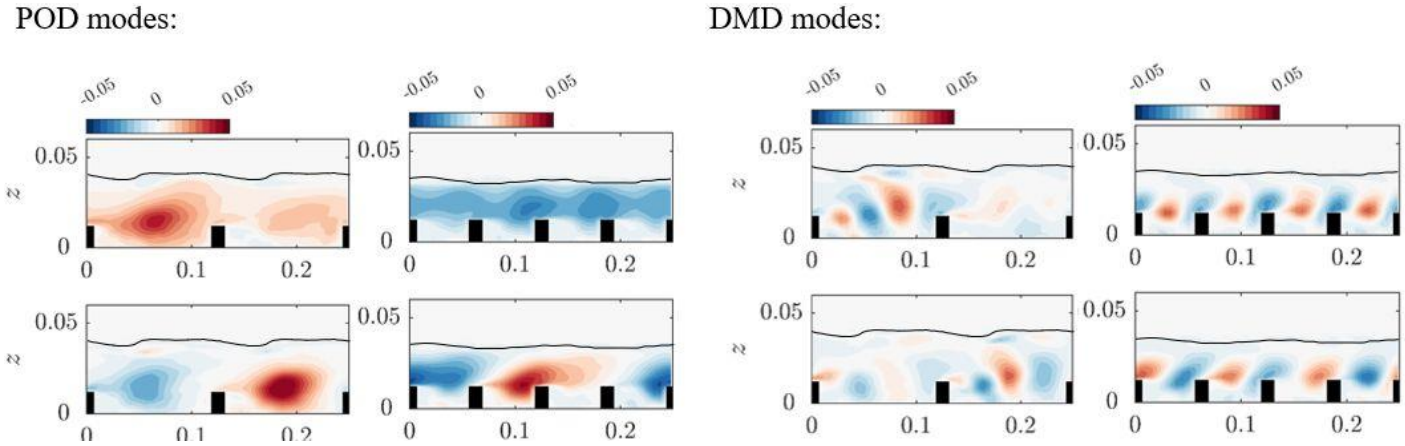

Figure 1. The first two dynamic modes extracted using POD and DMD approaches for the two bar spacing.

Jalalabadi, R., Stoesser, T., Ouro, P., Luo, Q., Xie, Z., 2021, Free surface flow over square bars at different Reynolds numbers. J. Hydro-Environ. Res. 36, 64.

Jalalabadi, R., Stoesser, T., 2022, Reynolds and dispersive shear stress in free-surface turbulent channel flow over square bars. Phys. Rev. E 105, 035102.

Yang, R., Zhang, X., Reiter, P., Lohse, D., Shishkina, O., Linkmann, M., 2022, Data-driven identification of the spatiotemporal structure of turbulent flows by streaming dynamic mode decomposition, GAMM-Mitteilungen. 45, e202200003.

ADV/015: A Novel Mesh Morphing Methodology for Computational Aerodynamic Shape Optimisation

[1*]Salamoun, Joelle; [2*]Smith, Ben; [3]Evans, Ben; [4]Walton, Sean; [5]Dodds, Martin; [6]Taylor, Neil

[1]Swansea, Wales 2268086@swansea.ac.uk. [2]Swansea, Wales benhicklingsmith@gmail.com. [3]Swansea, Wales b.j.evans@swansea.ac.uk. [4]Swansea, Wales s.p.walton@swansea.ac.uk. [5]Oxford, England. [6]Swansea, Wales n.v.taylor@swansea.ac.uk. *Presenting Author

Mesh deformation plays a critical role in aerodynamic shape optimisation, enabling efficient geometry modifications without requiring full mesh regeneration. This paper presents a mesh deformation method based on **Radial Basis Function (RBF)** interpolation, offering a computationally efficient and robust alternative to traditional physical analogy and interpolation-based approaches. The proposed method is integrated into a gradient-free optimisation framework, incorporating **Bayesian Optimisation (BO)** to efficiently navigate complex, multi-modal design spaces. The developed framework is tested on three aerodynamic shape optimisation case studies, demonstrating its ability to maintain mesh quality, improve computational efficiency, and enhance convergence towards optimal designs. Results show that RBF-based mesh deformation effectively accommodates large shape changes while reducing numerical noise, making it a promising approach for high-fidelity aerodynamic optimisation. The findings highlight the advantages of combining advanced mesh deformation techniques with Bayesian Optimisation, paving the way for more efficient and automated aerodynamic design methodologies.

ADV/016: Corneal Material Characterisation via PINNs-Based Modelling of Impinging Jets: *Poster*

[1*]Maklad, Osama; [2]Hao, Muting

[1]*Centre for Advanced Manufacturing and Materials, University of Greenwich, London, UK.*

[2]*Oxford Thermofluid Institute, University of Oxford, Oxford, UK.*

*Presenting Author, o.maklad@gre.ac.uk

This study investigates fluid-structure interaction (FSI) models of the air puff test; a diagnostic method used for assessing corneal biomechanics. Using Abaqus, simulations were conducted on eyes with varying biomechanical parameters, including material properties, corneal thickness, and radius. A reduced-order model of the air puff, represented as a turbulent impinging jet, was developed to significantly decrease computation time from 48 hours for the FSI model to approximately 12 minutes for finite element analysis (FEA) alone [1, 2]. To further optimize simulations and enhance model fidelity, Physics-Informed Neural Networks (PINNs) are incorporated into the reduced-order model. This integration aims to expand the dataset, improve intraocular pressure (IOP) estimation, and refine the corneal material characterization algorithm through inverse FEA, as illustrated in Figure 1.

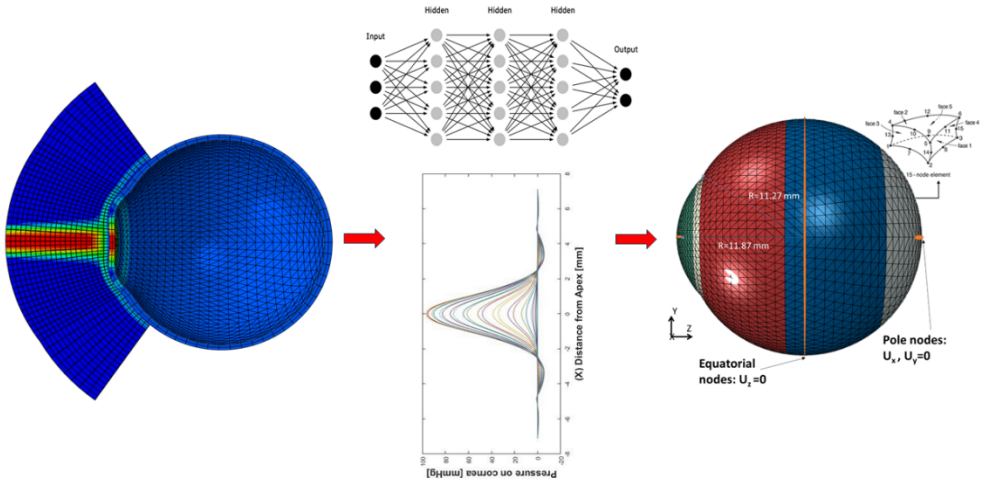

Figure 1: The FSI coupled model of the air puff test with the boundary conditions along with the proposed PINNs implementation.

Keywords: Physics-Informed Neural Networks (PINNs), air puff test, corneal biomechanics, impinging jets, turbulence, reduced order modelling, fluid structure interaction

[1] Osama Maklad, Ashkan Eliasy, Kai-Jung Chen, JunJie Wang, Ahmed Abass, Bernardo Teixeira Lopes, Vassilis Theofilis, and Ahmed Elsheikh. Fluid-structure interaction based algorithms for iop and corneal material behavior. Frontiers in Bioengineering and Biotechnology, 8:970, 2020.

[2] Osama Maklad, Vassilios Theofilis, and Ahmed Elsheikh. Role of impinging jets in the biomechanical correction of the intraocular pressure (iop) measurement. ICFD13, pages 1–8, 2018.

AER: Aerodynamics, Aeroelasticity and Aeroacoustics

AER/001: Wing Shock Buffet Prediction: From Conception to Aircraft Application

[1*]Nash, Daniel; [2]Timme, Sebastian

University of Liverpool, Liverpool, L69 3GH, United Kingdom

[1]d.j.nash@liverpool.ac.uk [2]sebastian.timme@liverpool.ac.uk.

*Presenting Author

Wing shock buffet is a cause of unsteady aerodynamic loads and associated structural vibrations which can limit the flight envelope. Despite its importance to aircraft design and certification, the physics within the multidisciplinary context remain an active area of research. The interaction of shock waves and turbulent boundary layers in the high Reynolds number flight regime naturally calls for computationally prohibitive scale-resolving simulations. However, to make numerical buffet prediction attainable, (Favre- and) Reynolds-averaged Navier-Stokes modelling combined with an appropriate choice of turbulence model is often resorted to, relying on the assumption of separation of unsteady scales between the lower frequency coherent buffet dynamics and the higher frequency turbulence. Even then, time-accurate time-marching simulations are too expensive for routine application. Instead, frequency-domain methods have grown in popularity, such as linear global stability analysis [1], that can directly predict critical parameters, coherent structures and associated frequencies, cf. figure 1.

Our contribution will look at three design philosophies of large airliners, all encountering the aerodynamic instability of shock buffet. Importantly, our final case, the Airbus XRF1 model, adds high levels of geometric complexity. The capabilities and limitations of two generations of industrial computational fluid dynamics solvers, including the legacy code DLR-TAU and the new-generation code CODA, will be discussed in this context, with a view on industrial adoption.

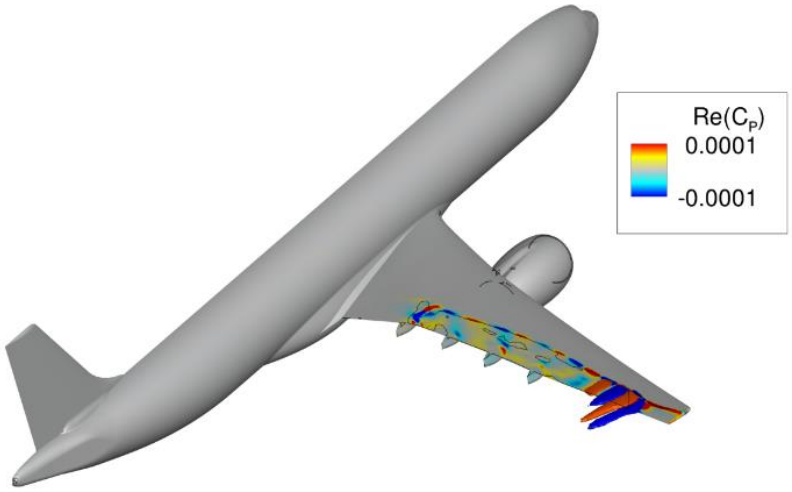

Figure 1. Shock buffet mode at angle of attack of 3.50^{o} *for the XRF1 model using DLR-TAU, showing real part of surface pressure distribution and zero skin-friction line. The isosurface is defined by the real part of x-momentum.*

[1] S. Timme. Global instability of wing shock-buffet onset. Journal of Fluid Mechanics, 885:A37, February 2020. doi: 10.1017/jfm.2019.1001

AER/002: Gust response of free-falling plates

[1*]Pandi, Jawahar Sivabharathy Samuthira; [1]Gungor, Ahmet; [2]Bose, Chandan;

[1]Attili, Antonio; [1]Viola, Ignazio Maria

[1]School of Engineering, University of Edinburgh, United Kingdom. [2]Aerospace Engineering, University of Birmingham, United Kingdom.
*jsamuthi@ed.ac.uk

Gusts have a significant impact on the performance of aerial vehicles affecting their stability, trajectory, and causing structural failure. A strong gust can hinder the manoeuvrers of small-scale flyers. We focus on understanding the free-fall dynamics of plates and their response to a transverse step gust for $10 \leq Ga \leq 50$. The Galilei number is $G_a = \hat{u}_g \hat{l}/\hat{v}$, where $\hat{u}_g$and $\hat{l}$ are the gravitational velocity and the length of the plate, and $\hat{v}$ is the kinematic viscosity of the fluid. The ratio of the plate and fluid density (ρ) is varied between 5 and 50. The gust ratio (G_R) is defined as the ratio of the gust velocity to the gravitational velocity and is varied between 0 to 5. It is found that the plate undergoes a steady fall for $Ga \leq 30$. For $Ga > 30$, the plate exhibits fluttering kinematics. The amplitude of oscillation of the fluttering motion increases with ρ up to $\rho = 20$ and decreases thereafter. Figure 1(a) shows the time-history of the nondimensional plate's descent velocity ($u_Z = \hat{u}_z/\hat{u}_g$) versus the convective time ($t = \hat{t}\,\hat{l}\,\backslash\hat{u}_g$) for various Ga falling freely in quiescent condition with no gust. The plate accelerates asymptotically towards its terminal velocity. The plate experiences lower nondimensional terminal velocity at low Ga due to higher drag coefficient. The impact of transverse gust on u_Z is showcased in figure 1(b) for $G_R = 4$. The gust causes a transient reduction in the terminal velocity. The increment in relative flow velocity experienced by the plate due to the gust-induced horizontal displacement results in an increased vertical force. The plate stabilises faster at low Ga because of the higher viscous effects. The amplitude and duration of the gust response increase with Ga. For $Ga > 30$, the gust triggers the fluttering kinematics. We also studied the stability characteristics of the plates, the effects of G_R and Ga on the vertical height gained, and the mechanism of upwards force generation driving this gain. The outcomes of this study are anticipated to inform the design of passively dispersed micro-drones, improving their control and prolonging their time afloat.

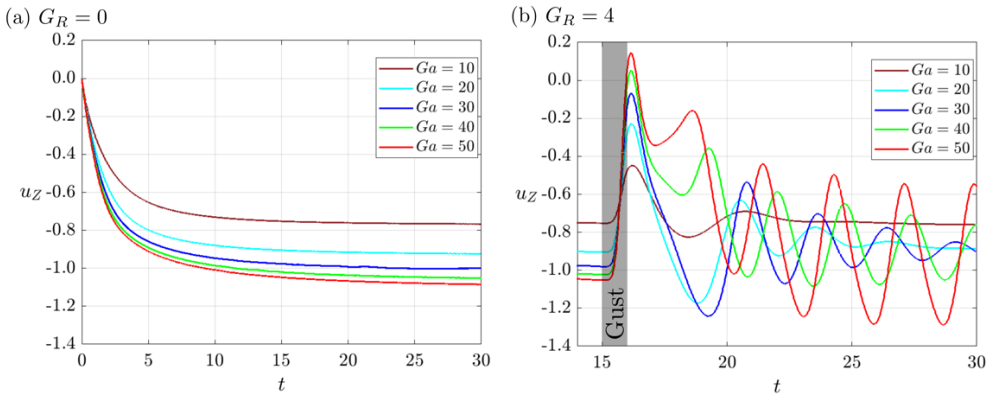

Figure 1. Free-falling plate for various Ga: time-history of descent velocity of the plate for (a) $G_R = 0$ and (b) $G_R = 4$. The grey shaded region in (b) denotes the gust. The start and end time of gust is $t_s = 15$ and $t_e = 16$. The period of gust $(t_G = t_s - t_e)$ corresponds to one.

1. Wu, Z., Cao, Y. & Ismail, M., 2019, Gust loads on aircraft. *The Aeronautical Journal* 123 (1266), pp 1216–1274.

2. Cummins, C., Seale, M., Macente, A., Certini, D., Mastropaolo, E., Viola, IM. & Nakayama, N., 2018, A separated vortex ring underlies the flight of the dandelion. Nature 562 (7727), pp 414–418.

AER/004: Hydrogen-Powered Aircraft Aerodynamics Analysis Through the Integration of OpenVSP and OpenFOAM.

[1*]Mejbil, Abdullah; [2]Thomson, Harvey; [3]Khan, Amirul; [4]Muir, Martin; [5]de Boer, Gregory

[1]University of Leeds, scaam@leeds.ac.uk. [2]University of Leeds, h.m.thompson@leeds.ac.uk. [3]University of Leeds, a.khan@leeds.ac.uk. [4]Airbus, martin.muir@airbus.com. [5]University of Leeds, g.n.deboer@leeds.ac.uk.

Commercial aircraft are highly efficient transport which play a significant role in the world economy. The aviation industry has boosted economic activity, but has also led to increased emissions. Technological advances have reduced emissions, yet this falls short of net-zero goals, and this drives the need for sustainable aviation. Hydrogen-powered aircraft have the potential to significantly reduce climate impact. Optimised conventional aircraft designs have evolved through years of experimentation and tool development, but frameworks for sizing hydrogen-powered aircraft designs do not exist. Using high-fidelity analysis tools in optimisation frameworks is necessary when designing novel aircraft configurations due to the limitations of low-fidelity tools. This study aims to build a workflow of high-fidelity aero-structural analysis using open-source tools for the purpose of optimising novel aircraft configurations. The study introduces a workflow from geometry generation using OpenVSP, to running CFD simulations using OpenFOAM. The validation case considered was the Onera M6 wing. In addition, the NASA Common Research Model (CRM) was considered as a full aircraft design. This workflow paves the way for aerostructural design optimisation using open source tools and allows for the construction of a design optimisation framework for novel hydrogen aircraft configurations.

AER/005: Coherent structures from round and serrated turbulent jets

Cassim, Amrit; Wang, Zhong-Nan

University of Birmingham, awc453@student.bham.ac.uk University of Birmingham z.n.wang@bham.ac.uk, Presenting author: Cassim, Amrit.

Prior studies have shown that serrated nozzles are capable of reducing low-frequency jet noise (St <~1) compared to round nozzles, with a maximum reduction of about 5 dB observed at aft-angles, while increasing high frequency noise (St>~1). The increase of high-frequency sideline noise has been linked to an increase in fine-scale turbulence caused by enhanced mixing due to the chevron-induced streamwise vortices. The reduction of low-frequency aft-angle noise is caused by a disruption of azimuthally coherent structures in the turbulent flow field from the serrated nozzle. However the exact modifications to coherent structures and how this links to low-frequency noise reduction have yet to be studied in detail. This talk presents results with the aim of addressing these questions.

We show Spectral POD (SPOD) results of LES data for a Mach 0.7 compressible turbulent serrated jet with 16 chevrons, and of a round jet with the same configuration. The way in which the chevrons modify and redistribute energy between Kelvin-Helmholtz (KH) and Orr wavepackets as well as streaks will be demonstrated. Chevrons decrease the relative energy of KH wavepackets close to the nozzle while increasing the relative energy of streaks, with this effect being most pronounced as St approaches 0. In addition, the chevrons modify the near-field optimal SPOD spectrum in a similar way to the far-field acoustics. The link between the near and far field is investigated further using acoustic matching calculations through the use of Lighthill's acoustic analogy. We show resolvent analysis results to elucidate the physical mechanisms by which chevrons achieve the above-mentioned disruption to coherent structures. Finally, the chevron-induced modifications to triadic interactions in the near-field of the jet and the resulting implications for far-field noise, studied using Bispectral Mode Decomposition, are presented.

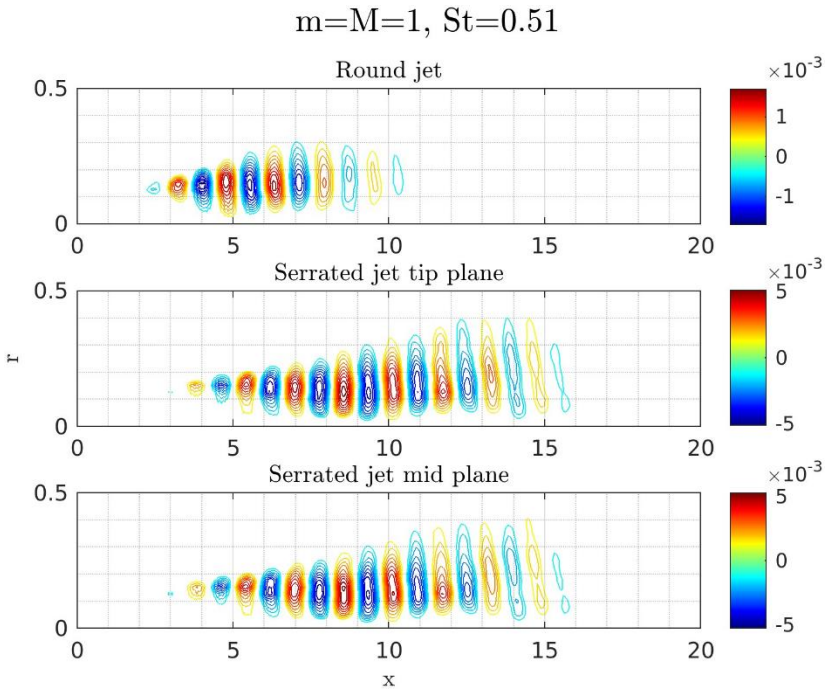

Figure 1: The leading SPOD mode (a KH wavepacket) for the indicated azimuthal wavenumbers and Strouhal number for the round jet and serrated jet, both in the tip and midplanes. Serrations destroy the KH wavepacket close to the nozzle.

AER/006: GUST RESPONSE OF BIO-INSPIRED MORPHING WINGS

Hibah Saddal[1*], Lucky Jayswal[1], Chandan Bose[1]
[1] Aerospace Engineering, The University of Birmingham, United Kingdom
(Email for Correspondence: c.bose@bham.ac.uk)

Nature-inspired small-scale unmanned-aerial vehicles are susceptible to unsteady gusty environments, particularly when environmental flow disturbances approach the scale of the vehicles' airspeed [1]. In such scenarios, wind gusts can lead to pronounced flow separation over aerodynamic surfaces, significantly affecting performance and stability. To address this, wings with variable flexibility, drawing inspiration from the adaptability of bird wings have emerged as a promising research direction for enhancing aerodynamic efficiency across various flight conditions [2]. This study conducts a numerical investigation into the dynamic response of oscillating wings with varying flexibility, subjected to canonical gust profiles including transverse, vortex and streamwise gusts.

A two-way coupled fluid-structure interaction framework is employed using a partitioned strong coupling strategy. The incompressible fluid flow is governed by the Navier-Stokes equations and solved using the finite volume method-based code - OpenFOAM. Mesh deformation during the wing movement is enabled through a quadratic inverse-distance diffusion-based dynamic meshing technique. The structural part is simulated using the finite element method-based solver CalculiX, governed by the St. Venant–Kirchhoff constitutive law. The coupling between fluid and structural solvers is facilitated via preCICE, with radial basis function interpolation ensuring accurate data exchange across the fluid-solid interface. A parallel implicit coupling scheme, accelerated using the Interface Quasi-Newton Inverse Least Squares scheme, ensures convergence.

This work investigates the effects of time-varying bending stiffness on the propulsion performance and gust mitigation of a morphing wing section. Figure 1 presents representative results from this study. Additionally, the influence of spatially varying stiffness is analysed with a particular focus on periodic structure of the phononic material to study the wing's interaction with vortical gusts. Results will be compared against rigid and uniformly flexible flapping wings. The outcomes of this study aim to inform the design of next-generation aerial vehicles capable of improved performance and robustness in various conditions.

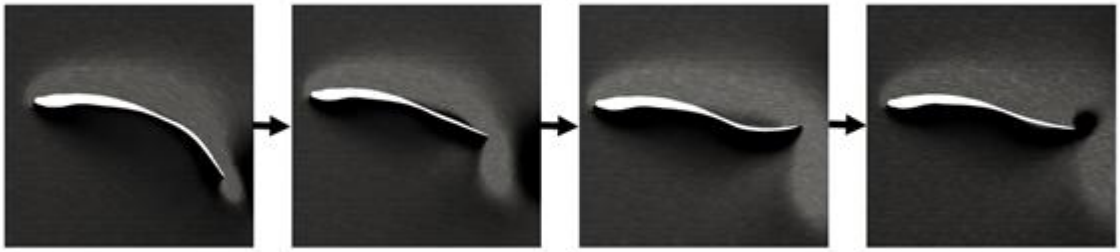

1. Jones, A. R. (2020). Gust encounters of rigid wings: Taming the parameter space. Physical Review Fluids, 5(11), 110513.

2. Yudin, D., Floryan, D., & Van Buren, T. (2023). Propulsive performance of oscillating plates with time-periodic flexibility. Journal of Fluid Mechanics, 959, A31.

AER/007: Roughness induced transition of compressible flow over an ablated surface

[1*]Matera, Giuseppe; [1]Sandham, Neil D.

[1] University of Southampton, Boldrewood Innovation Campus, Southampton, SO17 1BJ. Email: gm6g19@soton.ac.uk *Presenting Author

Surface ablation is a recurring phenomenon in re-entry capsules, characterised by the heterogeneous regression of heat shield material, leading to surface roughness. Numerous studies have shown that surface irregularities can shift the transition location upstream and increase both turbulent wall-shear stress and heat flux. Although several empirical correlations exist in the literature, they are often based on specific roughness configurations (e.g., distributed vs. isolated), flow geometries (e.g., flat plate vs. cone), or gas compositions (e.g., air vs. CO_2), highlighting a lack of general applicability. The aim of the present study is to advance the understanding of the physical mechanisms that promote early transition by identifying the key surface features responsible for this behaviour. The full three-dimensional, compressible Navier–Stokes equations are solved using a high-order finite-difference Direct Numerical Simulation (DNS) code to investigate the effects of distributed roughness on hypersonic boundary-layer transition over an isothermal flat plate, under Mars atmospheric entry conditions and assuming an ideal gas. Conditions at the inflow are representative of those behind the bow shock of the Mars 2020 capsule flying at approximately Mach 26. Simulations are carried out using a post-shock Mach number of 1.5 and a temperature ratio (wall to post-shock) of 0.5. The start of the computational domain corresponds to a Reynolds number of 2000, based on the displacement thickness and post-shock flow properties. The rough section is obtained from scans of an ablated surface. The roughness characteristic length is set to half the displacement thickness at the inflow. Preliminary results show the formation of hairpin vortices that evolve into sustained turbulence, driven solely by the surface roughness, without any external perturbations, as shown in Figure 1. Streamwise structures are observed to originate near the middle of the domain, close to the wall. These are progressively amplified as they convect downstream, eventually leading to the formation of coherent vortical structures and transition to turbulence. Furthermore, the influence of roughness extends upstream into the nominally smooth region. Future work will investigate the sensitivity of the transition process to variations in flow conditions and roughness characteristics, with the goal of developing more general transition criteria applicable to a wider range of rough surfaces.

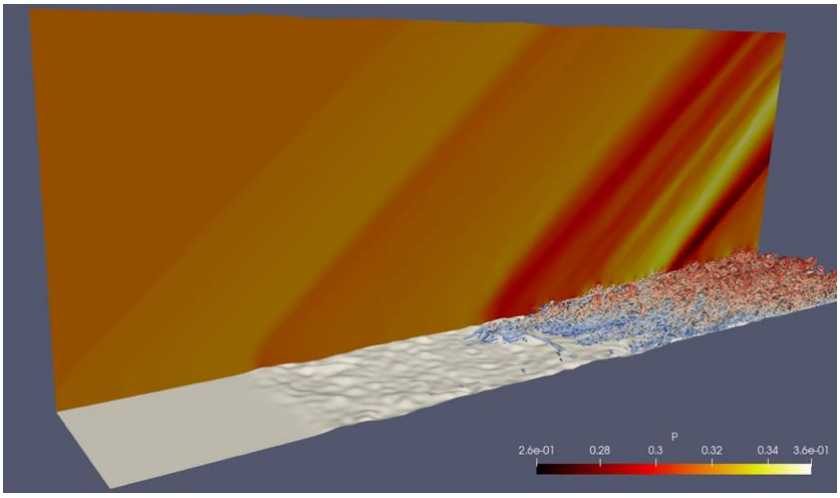

Figure 1. Iso-surfaces of normalised Q-criterion showing the formation of hairpin vortices coloured by the local value of the streamwise velocity; and contour of the normalised pressure at the edge of the domain.

AER/008: DIRECT MECHANICAL POWER MEASUREMENT OF A MINIATURE WIND TURBINE

[1*]Board, Lily; [2]Sampath, Ahren; [3]Mandre, Shreyas

[1*]University of Cambridge, lb2013@cam.ac.uk . [2]University of Oxford. [3]University of Cambridge. *Presenting Author

Miniature wind turbines are used in the study of wind farms and their wake interactions in wind tunnel experiments. It is often desirable in such experiments to measure the power that is mechanically extracted from the flow by the wind turbine. Typically, the power is measured indirectly via the electrical power generated by a motor in the hub of the turbine. However, this is not a perfect substitute due to electrical losses obfuscating the relationship between the fluid dynamics and the mechanical power. Here a new design for directly measuring the mechanical power of a miniature wind turbine is proposed. Strain gauges are applied to webbed sections of spring steel at the base of the tower, one parallel and one perpendicular to the flow, to measure the torque and drag. Mechanical power is then obtained by multiplying the measured torque by the rotor's angular velocity. Existing designs have employed strain gauges but face problems such as bearing friction [1]. This new design eliminates the need for bearings and has the potential to be used with slimmer nacelle designs. The turbine performance is characterized using the directly measured mechanical power and results are supported through calibration of the electrical power and measuring the velocity deficit in the wake.

Figure 1. Miniature wind turbine. This turbine employs strain gauges at the base of the turbine tower below the ground board (not pictured) to measure the torque and drag it experiences. The turbine rotor used here is WiRE-01, by Bastankhah and Porté-Agel [2] and modified by Sampath [3].

[1] H. S. Kang and C. Meneveau, "Direct mechanical torque sensor for model wind turbines," Measurement Science and Technology, vol. 21, no. 10, p. 105206, 2010

[2] M. Bastankhah and F. Porté-Agel, "A New Miniature Wind Turbine for Wind Tunnel Experiments. Part I: Design and Performance", Energies, vol. 10, no. 7, p. 908, 2017.

[3] A. Sampath, "Design and characterisation of performance of a wind tunnel scale wind turbine," Master's thesis, University of Cambridge, 2024.

AER/009: FLUTTERY FLIGHT OF BUTTERFLY SWARMS

Chandan Bose[1*], Ethan Warman[1], Debajyoti Kumar[2], Siddharth Sharma[2], Somnath Roy[2,3]
[1] Aerospace Engineering, The University of Birmingham, United Kingdom
[2] Centre for Computational and Data Sciences, IIT Kharagpur, India
[1] Department of Mechanical Engineering, IIT Kharagpur, India
(Email for Correspondence: c.bose@bham.ac.uk)

The study of robotic butterfly swarms presents futuristic opportunities for understanding complex aerodynamic interactions in bio-inspired flight formations. However, simulating large-scale robotic swarms is computationally intensive due to intricate flow interactions, moving boundaries, and nonlinear phenomena. In this research, we harness the power of GPU-accelerated computing to accelerate aerodynamic simulations significantly using an Immersed Boundary Method [1] and overset meshing strategy. Our GPU-accelerated flow solver efficiently handles the complex flow interactions inherent to the flapping wings of robotic butterflies, enabling detailed characterization of aerodynamic performance metrics such as lift, thrust, and propulsion efficiency. Through high-resolution computational fluid dynamics simulations, we explore critical aerodynamic features emerging within robotic butterfly swarms, including wake interactions, vortex formation, and aerodynamic synchronization between multiple units. These insights not only deepen our fundamental understanding of swarm aerodynamics but also directly inform the design principles of next-generation robotic aerial systems. Ultimately, this study demonstrates the transformative potential of GPU-computing in computational aerodynamics, offering robust and scalable tools capable of unlocking new paradigms in bio-inspired engineering and robotics research. Figure 1 presents a representative snapshot of the unsteady flow-field around two fluttering butterflies following each other in a sinusoidal trajectory.

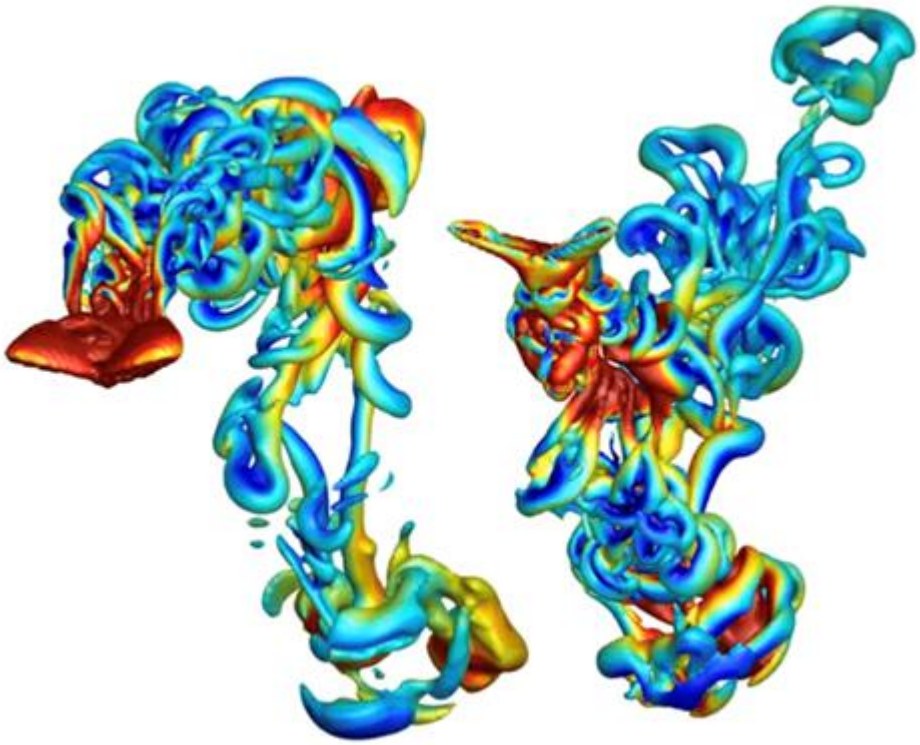

1. Raj, A., Khan, P. M., Alam, M. I., Prakash, A., & Roy, S. (2023). A GPU-accelerated sharp interface immersed boundary method for versatile geometries. Journal of Computational Physics, 478, 111985.

AER/011: Effect of One-Minus-Cosine Discrete Gusts on an Isolated Propeller Performance in Axial Flight

[1*]Finnemore, Aron; [2]Westin, Michelle; [3]Yuan, Ye; [4]Yuying, Xia; [5]Celik, Alper

[1*]Faculty of Science and Engineering, Swansea University, Swansea, SA1 8EN, UK; a.p.finnemore@swansea.ac.uk. [2]Embraer S.A., São José Dos Campos, SP 12227-901, Brazil; michelle.westin@embraer.com.br. [3]School of Engineering, University of Glasgow, Glasgow, G12 8QQ, UK; ye.yuan@glasgow.ac.uk. [4]Faculty of Science and Engineering, Swansea University, Swansea, SA1 8EN, UK; yuying.xia@swansea.ac.uk. [5]Faculty of Science and Engineering, Swansea University, Swansea, SA1 8EN, UK; alper.celik@swansea.ac.uk.

Electric Vertical Take-off and Landing (eVTOL) aircraft are key to future sustainable air transport and urban air mobility (UAM), enabling low-altitude, intra-city flight. Operating near urban structures exposes these vehicles to frequent high-magnitude gusts, which can affect stability and increase pilot workload. These challenges have prompted growing research into multi-propeller interactions under unsteady flow conditions. This study presents an experimental investigation into the effect of a one-minus-cosine shaped discrete gust on an isolated propeller in axial flight. Experiments were carried out at Swansea University wind tunnel facility, which is temperature-controlled, closed-circuit and has closed test section with dimensions of 1.5 m x 1 m x 2.5 m (width x height x length). An off-the-shelf APC 12”x4.5” propeller was used for the experiments. Flow characteristics and aerodynamic loads were measured using a crosswire probe and an ATI Mini40E load cell, respectively. The discrete gusts were generated using two NACA0015 vanes at the wind tunnel inlet. Gust strength was varied by adjusting the amplitude and rate of vane rotation. Gust characteristics were quantified at the propeller plane, located 1.7 m downstream of the inlet. The resulting gust ratios ranged from 0.1 to 0.3, defined as the vertical gust velocity divided by the free stream velocity. Tests were performed across rotational speeds from 4000 to 6000 Revolutions Per Minute (RPM) at a free stream velocity of 10 m/s. Load measurement results showed that thrust deviates significantly under discrete gusts, with greater deviation at lower RPMs. At higher RPMs, thrust deviation is reduced but accompanied by significant fluctuations in yaw and pitch torques. These torque fluctuations were driven by the gust’s vertical component, which temporarily creates an edgewise flight condition. Under gust conditions, the wake shifts toward the instantaneous advancing side of the propeller blade, deviating from the symmetric wake observed in steady flow. This shift aligns with the torque imbalances recorded by the load cell, providing valuable insight for propeller design, control strategies and overall vehicle stability. These observations regarding flow field are presented Figure 1, which displays the ratios of vertical velocity to streamwise velocity for steady and unsteady inflow conditions.

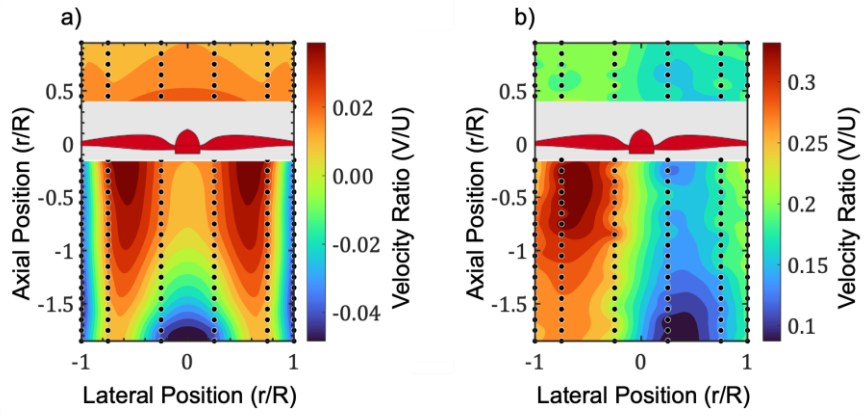

Figure 1. a) Flow field of isolated propeller in steady flow conditions. b) Flow field of isolated propeller in a gust ratio of 0.3.

AER/012: Effect of Discrete One-Minus-Cosine Gusts on UAM Aerodynamics

[1*]Lobb, Morgan; [2]Westin, Michelle; [3]Yuan, Ye; [4]Yuying, Xia; [5]Celik, Alper

[1]Swansea University; m.j.o.lobb@swansea.ac.uk. [2]Embraer; michelle.westin@embraer.com.br

. [3]University of Glasgow; Ye.Yuan@glasgow.ac.uk. [4]Swansea University; x.yuying@swansea.ac.uk. [5]Swansea University; alper.celik@swansea.ac.uk.

Interest in both Urban Air Mobility (UAM) and Micro Air Vehicles (MAVs) has increased in recent years. Both MAVs and UAM vehicles operate at low altitudes in urban environments, where atmospheric turbulence intensities can be high and gusts highly pronounced. However, there has been limited research into the aerodynamic effects of turbulence and gust on these vehicles, presenting a significant gap in existing literature. A propeller-wing rig has been designed and manufactured to investigate the effects of the one-minus-cosine gusts on propeller-wing aerodynamics. Propeller and wing forces were recorded using a six-component ATI Mini40E load cell and a six-component AMTI MC12-1000 force balance. Pressures on the suction and pressure side of the wing were recorded using a series of static and high frequency pressure sensors to investigate the effect of gust on the mean and unsteady loading on the wing. A two-vane gust generator is used to produce gusts at frequencies of 2 Hz, 3 Hz, and 4 Hz at amplitudes of 10°, 15°, and 20°. The tests were performed at propeller rotational speeds of 5000 rpm, 6000 rpm, and 7000 rpm at free stream velocities for 10 m/s, 15 m/s, and 20 m/s, which corresponds to a chord-based Reynolds number of $176000 < Re < 352000$ and advance ratio of $0.34 < \mu < 0.94$. The pressure measurement results show a dramatic change in the pressure distribution under gust compared to steady case, accompanied by a significant change in propeller trust and overall loading on the wing.

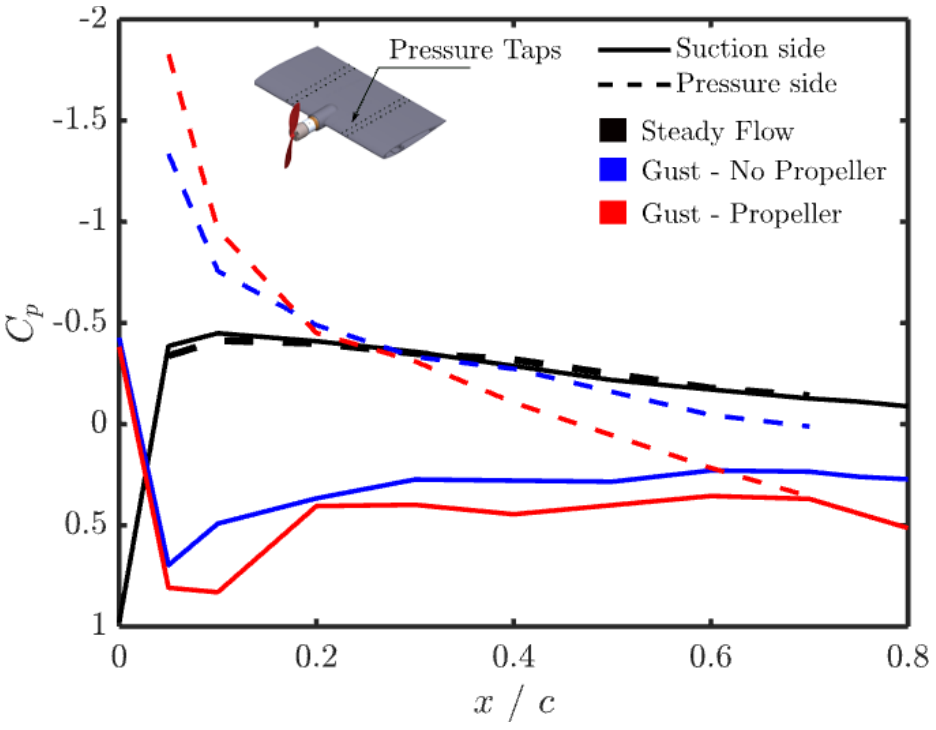

Figure 1 – Non-dimensional pressure coefficient distribution, Cp, over NACA0012 aerofoil in a one-minus-cosine gust interaction for . Gust was generated at 2Hz and 10° Amplitude at 10ms, with a propeller rotational speed of 7000RPM (Retreating Side)

AER/013: An Experimental Investigation of Active Leading-Edge Flow Control Mechanism

[1*]Modrzyński, Jan; [2] Çelik, Alper

[1,2] Faculty of Science and Engineering, Swansea University Bay Campus, Fabian Way, Swansea, UK

[1]jan.modrzynski@swansea.ac.uk, [2]alper.celik@swansea.ac.uk

,

With the growing interest in Urban Air Mobility (UAM) aircraft, where STOL and VTOL capabilities are essential, particular attention is currently being paid to developing new, highly efficient aerofoils. The Moving Surface Boundry Layer Control (MSBC) system has been proven to provide exceptional improvements compared to standard airfoils in literature. This study focuses on investigating the underlying mechanisms of the system by using 2D Particle Image Velocimetry (PIV) to study the flow field around the aerofoil. Building on the previous designs from the literature, a model equipped with four different cylinder geometries was tested at a chord-based Reynolds number of 200 000 and at three different speed ratios, i.e. surface speed of the cylinder to the free-stream velocity, of 0, 1 and 2. PIV results were supported by pressure and load measurements. The results show that the Scooped design performs better compared to other test cases and baseline. The stall angle is doubled with over 64% increase in lift compared to the baseline. Non-dimensional pressure distribution over the aerofoil shows significant increase at low angles of attack near the leading edge, which hasn't been observed in previous studies. Flow field results obtained from PIV experiments highlight the added momentum to the flow and underpins the improved performance. New methods of efficiency analysis were proposed, including histograms of the flow field to precisely capture all changes among the cases.

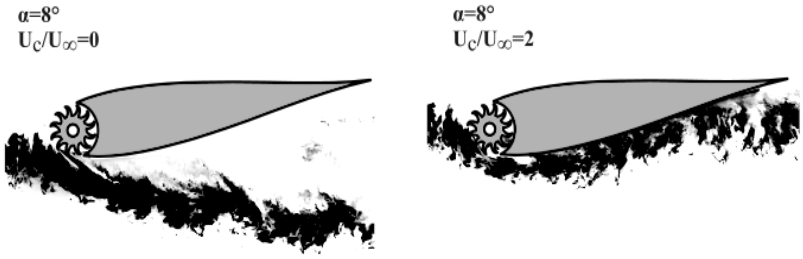

Figure 1. Smoke flow visualization of active leading-edge flow control mechanism in form of a scooped cylinder at 8° angle of attack and speed ratio U_c/U_∞ of 0 and 2.

AER/014: The effects of cascaded AC DBD-Plasma actuators with linear active electrode on the aerodynamic performance of a non-planar flying wing aircraft

Kontis, Konstantinos; *Eleghasim, Chigozie; Abbas, Hasan

Aerospace Sciences Division, James Watt School of Engineering, University of Glasgow

*Presenting Author

The dielectric barrier discharge plasma actuator is still attracting research attention because of its desirable active aerodynamic flow control features and wide application projections in aerospace. Since the exact description of the net volumetric body force induced by alternating current DBD actuator for momentum transfer is not yet available but experimental studies and numerical predictions show that the body force increases as a function of applied voltage and frequency, hence requires approximate description of the body force. This study presents the findings of multi-DBD actuators in cascaded formation with linear active electrode. The investigation applied an upgraded phenomenological model for DBD-Plasma actuator. Multi-DBD actuators are placed at different positions with different alignments on the suction sides of a non-planar flying wing model at low speed. Initially, the computational fluid dynamic simulation (CFD) results of single actuators in OpenFOAM software are validated with wind tunnel experiments. Finally, the CFD results of multi-DBD actuators show tremendous improvement on the aerodynamics of the flying wind model at low speed for angle of attack (AOA) between 0° and 24° considered.

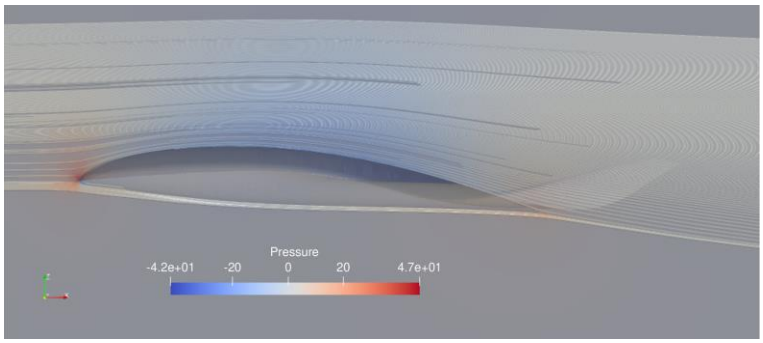

Figure 1: Pressure contour plots and streamlines result of the non-planar flying wing model at 0° AOA.

BIO: Biological flows including health applications (including biofluids)

BIO/001: A Systematic Review and Meta Analysis: How are Pathogens Distributed in Respiratory Emissions?

*[1]Blundell, D; [1]Noakes, C, [1]Fletcher, L; [1]King, M-F; [2]Lopez Garcia, M; [1]Hiwar, W

*Presenting Author Email: scdapb@leeds.ac.uk

[1]University of Leeds, School of Civil Engineering; [2]University of Leeds, School of Mathematics

Pathogen-laden aerosols are the mechanism of choice for a myriad of airborne transmissible diseases and present a significant health risk in the indoor environment. Much has been done to build a picture of the physics, biology, generation, and transport of these bioaerosols in the hopes of mitigating infection risk to those susceptible. However, the initial distribution of pathogens across different respiratory aerosol sizes remains unclear due to the demanding experimental challenges in measuring particle size segregation and working with microorganisms. This problem is further magnified when considering the role played by evaporation in the air and the implications aerosol and droplet sizes have on the transport of the pathogens to those susceptible. The systematic review aimed to extract and collate data from the current literature to answer the question: “What is the concentration of pathogens throughout the range of aerosol sizes produced in respiratory emissions?” The review employed a systematic methodology, as laid out by PRISMA, to identify and examine the experimental methods capable of measuring aerosol size segregation and the quantity of pathogens/microorganisms present across different sizes released during respiratory activities. The systematic review collated 55 papers from an initial 1247, reporting on a myriad of experiments utilising a range of different sampling techniques to measure data on pathogen concentration in human exhaled breath. To combine and quantify these findings, a meta-analysis on experiments used to quantify SARS-COV-2 and mycobacterium tuberculosis has been conducted. The analysis has made use of a novel model that incorporates particle size distributions emitted from the respiratory system by different respiratory activities. Initial results support the hypothesis that pathogens tend to be concentrated in smaller aerosols and suggests that pathogens are not distributed by a constant concentration by aerosol volume. This has important implications for modelling exposure using tools such as computational fluid dynamics, as a distribution by volume is the current assumption made by most studies.

BIO/002: A CFD ANALYSIS OF TOILET PLUME AEROSOL DISPERSION IN SHARED INDOOR TOILET FACILITIES

[1*] Higham, Ciara A.; [2] Noakes, Catherine J.; [3] López-García, Martín; [4] Fletcher, Louise A.

[1]C.A.Higham1@leeds.ac.uk; School of Civil Engineering, University of Leeds, Leeds, LS2 9JT,

[2]C.J.Noakes@leeds.ac.uk; School of Civil Engineering, University of Leeds, Leeds, LS2 9JT,

[3]M.LopezGarcia@leeds.ac.uk; School of Mathematics, University of Leeds, Leeds, LS2 9JT,

[4]L.A.Fletcher@leeds.ac.uk; School of Civil Engineering, University of Leeds, Leeds, LS2 9JT.

Toilet flushing in shared facilities can release droplets and aerosols into the surrounding air, known as the toilet plume. These aerosols may contain microorganisms as large as bacteria, leading to both airborne and surface contamination, with potential infection risks through inhalation or surface contact. Although expiratory aerosols have been widely studied, the behaviour and dispersion of toilet plume aerosols is less well understood.

This study uses Computational Fluid Dynamics (CFD), employing the Lagrange-Eulerian Discrete Phase Model (DPM) in ANSYS Fluent to simulate particle transport and fate following a toilet flush event. Particle sizes ranging from submicron aerosols to droplets up to 10 µm were modelled based on experimental size distributions. Simulations captured transient aerosol dynamics over a 10-minute post-flush period in a controlled mechanically ventilated chamber, testing three ventilation rates (1.5, 3, and 6 air changes per hour) and two spatial configurations: an isolated toilet (scenario 1) and a toilet within a cubicle (scenario 2).

Results show that higher ventilation rates improve overall particle removal after a 10-minute period but, in some instances, can increase exposure by dispersing particles into the breathing zone. Cubicle partitions alter airflow patterns, leading to prolonged particle suspension for all ventilation rates and an increase in surface deposition, highlighting the role of room layout in exposure risk.

Alternative ventilation strategies involving ceiling-mounted extract outlets positioned directly above the cubicles (adapted scenario 2) demonstrated improvements in aerosol removal efficiency. At 6 air changes per hour, 91% of particles were removed after 10 minutes with this strategy, compared to 48% in the baseline layout. These findings underscore the role of ventilation design in mitigating exposure to toilet plume aerosols.

This research provides insights for the design of shared toilet facilities in workplaces, healthcare settings, and public venues. By optimising ventilation rates and outlet placements, facility managers can significantly reduce aerosol transmission risks, supporting healthier indoor environments and informing future building designs and public health guidelines.

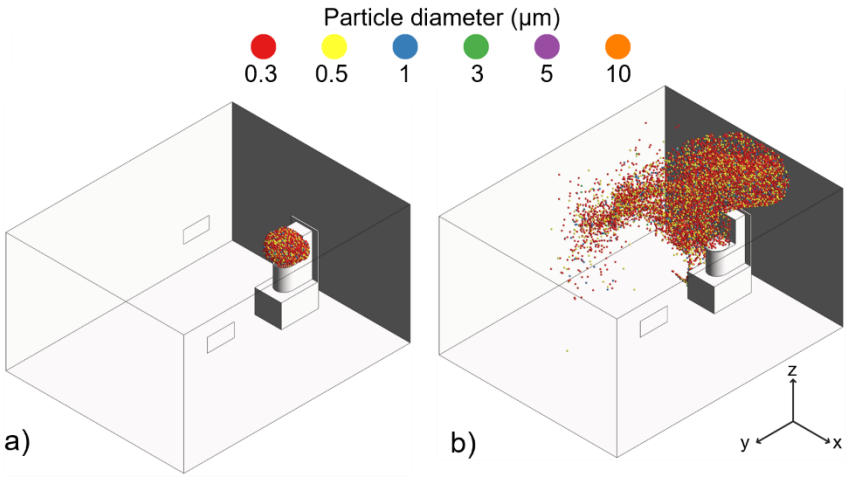

Figure 1. Particle locations (a) immediately after flushing and (b) 10 minutes post-flush for the isolated toilet scenario (scenario 1) under a low ventilation rate of 1.5 air changes per hour. For visual clarity, the number of particles displayed has been reduced by approximately half. All particle sizes are represented uniformly in size, with colours used to distinguish between different size categories.

BIO/003: The Role of Arteriovenous Graft Curvature in Haemodynamics: an Image-Based Approach

[1*]Wang, Guanqi; [1]Abadie, Thomas; [1]Esteban, Patricia Pérez

[1]School of Chemical Engineering, University of Birmingham. *Presenting Author

Vascular access, such as arteriovenous grafts, is crucial for patients undergoing haemodialysis as part of kidney replacement therapy. One of the primary causes of arteriovenous graft failure and loss of patency is disordered blood flow, as the vein is exposed to the arterial environment with high flow rates and shear stress. We hypothesize that secondary flow downstream of the vein-graft anastomosis plays a critical role in generating low shear regions, thereby promoting neointima hyperplasia. The secondary flow highlighted in the present study also promotes high oscillatory shear index regions downstream of the vein-graft anastomosis, further contributing to graft failure. Figure 1 illustrates the correlations between the failure areas. To our knowledge, no studies in arteriovenous haemodynamics have explicitly examined the impact of curved bends or the potential correlations between failure metrics and such geometric features. To prolong the overall graft survival and patency, we aim to develop a strategy to optimize graft configurations with reduced levels of disturbed haemodynamics. We developed an image-based approach to build three-dimensional geometries for subsequent computational fluid dynamics (CFD) numerical simulations. This simple, yet accurate, method allowed us to improve the accuracy of geometries, thus facilitating comparisons between different vein-graft anastomotic angles.

Our results reveal that overall graft curvature (looped vs. straight) plays a dominant role in characterising the failure metrics. Looped grafts, particularly at moderate vein-graft anastomotic angles (30°-45°), exhibited the most favourable metrics, including reduced values of low wall shear stress, high wall shear stress, and high oscillatory shear index. These findings provide critical insights to inform medical professionals about graft areas that are subject to high shear stresses due to the oscillating nature of blood flow as well as the graft geometric configuration when performing surgery. The model developed in this work offers a framework enabling personalized vascular access strategies tailored to individual patient needs.

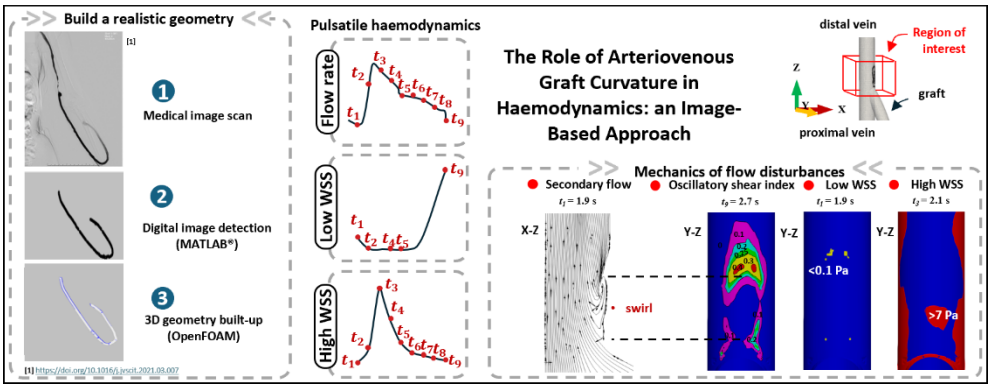

Figure 1. The correlations between the failure areas and the Dean vortice at the curved bend of the vein-to-graft anastomosis

BIO/004: Developing numerical tools to improve the diagnosis of peripheral artery disease - *POSTER*

[1]*Barratt, Luke; [2]Somani, Yasina; [3]Benson, Al; [4]Lassila, Toni; [5]Bailey, Marc

[1]University of Leeds, LS2 9JT and scljb@leeds.ac.uk.

[2]University of Leeds, LS2 9JT and Y.Somani@leeds.ac.uk.

[3]University of Leeds, LS2 9JT and A.P.Benson@leeds.ac.uk.

[4]University of Leeds, LS2 9JT and T.Lassila@leeds.ac.uk.

[5]University of Leeds, LS2 9JT and M.A.Bailey@leeds.ac.uk.

*Presenting Author

Peripheral artery disease (PAD) is an age-related condition present in >10% of adults over 65 years [Houghton et al, 2024] and is characterized by atherosclerotic narrowing of arteries classically affecting the legs. This reduces oxygen delivery to skeletal muscle and leads to pain during walking (intermittent claudication, IC) [Fowkes et al, 2013]. Early diagnosis of PAD is key to reducing risk of cardiovascular events; a risk that is 2-fold greater in PAD than in those with stable coronary artery disease [Sprenger et al, 2021]. The gold-standard diagnostic method for PAD is the ankle-brachial index (ABI; the ratio of leg to arm systolic blood pressure), sometimes supplemented with ultrasound, MRI or CT [Parwani, 2023]. However, traditional diagnostic methods do not always detect PAD, particularly in patients with calcified arteries or atypical presentations often occurring in women. As a result, PAD frequently remains underdiagnosed and undertreated compared with other cardiovascular disease conditions [Pabon et al, 2022].

To address the limitations of current diagnostic methods, we are developing numerical methods to improve risk prediction algorithms by assessing factors local to the occluded limbs. Two mathematical models are being developed that can assess the two physiological functions responsible for IC: blood flow in the leg and oxygen utilisation in skeletal muscle. The first is a 1D haemodynamic model which uses 1D Navier-Stokes for flow in compliant tubes, solved with finite element methods using FEniCS [Logg et al, 2012]. This simulates arterial networks and the impact of atherosclerotic plaques on blood transport. The peripheral resistances at terminal branches are represented by Windkessel models. The second model is a mathematical representation of oxygen transport and utilisation within skeletal muscle, driven by the inflow rates provided by the haemodynamic model. It includes a system of coupled differential equations representing oxygen transport in capillary networks and muscle fibres and cellular metabolism [Lai et al, 2009]. The models will be validated using ultrasound and near-infrared spectroscopy during transition to light exercise. Future work will extend the flow model to include shear-dependent vascular function, enabling the capture of endothelial cell dysfunction involved in vessel contraction and dilation.

These two coupled models will be used to assess the impact of vascular anatomy and function, plaque development, and muscle metabolism on oxygen dynamics. This will help identify key causes of IC in PAD patients and support targeted strategies for improved diagnosis.

Houghton, J. S. M., Saratzis, A. N., Sayers, R. D., & Haunton, V. J. (2024). New Horizons in Peripheral Artery Disease. Age and Ageing, 53(6), afae114.

Fowkes, F. G. R., Rudan, D., Rudan, I., Aboyans, V., Denenberg, J. O., McDermott, M. M., Norman, P. E., Sampson, U. K. A., Williams, L. J., Mensah, G. A., & Criqui, M. H., 2013, Comparison of global estimates of prevalence and risk factors for peripheral artery disease in 2000 and 2010: a systematic review and analysis. The Lancet, 382(9901), pp. 1329–1340.

Sprenger, L., Mader, A., Larcher, B., Mächler, M., Vonbank, A., Zanolin-Purin, D., Leiherer, A., Muendlein, A., Drexel, H., & Saely, C. H. (2021). Type 2 diabetes and the risk of cardiovascular events in peripheral artery disease versus coronary artery disease. BMJ Open Diabetes Research & Care, 9(2), e002407.

Parwani, D., Ahmed, M. A., Mahawar, A., & Gorantla, V. R. (2023). Peripheral Arterial Disease: A Narrative Review. Cureus, 15(6), e40267.

Pabon, M., Cheng, S., Altin, S. E., Sethi, S., Nelson, M. D., et al. (2022). Sex differences in peripheral artery disease. Circulation Research, 130(4), 496–511.

Logg, A., Mardal, K.-A., Wells, G. N., et al., 2012, Automated Solution of Differential Equations by the Finite Element Method. Springer.

Lai, N., Zhou, H., Saidel, G. M., Wolf, M., McCully, K., Gladden, L. B., and Cabrera, M. E., 2009, Modeling oxygenation in venous blood and skeletal muscle in response to exercise using near-infrared spectroscopy. Journal of Applied Physiology, 106(6), pp. 1858–1874.

BIO/005: Inhaler aerosol transport in lung airways with two-way and four-way coupling

[1*]Williams, Josh; [2]Wolfram, Uwe; [3]Ozel, Ali

[1]Hartree Centre, STFC Daresbury Laboratory, Warrington, UK (josh.williams@stfc.ac.uk). [2]Institute for Material Science and Engineering, TU Clausthal, Clausthal-Zellerfeld, Germany. [3]School of Engineering and Physical Sciences, Heriot-Watt University, Edinburgh, UK. *Presenting Author

Inhalers transport drugs as aerosolised solid particles or liquid droplets (henceforth called 'particles'), by spraying a large number of particles ($N_p > 10^8$ for a 100 µg dose) into the airways. We expect this spray to create a significant momentum transfer between particle and gas phases. Due to the large computational resources required to simulate 10^8 particles for realistic dosages of 50 − 100 µg, the effect of fluid-particle interaction modifying fluid transport (two-way coupling) or particle-particle interaction (four-way coupling) on deposition has not been studied previously. In this study, we aimed to evaluate the influence of a realistic number of particles with two-way and four-way coupling on deposition. We used the multiphase particle-in-cell[1] OpenFOAM solver MPPICFoam to track fluid and particle motion in patient-specific airways from a healthy adult male patient[2]. Particle motion is computed by Newton's equations of motion including drag force and gravity. Four-way coupled simulations also include contributions of the particle-phase granular pressure[3], computed on the fluid grid and interpolated to the particles. We studied particle diameters d_p = 4 − 20 µm at doses 10, 50 and 100 µg. For the case of d_p = 10 µm, the number of particles was 16×10^6, 80×10^6, 160×10^6 for a dosage of 10, 50, 100 µg, respectively. We observed a significant increase in deposition fraction for all particle sizes. Compared to one-way coupled simulations, deposition with d_p = 10 µm and 100 µg was 2.6 times larger. Four-way coupling effects became important at 100 µg, causing a decrease in deposition. These findings show that future deposition simulations must include four-way coupling to accurately predict drug transport and deposition that will be used for tailoring of clinical treatments.

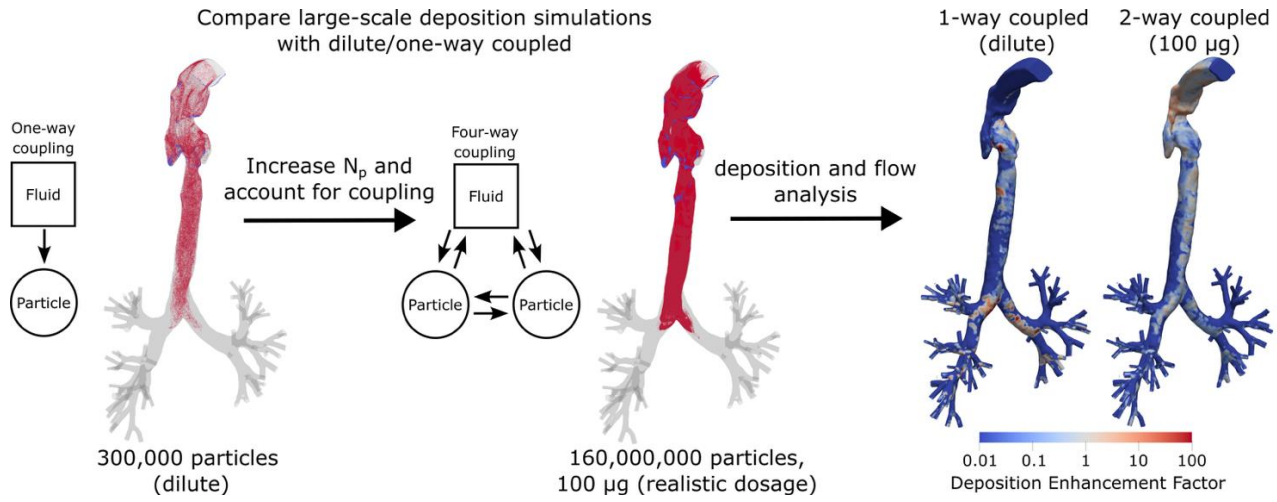

Figure 1. Overview of the study, showing comparison between one-way coupled approach widely used in literature under the assumption of dilute flow with a realistic number of particles (160 million), where two-way and four-way coupling are influential. This leads to an enhanced deposition in the upper airways (mouth) and more uniform deposition pattern.

[1] Snider, D. M., Journal of computational physics, Vol. 170, No. 2, 2001, pp. 523–549. [2] Williams, J. et al., International Journal of Pharmaceutics, Vol. 612, 2022, pp. 121321. [3] Harris, S. and Crighton, D., Journal of Fluid Mechanics, Vol. 266, 1994, pp. 243–276.

BIO/006: A theoretical maximum for bacterial surface adhesion in fluid flow: an active Lévêque boundary layer

E.Yeo, B. Walker, P. Pearce, M.P. Dalwadi

The mitigation of bacterial adhesion to surfaces and subsequent biofilm formation is a key challenge in healthcare and manufacturing processes. To accurately predict biofilm formation you must determine how changes to bacteria behaviours and dynamics alter their ability to adhere to surfaces. In this work we examine the flow of a dilute suspension of motile bacteria over a flat absorbing surface, developing an effective model for the bacteria density near the boundary inspired by the classical Lévêque boundary layer problem. We use our effective model to derive analytical solutions for the bacterial adhesion rate as a function of fluid shear rate and individual motility parameters of the bacteria, validating against numerical simulations of individual bacteria. We find that bacterial adhesion is greatest at intermediate flow rates, since at higher flow rates shear-induced upstream swimming limits adhesion.

BIO/007: Predicting Retinal Haemorrhage Following Retinal Vein Occlusion

[1*]Bhattacharya Atrayee; [2]Stewart, Peter; [3]Gao, Hao; [4]Husmeier, Dirk

[1]University of Glasgow and a.bhattacharya.2@research.gla.ac.uk. [2]University of Glasgow and Peter.Stewart@glasgow.ac.uk

*Presenting Author

The retina is the layer of sensory tissue that lines the interior surface of the human eye. The retinal cells are nourished by a dense network of blood vessels which enter and exit through the optic nerve. Retinal vein occlusion is a blockage in one of the veins of the retinal circulation, which can subsequently lead to retinal haemorrhage. Such blockages often occur at points of arterio-venous crossing where the retinal vein and artery share a common sheath; gradual swelling of the artery (due to arteriosclerosis) results in compression of the adjacent vein, narrowing the blood vessels, damaging their wall and eventually leading to a venous thrombus [1]. We aim to understand how occlusion in one vessel can lead to haemorrhage in distant parts of the network using a combination of cutting-edge image analysis and mathematical modelling based on continuum mechanics. The clinical images suggest that bursting of vessels can occur several generations upstream of the site of arterio-venous crossing. To investigate this observation, we consider a model retinal network with a locally applied (external) perturbation to mimic a thrombus, and examine when this perturbation can lead to a rapid expansion of a vessel upstream of the occlusion site. We find that wave propagation only plays a significant role on timescales much faster than the typical timescale of thrombus growth. Instead, the rapid expansion of upstream vessels is more clearly aligned with the accumulation of blood upstream of the constriction due to the reduced outflow.

[1] Hayreh SS. Retinal vein occlusion. Indian J Ophthalmol. 1994 Sep;42(3):109-32. PMID: 7829175.

BIO/009: THE HYDRODYNAMIC INTERACTION OF A PAIR OF SEDIMENTING SEMI-FLEXIBLE BROWNIAN FIBRES

[1*]Hajaliakbari, Nasrollah; [1]Head, David; [2]Harlen, Oliver

[1] School of Computer Science, Faculty of Engineering and Physical Science, University of Leeds, Leeds, UK, scnhv@leeds.ac.uk. d.head@leeds.ac.uk. [2] School of Mathematics, Faculty of Engineering and Physical Science, University of Leeds, Leeds, UK, o.g.harlen@leeds.ac.uk. *Presenting Author

The sedimentation of a collection of semiflexible fibres is a vital process in producing a range of materials and composites such as paper and fibre-reinforced composites. Due to the Brownian, gravitational and hydrodynamic forces, fibres undergo various deformations, translations and rotations. A predictive numerical tool that can evaluate the dynamics of these fibres would be useful in the design of novel fibre materials.

In this study, the Rotger-Prager-Yamakawa (RPY) singularity representations have been used to accurately capture the fluid-structure interaction of multiple fibres, including the case when the nonlocal hydrodynamic interactions add more complexities to the problem. In addition, a continuum model based on the Oseen approximation was introduced to evaluate the early time dynamics for rigid fibres to compare its results against the numerical RPY model.

For a pair of semi-flexible fibres in various initial geometries, we firstly determine whether the system belonging to hydrodynamic-dominated or Brownian-dominated regimes. We then quantify the temporal dynamics of the system and showed that the early time behaviour agrees the prediction of the continuum model. For late times, we evaluated the final sedimentation velocity and the fibre configuration as measured by the gyration tensor. We conclude by discussing possible future for this accurate numerical approach.

BIO/011: Characterizing Zipping-Driven Fluid Flow in Soft Electrostatic Actuators

[1]Ahmad, Faisal; [1]Brandenbourger, Martin, [2]Marthelot, Joël

[1]CNRS, Aix-Marseille Univ, Centrale Marseille, IRPHE (UMR 7342), Marseille, France [2]IIUSTI, CNRS Aix-Marseille University, France

Soft hydro-electronic systems offer a novel approach to designing soft robotics compared to conventional rigid robots. These systems operate on the principle of capacitors and typically consist of soft thin films, a liquid dielectric, and electrodes. When a voltage is applied, electrostatic forces induce muscle-like linear contraction, known as the zipping mechanism. Previously, small-scale HASELs (hydraulically amplified self-healing electrostatic actuators), typically around 15 cm in length, have been studied to achieve limited fluid displacement [1,2].

In this study, we investigate fluid transport in larger rectangular channels (length≈100 cm) to characterize the effect of varying voltage and electrode width on zipping-induced flow. Actuation begins at the end of the channel where the electrode spacing is minimal. Upon applying a voltage, electrostatic forces deform the channel along the entire electrode length, generating unidirectional fluid transport. We used high-speed camera imaging to track the evolution of the zipping front over time. Further, we also studied the dynamics of the two and three zipping fronts meeting at a junction.

We hypothesized that the zipping front position would follow a first-order exponential model due to viscous damping from the dielectric fluid. By balancing electrostatic and viscous forces, we confirmed this behavior experimentally. Furthermore, we found that the zipping dynamics are independent of fluid volume and electrode width, and can be rescaled with applied voltage.

This study advances the understanding of electrohydraulic actuation dynamics and supports the development of scalable, geometry-independent soft actuators.

Figure 1.

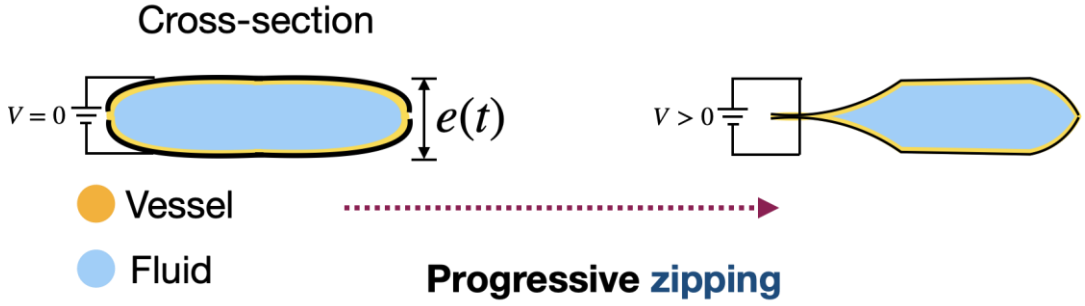

1 - Mitchell et al. ”An easy-to-implement toolkit to create versatile and high-performance HASEL .” Advanced Science (2019).

2 - Sırbu et al. ”Electrostatic actuators with constant force.” Nature Electronics (2023)

CFD: Computational fluid dynamics

CFD/002: IMPROVING ACCURACY IN HYBRID RANS–LES FOR FLOW OVER A HEMISPHERE WITH SYNTHETIC EDDY FORCING

[1*]Yudianto, Aan; [2]Revell, Alistair; [2]Harish, Ajay; [2]Razaeiravesh, Saleh; [2]Quinn, Mark

[1]Modelling and Simulation Centre, The University of Manchester, UK. email: aan.yudianto@postgrad.manchester.ac.uk *Presenting Author

This study investigates the influence of synthetic turbulence generation on hybrid RANS–LES simulations by employing the Synthetic Eddy Method (SEM) in the flow around a wall-mounted hemisphere at a Reynolds number of $Re_D = 50{,}000$ based on the hemisphere diameter. The simulations are conducted with prescribed inflow conditions to replicate the experimental setup and match available high-fidelity Large Eddy Simulation (LES) reference data. A series of turbulence models are assessed, including the standard Delayed Detached Eddy Simulation (DDES) based on maximum grid length scale (Δ_{max}), DDES with shear layer adaptation (Δ_{SLA}), and Improved DDES (IDDES) also using both Δ_{max} and SEM-augmented variants. All models use the $k-\omega SST$ formulation for the RANS background. Results show that in the absence of SEM, all models experience a delayed onset of turbulence near the separation region, leading to underprediction of turbulent mixing and flow reattachment. Incorporating SEM substantially enhances the accuracy of the hybrid simulations by triggering earlier and more realistic transition to resolved turbulence. Notably, SEM improves agreement with experimental and LES data in terms of mean velocity profiles, Reynolds stresses, and turbulence intensity distributions. Accurate implementation of SEM requires modifying the blending function to enforce$f_d = 1$ in order to activate synthetic turbulence consistently within the LES zone. Comprehensive comparisons of the flow field are presented, including streamwise velocity contours, streamlines in the symmetry plane and near-wall region, and skin friction coefficient distributions. Key flow features such as the reattachment point, separation location, stagnation region, and horseshoe vortex formation are also analysed. Across all metrics, the application of SEM leads to improved correspondence with reference data, especially in capturing near-wall behaviour and complex vortical structures. The study demonstrates that synthetic turbulence forcing is a critical component for enhancing the predictive capability of hybrid RANS–LES methods, particularly for bluff body flows where shear layer development and separation dynamics are essential. These findings provide guidance for accurate hybrid modelling and highlight the importance of inflow condition treatment in external aerodynamic simulations.

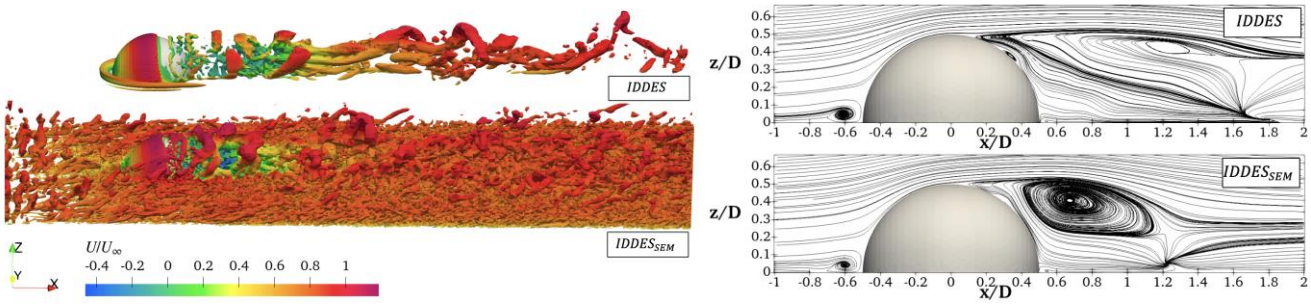

Figure 1. Isosurface base on Q-criterion comparison between IDDES without and with SEM (left) and streamlines comparison at symmetry plane calculated by IDDES and IDDES with SEM (right). The use of SEM significantly enhances the simulation accuracy.

CFD/003: TURBULENT DRAG-REDUCTION VIA PIEZOELECTRIC REALISTIC WAVES

[1*]Amjadimanesh, Amir; [2]Kidanemariam, Aman; [3]Chappel, David; [4]Bodaghi, Mahdi; [5]Rouhi, Amirreza

[1*] Nottingham Trent University, amir.amjadimanesh@ntu.ac.uk. [2]University of Melbourne, Aman.Kidanemariam@unimelb.edu.au. [3]Nottingham Trent University, david.chappell@ntu.ac.uk. [4]Nottingham Trent University, mahdi.bodaghi@ntu.ac.uk. [5]Nottingham Trent University, amirreza.rouhi@ntu.ac.uk.

We study drag reduction (DR) in turbulent open-channel flow through piezoelectric surface actuation. The actuated surface is modeled as a thin aluminum sheet with piezoelectric patches bonded beneath it. Finite Element Analysis is employed to simulate the resulting deformations, which consist of out-of-plane, multi-frequency standing and streamwise-travelling waves. These deformations show strong agreement with semi-analytical predictions from Euler–Bernoulli beam theory. A dimensional analysis links the actuation parameters—such as piezoelectric layout, material properties, and electrical signals—to the resulting deformation characteristics, including modal frequencies (ω_i), wavelengths (λ_i), and amplitudes (η_i). Unlike most numerical studies, we do not treat surface deformation parameters as independent inputs; instead, we model the physical coupling between actuation inputs and surface response. The deformation characteristics are non-dimensionalised using viscous scales, based on the experimental setup described by Ding et al. (2024). These surface deformations are applied as bottom boundary conditions in Direct Numerical Simulations of turbulent open-channel flow at a friction Reynolds number of $Re_\tau = 200$, using a validated curvilinear boundary-deforming solver. A range of actuation configurations is explored to generate both upstream (UTW) and downstream (DTW) travelling waves, covering the frequency range $-0.3 < \omega_1^+ < 0.6$ and amplitude range $2 < A_1^+ < 34$. A peak drag reduction of 7% is achieved for DTWs at $\omega_1^+ = 0.3$ and $A_1^+ = 15$. Further increases in amplitude lead to reduced DR, a trend associated with the weakening of near-wall streaks in the buffer layer ($y^+ \approx 15$).

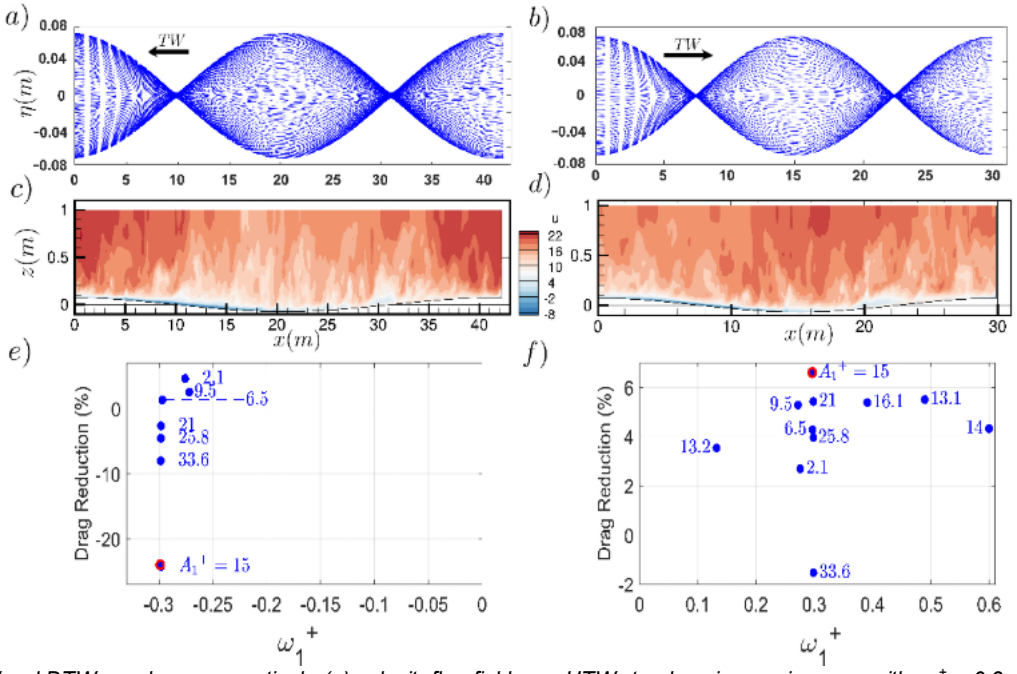

Figure 1. (a,b) UTW and DTW envelops, respectively. (c) velocity flow field over UTW at a drag-increasing case with ω_1^+= -0.3, A_1^+= 15, DR = -24% (as marked in e). (d) velocity flow field over DTW at an optimal drag-reducing case with ω_1^+= 0.3, A_1^+= 15, DR = 7% (as marked in f), respectively. (e,f) drag reduction versus dominant angular frequency for the UTW and DTW, respectively.

CFD/004: EFFECT OF TURBULENCE MODELS ON NUMERICAL MODELLING OF FLOW AROUND A WAVE ENERGY CONVERTER LOCATED IN A MARINA

[1*]Yildiz, Burhan; [1]Dapelo, Davide; [1]Bashir, Musa

[1]University of Liverpool, School of Engineering, L69 3BX Brownlow Hill, Liverpool burhan.yildiz@liverpool.ac.uk. *Presenting Author

Wave energy is a promising renewable energy source, offering higher power intensity, availability and predictability compared to solar and wind energies (López et al. 2013). Despite ongoing research demonstrating significant advances in wave energy extraction through wave energy converters (WECs), their deployment remains limited, with only a few examples worldwide. This limited adoption is largely due to economic and engineering challenges—particularly those associated with deploying WECs in open seas, where costs increase significantly due to the need for mooring systems and underwater electrical cabling (Astariz & Iglesias 2015). In addition, harsh marine conditions can cause structural damage or loss of devices. Installing WECs in more sheltered environments, such as marinas, can mitigate these risks and costs. However, wave energy intensity is significantly lower in such locations, raising concerns about the feasibility of these projects (Foteinis 2022).

Accurately predicting the motion of WECs is essential for estimating their power output, which relies on hydrodynamic modelling. The accuracy of the results depends on the type of numerical model used, which can range from low-fidelity approaches (e.g., potential flow assumptions) to high-fidelity methods such as computational fluid dynamics (CFD), depending on the flow conditions. In marina settings, the proximity of WECs to vertical walls and other boundaries increases flow complexity through enhanced vorticity. This makes low-fidelity models—which are often favoured for their computational efficiency but typically neglect turbulence or vorticity—less suitable for accurate simulations in such environments.

In this study, a CFD model based on finite-volume method was employed to simulate flow around a cylindrical WEC beside a vertical wall (Figure 1). The simulations were carried out using the OpenFOAM software and its interFoam solver module. A morphing mesh technique was implemented to capture the oscillating motion of the WEC. The Reynolds-Averaged Navier-Stokes (RANS) equations were solved using the k-ε and k-Ω SST turbulence models, which are the two most widely used ones in this field (Windt et al. 2020). Several computational mesh alternatives were developed to assess model performance and ensure reliability. Verification of the models included testing the convergence of turbulence-related quantities—an approach that is rarely applied in existing literature.

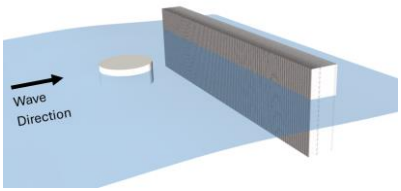

Figure 1. Schematic representation of a cylindrical WEC beside a vertical wall

López, I., Andreu, J., Ceballos, S., De Alegría, I. M., & Kortabarria, I. (2013). Review of wave energy technologies and the necessary power-equipment. Renewable and sustainable energy reviews, 27, 413-434.

Astariz, S., & Iglesias, G. (2015). The economics of wave energy: A review. Renewable and Sustainable Energy Reviews, 45, 397-408.

Foteinis, S. (2022). Wave energy converters in low energy seas: Current state and opportunities. Renewable and Sustainable Energy Reviews, 162, 112448.

Windt, C., Davidson, J., & Ringwood, J. V. (2020). Investigation of turbulence modeling for point-absorber-type wave energy converters. Energies, 14(1), 26.

CFD/005: Flow transition over surface gaps in incompressible laminar boundary layers

[1*]Víctor Ballester Ribó; [2]Jeffrey Crouch; [1]Yongyun Hwang; [1]Spencer Sherwin

[1]Department of Aeronautics, Imperial College London, UK. [2]The Boeing Company, USA. *Presenting Author

Aircraft wings are not perfectly smooth; they often have spanwise gaps due to manufacturing tolerances, structural components, or control surface discontinuities. These geometric irregularities can significantly influence boundary layer transition, potentially affecting aerodynamic performance and efficiency. In this study, we investigate the interaction between such gaps and the transition process, with a particular emphasis on the enhanced amplification of Tollmien-Schlichting waves and bypass mechanisms. Specifically, we examine the role of gap-induced modes in triggering or enhancing natural boundary layer instabilities [1]. The analysis is conducted at low Mach number under incompressible flow conditions at a Reynolds number of $Re_{\delta^*} = 1000$, where δ^* denotes the displacement thickness measured at the upstream edge of the gap on a smooth surface free of discontinuities. The depth of the gaps considered lies in the interval $d / \delta^* = 1\text{-}4$, while the width is varied within the range $w / \delta^* = 10\text{-}30$ to assess the onset of global instability. High-fidelity numerical simulations are performed using the spectral/hp element method implemented in the open-source framework Nektar++ [2]. The results provide new insights into the transition mechanisms induced by geometric discontinuities, contributing to the design of more aerodynamically efficient wings. Future work will extend the study to compressible flow regimes and three-dimensional configurations to account for sweeping effects.

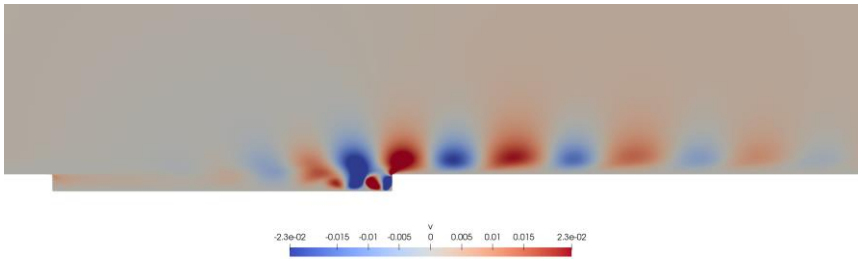

Figure 1. v-component of the flow field illustrating an absolute instability near the downstream edge of a gap of dimensions $d = 2\delta^*$ and $w = 40\delta^*$, where δ^* denotes the displacement thickness of the boundary layer.

References:

[1] Crouch JD, Kosorygin VS, Sutanto MI, Miller GD. Characterizing surface-gap effects on boundary-layer transition dominated by Tollmien Schlichting instability. Flow. 2022;2:E8. doi:10.1017/flo.2022.1

[2] Nektar++. https://www.nektar.info/. Accessed: 29/05/2025.

CFD/006: Turbulent drag decomposition over porous substrates

[1*]Faure, Noe; [1]Garcia-Mayoral, Ricardo

[1]Department of Engineering, University of Cambridge, Trumpington Street, Cambridge CB 1PZ, UK.
Corresponding author: Ricardo Garcia-Mayoral, r.gmayoral@eng.cam.ac.uk ; *Presenting Author : nf399@cam.ac.uk

While roughness generally increases drag, small anisotropic permeable textures have been proposed to reduce drag while leaving the turbulence smooth wall-like. The efficiency of these surfaces is limited to small texture sizes due to the appearance of additional flow features disrupting the near-wall cycle. This is set by the competing contributions of a known drag-reducing slip effect and by adverse mechanisms which we do not fully understand, both of which increase with texture size. We anticipate that the prevalent features will be Kelvin-Helmholtz rollers and a texture-coherent flow, whose effect on the flow is drag-degrading.

Our understanding of these mechanisms is nonetheless partial and the respective contributions of each flow component to the drag-degradation are difficult to evaluate.

When the texture scale is much smaller than that of the near-wall cycle, the footprint of the texture-induced flow on the energy spectra appears distinct from the background turbulence. The footprint of the latter can nonetheless be altered even when the separation of scales holds, indicating a non-linear interaction. As the signature of the Kelvin-Helmholtz rollers and the near-wall cycle overlap, spectral filtering is to be used cautiously.

Motivated by this, we have conducted fully resolved direct numerical simulations (DNS) of turbulence in the 'transitionally rough' regime, where the physics are not well understood and also where the optimal performance for drag-reducing surfaces occurs. Using temporal information from the advection velocities, we decompose the flow into three components (an amplitude-modulated texture-induced flow, Kelvin-Helmholtz rollers and the background turbulence) and quantify their respective contribution to the total Reynolds stress.

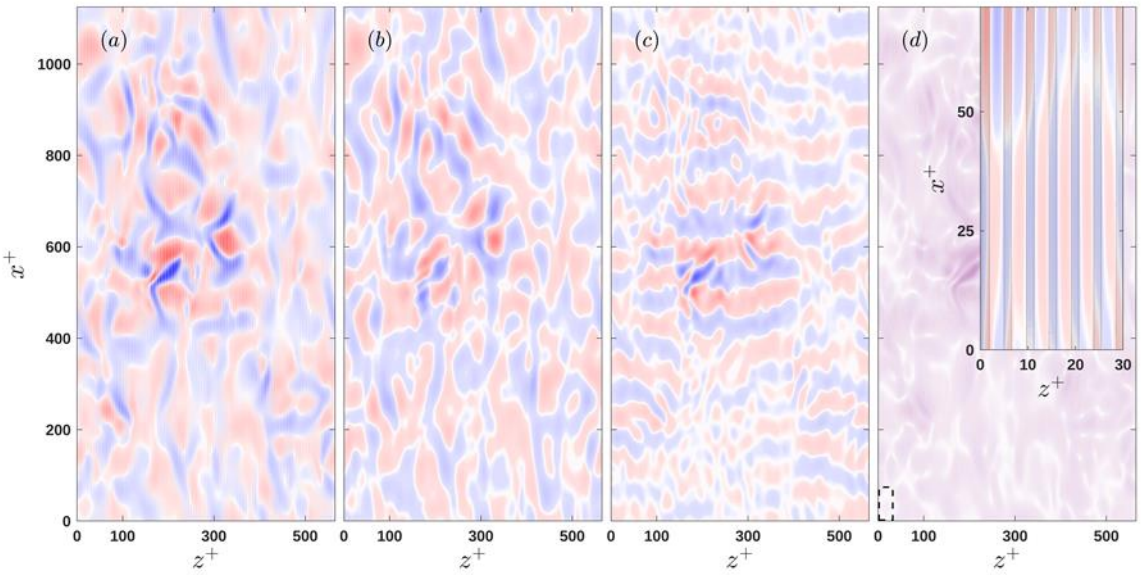

Figure 1 : Instantaneous realisation of the v component at $Re_\tau = 180$ at $y^+ \approx 0.5$ over an anisotropic permeable substrate of pitch $L^+ \approx 5$. a) Full signal b) Filtered background turbulence c) Kelvin-Helmholtz rollers d) Amplitude-modulated texture-coherent flow with dashed region magnified in the inset. Colours range from red to blue $v = [-1,1]u_\tau$ and $v = [-0.25,0.25]u_\tau$ for the inset.

CFD/007: Evaluating Neighbor Search Algorithms in SPH: A Comparison between Cell-Linked List and cKDTree

Tang, Yanchi

1st year PhD student

University of Liverpool, Brownlow Hill, Liverpool, L69 7ZX.

Tyc@liverpool.ac.uk

In Smoothed Particle Hydrodynamics (SPH) simulations, neighboring particle search conducted at every timestep is computationally intensive. The cell linked list (CLL) method is widely used in engineering SPH for its simplicity and efficiency in uniformly distributed systems. Alternatively, k-d trees, commonly applied in astrophysical SPH, are used to address highly inhomogeneous particle distributions or variable smoothing lengths. However, their performances in engineering SPH context remain unclear.

This study compares the performance of CLL and k-d tree algorithms through single-phase SPH benchmarks. Both methods are analyzed for search time and memory behavior for a wide range of numbers of SPH particles in Python. Although previous literature suggests that k-d trees may outperform CLL in small-scale 2D cases, our results show that an optimized CLL consistently outperforms across number of particles up to two million. At larger scales, performance becomes more nuanced, reflecting a stronger interplay between algorithmic structure and implementation choices.

CFD/008: NUMERICAL MODELLING OF NON-NEWTONIAN LAMINAR FLOW IN PARTIALLY FILLED PIPES

[1*]Federico, Peruzzini, [2]Jonathan M., Dodds, [2]Christopher J., Cunliffe, [1]Henry C.-H, Ng, [1]Robert J., Poole

[1] School of Engineering, University of Liverpool, Liverpool L69 3GH, United Kingdom (f.peruzzini@liverpool.ac.uk, robpoole@liverpool.ac.uk).

[2] United Kingdom National Nuclear Laboratory, Workington CA14 3YQ, United Kingdom.

*Presenting Author

Flow prediction of partially filled pipes is a challenging task for non-Newtonian fluids, which is essential for many industrial applications, such as pharmaceuticals, nuclear energy, and mining. Particularly in the nuclear industry, liquid waste is generated during reprocessing and decommissioning operations. Typically, the waste is in the form of a slurry containing solid particles suspended in a shear-thinning matrix, which requires careful handling during the extraction and transportation processes. Generation and disposal of nuclear waste are among the greatest challenges for the nuclear industry, and improving waste treatment strategies will enhance safety and protect the environment (Paul et al., 2013).

This research presents a Computational Fluid Dynamics (CFD) study to improve understanding and modelling of these specific flow conditions. Our methodology involved simulating non-Newtonian fluid behaviour using a power-law model with various flow behaviour indices (n), as well as the Cross model with different Carreau numbers (Cu). The simulations were conducted in laminar flow at 14 different fill heights, ranging from 25% to 95% of the pipe diameter, with a $Re = 1$ and $Fr = 0.15 - 0.55$ (subcritical flow).

A rigorous validation process has been used, which involved benchmarking the simulations against Newtonian CFD results (validated with analytical solutions for partially-filled pipes by Guo, 2013), Particle Image Velocimetry (PIV) experimental data for similar Newtonian flows (Ng et al., 2018), and analytical solutions for full-pipe non-Newtonian (power-law) flow (Barnes et al., 1989).

This study will contribute to an improved understanding of the fluid dynamics governing these complex systems. Results will contribute to improved predictive capabilities, critical to optimising slurry transportation operations and supporting safety assessments essential to the UK's nuclear decommissioning program.

Paul, Neepa, et al. "Characterising highly active nuclear waste simulants." Chemical Engineering Research and Design 91.4 (2013): 742-751.

Guo, Junke, and Robert N. Meroney. "Theoretical solution for laminar flow in partially-filled pipes." Journal of hydraulic research 51.4 (2013): 408-416.

Ng, Henry C-H., et al. "Partially filled pipes: experiments in laminar and turbulent flow." Journal of Fluid Mechanics 848 (2018): 467-507.

Barnes, Howard A., John Fletcher Hutton, and Kenneth Walters. An introduction to rheology. Vol. 3. Elsevier, 1989.

CFD/009: Analysis of Turbulence in Open Channel Flows using Direct Numerical Simulations

[1*]Malkeson, Sean; [2]Brearley, Peter; [3]Ahmed, Umair

[1]Liverpool John Moores University, UK, s.p.malkeson@ljmu.ac.uk. [2]Imperial College London, UK, p.brearley@imperial.ac.uk. [3]Newcastle University, UK, umair.ahmed@newcastle.ac.uk

Turbulence close to approximately flat, shear-free surfaces (i.e., below a critical Froude number [Nezu & Nakagawa (1993)]) is found in flows of engineering and environmental relevance (e.g., for tidal stream turbines). Understanding turbulent structures and their effects on the flow field is key for maximising tidal energy extraction and device lifetime. Given the drive to net-zero power generation, an increased understanding of turbulence near shear-free surfaces is essential for improving the design of tidal energy extraction devices. Closed and open channel flows have previously been examined with studies considering Direct Numerical and Large Eddy Simulations of open channel flows [Taylor et al. (2005), Walker et al. (2014), Pirozzoli (2023), Ahmed et al. (2021)]. Understanding the behaviour of turbulent features, including the integral length scale and the velocity structure functions, is limited for different Re_τ conditions. This information is needed for the accurate estimation of the bending moments experienced by tidal energy extraction devices.

In this study, a database of open channel flow DNS isothermal cases ($Re_\tau = 180,\ 400,\ 1000,\ 2000$) has been developed using the 3D, incompressible solver, Xcompact3d [Laizet & Lamballais (2009), Bartholomew et al. (2020)]. Figure 1a shows the considered configuration and Fig. 1b provides instantaneous u velocity contours on the central x-z plane for the $Re_\tau = 180$ fully developed case. The flow is driven by a uniform pressure gradient aligned with the x axis and is fully developed. The average pressure gradient is related to the average shear stress ρu_τ^2 as $-\partial\bar{p}/\partial x = \rho u_\tau^2/h$ where ρ is density, p is pressure, h is channel height, $u_\tau = \sqrt{\tau_w/\rho}$ is friction velocity and $\tau_w = \mu(\partial\tilde{u}/\partial x)_{y=0}$ is bed shear stress where μ is dynamic viscosity. Boundary conditions considered in the y direction are given in Fig. 1a (i.e., no-slip wall condition at $y = 0$, and, under the low Froude number approximation, a no-stress, undeformed surface is implemented at $y = h$). Time advancement (spatial discretisation) is achieved using a 3rd order Runge-Kutta scheme (6th order compact finite-difference scheme). The DNS data is used to study turbulent structures, length scales, and velocity structure functions. In particular, the behaviour of these features is analysed close to the free surface with important differences observed compared to closed channel flow cases.

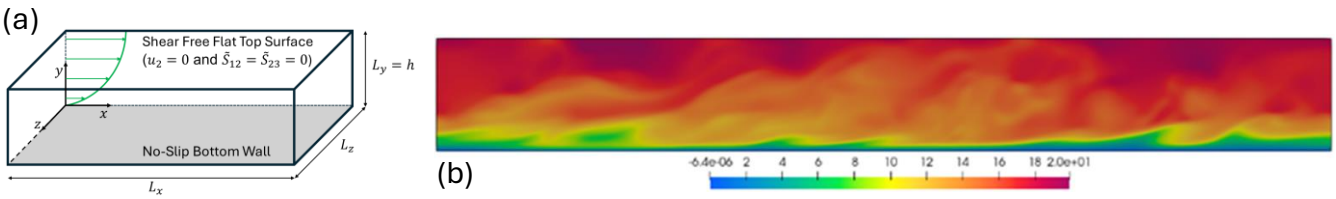

Figure 1. (a) Computational domain and coordinate system with indicative velocity profile and considered boundary conditions, and (b) instantaneous u velocity contours on the central x-z plane for $Re_\tau = 180$ fully developed case.

Ahmed, U., Apsley, D., Stallard, T., Stansby, P., Afgan, I., 2021, Turbulent length scales and budgets of Reynolds stress-transport for open-channel flows; friction Reynolds numbers (Re_τ) = 150, 400 and 1020. Journal of Hydraulic Research. 59, pp. 36-50.

Alexander, S. R., Hamlington, P.E., 2015, Analysis of turbulent bending moments in tidal current boundary layers. Renewable Sustainable Energy. 7, 063118.

Bartholomew P., Deskos G., Frantz R.A.S., Schuch F.N., Lamballais E., Laizet S, (2020), Xcompact3D: An open-source framework for solving turbulence problems on a Cartesian mesh. SoftwareX. 12, 100550.

Laizet, S., Lamballais, E, 2009, High-order compact schemes for incompressible flows: A simple and efficient method with quasi-spectral accuracy. Journal of Computational Physics. 228(16), pp. 5989-6015.

Nezu, I., Nakagawa, H., 1993, Turbulence in Open-Channel Flows. IAHR Monograph, A. A. Balkema, Rotterdam.

Pirozzoli, S., 2023, Searching for the log law in open channel flow. Journal of Fluid Mechanics. 971, A15-1.

Taylor, J.R., Sarkar, S., Armenio, V., 2005, Large eddy simulation of stably stratified open channel flow. Physics of Fluids. 17, 116602.

Walker, R., Tajeda-Martínez, A. E., Martinat, G., Grosch, C.E., 2014, Large-eddy simulation of open channel flow with surface cooling. International Journal of Heat and Fluid Flow. 50, pp. 209-224.

CFD/010: LES-based study of the combined effects of relative humidity and temperature on expiratory particle dispersion

[1*]Monka, Aleksandra; [2]Fraga, Bruño

[1] School of Engineering, University of Birmingham, Edgbaston, Birmingham, B15 2TT, UK. Email: akm522@student.bham.ac.uk [2]School of Engineering, University of Birmingham, Edgbaston, Birmingham, B15 2TT, UK. Email: b.fraga@bham.ac.uk. *Presenting Author

Indoor ambient conditions such as relative humidity and temperature play a critical role in the evaporation, settling, and dispersion of expiratory particles. Accurate prediction of the complex interaction between these conditions and the turbulent exhalation jet carrying respiratory particles is crucial in determining the exposure risk to airborne pathogens in shared indoor environments. In this study, large eddy simulation (LES) is employed within a Eulerian-Lagrangian framework to investigate the combined effect of relative humidity and temperature on expiratory particle dispersion between two seated individuals. Three seasonal indoor scenarios – winter, summer, and tropical – are examined to assess how variations in relative humidity and temperature influence particle transport when one person speaks for 60 s. A realistic polydisperse particle size distribution is used to capture the evaporation dynamics of expiratory particles across a broad size spectrum. The particles are composed of a binary water-NaCl solution, and their evaporation is stopped when the limit of NaCl solubility in water is reached. One additional case is also considered in which both individuals speak intermittently under summer conditions, to assess the influence of speaker configuration on exhalation jet mixing and local aerosol concentration.

Results show that winter indoor conditions accelerate the rate of evaporation by 29% and 70% when compared to summer and tropical conditions respectively. Analysis of the integrated average aerosol volume fraction in the breathing zone after 60 s shows an increase of 4.5% and 30% under summer and tropical conditions respectively when compared to winter. This reflects the combined effect of reduced evaporation rate and buoyancy in summer and tropical conditions, which result in a more horizontal jet trajectory before upward curvature, and a greater retention of larger aerosols within the breathing zone. While upward transport still continues, the slower evaporation rate under summer and tropical conditions results in larger aerosols remaining longer within the breathing zone, while in winter conditions more rapid evaporation occurs which entrains smaller aerosols faster toward the ceiling and away from the breathing zone. In the case of two speakers, a more symmetric particle dispersion pattern is generated, and the mixing of both exhalation jets leads to a 15% increase in aerosol concentration in the breathing zone, delaying ceiling accumulation. These results underscore the importance of considering seasonal indoor scenarios when assessing exposure risk to infectious pathogens.

CFD/011: Numerical studies on the hydrodynamic settling of solid particles in a quiescent fluid

[1*]Gaur, Abhimanyu; [2]Lee, Mortimer; [2]Fairweather, Mike; [3]Hodgson, David; [3]Peakall, Jeffrey; [3]Keevil, Gareth

[1*]School of Computer Science, University of Leeds, Leeds, LS2 9LA, United Kingdom, [*]scab@leeds.ac.uk. [2]School of Chemical and Process Engineering, University of Leeds, LS2 9LA, United Kingdom, l.f.mortimer@leeds.ac.uk, m.fairweather@leeds.ac.uk, [3]School of Earth and Environment, University of Leeds, LS2 9LA, United Kingdom, d.hodgson@leeds.ac.uk, j.peakall@leeds.ac.uk, g.m.keevil@leeds.ac.uk.

The hydrodynamic settling behaviour of spherical and non-spherical particles plays a critical role in understanding sedimentation processes in natural water bodies such as lakes, rivers, estuaries, and oceans. In this study, numerical simulations are conducted using NEK5000, a spectral element-based computational fluid dynamics (CFD) solver that integrates the Immersed Boundary Method within a unified framework. The investigation focuses on the settling dynamics of various particle geometries, including a sphere, disks with sharp and bevelled edges, and a prolate ellipsoid. Settling velocities, flow field contour maps, and wake structures downstream of the particles are analysed over time. The simulations capture particle Reynolds numbers up to 870, corresponding to the intermediate flow regime. The results reveal that hydrodynamic forces and torques acting on the particles are inherently unsteady and significantly influence motion characteristics such as secondary drift and rotational behaviour about the geometric axes. Among the non-spherical geometries, the disk with bevelled edges exhibits the highest settling rate. Furthermore, distinct wake structures are observed during the settling process, with shape-dependent patterns including spiral, hairpin, and horseshoe vortices. Velocity and pressure fields in a vertical plane intersecting the geometric centre of both disk types are examined in detail. These flow features are visualised at 0.3 seconds following the release of particles within a three-dimensional rectangular domain, as presented in Figure 1.

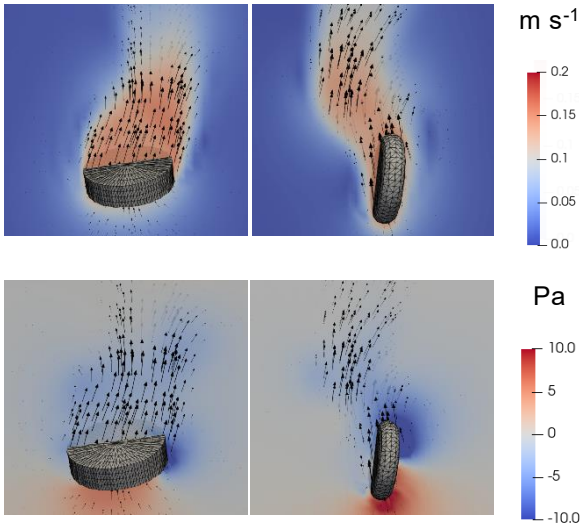

Figure 1. Contours of velocity magnitude (top) and pressure (bottom) for a disk with sharp edges (left), and bevelled edges (right).

CFD/012: Uncertainty Quantification of Volume-of-Fluid-Based Interface Capturing Methods Using a Gaussian Process Surrogate Model

[1*]Wahbah Makhoul, Elias;[2]Tabor, Gavin; [3]Shrestha, Saugat

[1]Department of Engineering, University of Exeter, Exeter, United Kingdom, ew838@exeter.ac.uk [2] Department of Engineering, University of Exeter, Exeter, g.r.tabor@exeter.ac.uk. [3]Department of Engineering, University of Exeter, Exeter, ss1604@exeter.ac.uk. *Wahbah Makhoul, Elias

Accurately predicting the evolution of the free surface in interfacial flows remains a central challenge in computational fluid dynamics (CFD), particularly in wave–structure interaction (WSI) problems where nonlinear interface dynamics, transient flows, and impact loading are critical. A key yet underexplored source of epistemic uncertainty arises from the Volume-of-Fluid (VoF) method, which lacks a clearly defined value of the volume fraction field that represents the free surface, an issue well-documented in the literature. This ambiguity is compounded by numerical artifacts such as interface smearing, unbounded values, and mesh dependency, especially when comparing VoF variants or applying adaptive mesh refinement (AMR). This study investigates these uncertainties through an uncertainty quantification (UQ) framework applied to a Gaussian Process Regression (GPR) surrogate model trained on high-fidelity CFD simulations of isothermal sloshing in a cylindrical tank. The CFD framework is based on OpenFOAM's one-fluid model of two phase immiscible flows, where the interface is implicitly captured through the volume fraction field and coupled to the incompressible Navier–Stokes equations. GPR not only provides point predictions but also estimates confidence intervals around them, making it particularly well-suited for scenarios where CFD data is costly or limited. A Latin Hypercube Sampling (LHS) design is employed to span a parameter space defined by mesh topologies, refinement strategies, and VoF-type interface capturing methods. The GPR model is trained over this space to emulate CFD outputs efficiently. A Latin Hypercube Sampling (LHS) is employed to design the input space defined by mesh topologies, refinement strategies, and different VoF-type interface capturing methods over which the surrogate model is trained. The uncertainty quantification framework will be implemented on the GPR model to study the Gaussian distribution of volume fraction fields that define the free surface, with the goal of identifying a representative global volume fraction value for interface reconstruction and assessing the sensitivity of this definition to discrete numerical choices in multiphase CFD.

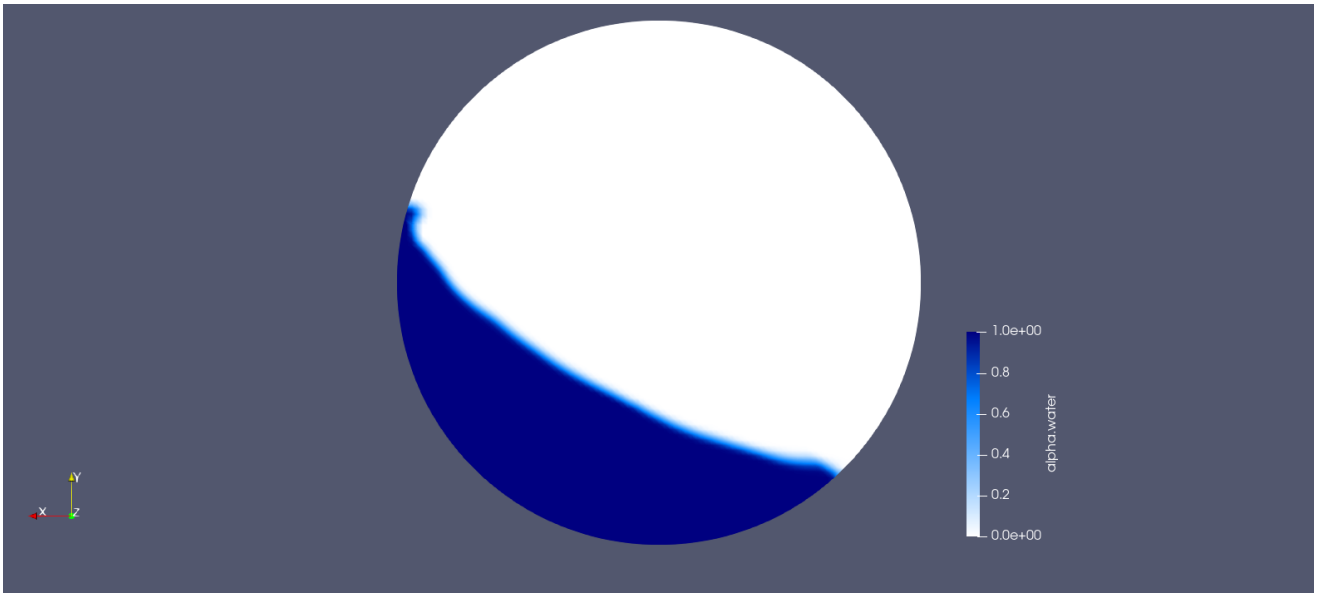

Figure 1. Snapshot of isothermal water sloshing simulation performed using OpenFOAM's Volume of Fluid (VOF) solver interFoam, which employs the MULES (Multidimensional Universal Limiter for Explicit Solution) algorithm for interface compression. The volume fraction scalar field α is shown, where dark blue indicates the water region ($\alpha = 1$) and white represents the air region ($\alpha = 0$), and light blue indicates diffused interface between phases.

CFD/014: Direct numerical simulation of simultaneous droplet impact on a solid substrate

[1*]Ziyao Zhang; [1]Alfonso A. Castrejón-Pita; [1]Wouter Mostert

[1]Department of Engineering Science, Oxford University, Parks Road, Oxford OX1 3PJ, UK. *Presenting Author

The impact of droplets on a substrate appears universally in nature and industrial applications. Many studies have focused on individual droplet impacts, while in fact the occurrence of multiple droplet impacts in close proximity is widespread. In this work, we present three-dimensional high-resolution direct numerical simulations of simultaneous pair droplet impacts. The governing dimensionless parameters in this problem are the impact Weber number (*We*, describing the relative effect of inertia to surface tension), Reynolds number (*Re*, inertia to viscosity) and Froude number (*Fr*, inertia to gravity). After impact on the substrates, the spreading droplets interact and form a vertical uprising sheet with a well-defined trajectory (Figure 1(a), (b)). The simulations are validated against recent experimental work (Goswami's (2023) thesis), showing good agreement for the height of the central sheet over time for various *We*, *Re*, *Fr*. We further investigate the detailed kinematics of the process, develop scaling for the height of central uprising sheet as a function of *We* and *Re*, and propose an energetic model for the maximum height with reliable predictive ability. The model indicates that kinetic energy and surface tension energy dominate, with viscous dissipation playing an important role via the Reynolds number, while gravitational potential energy is of secondary importance. These insights promise a more complete understanding of the central uprising sheet dynamics and lay the groundwork for further exploration of fragmentation processes associated with droplet impact.

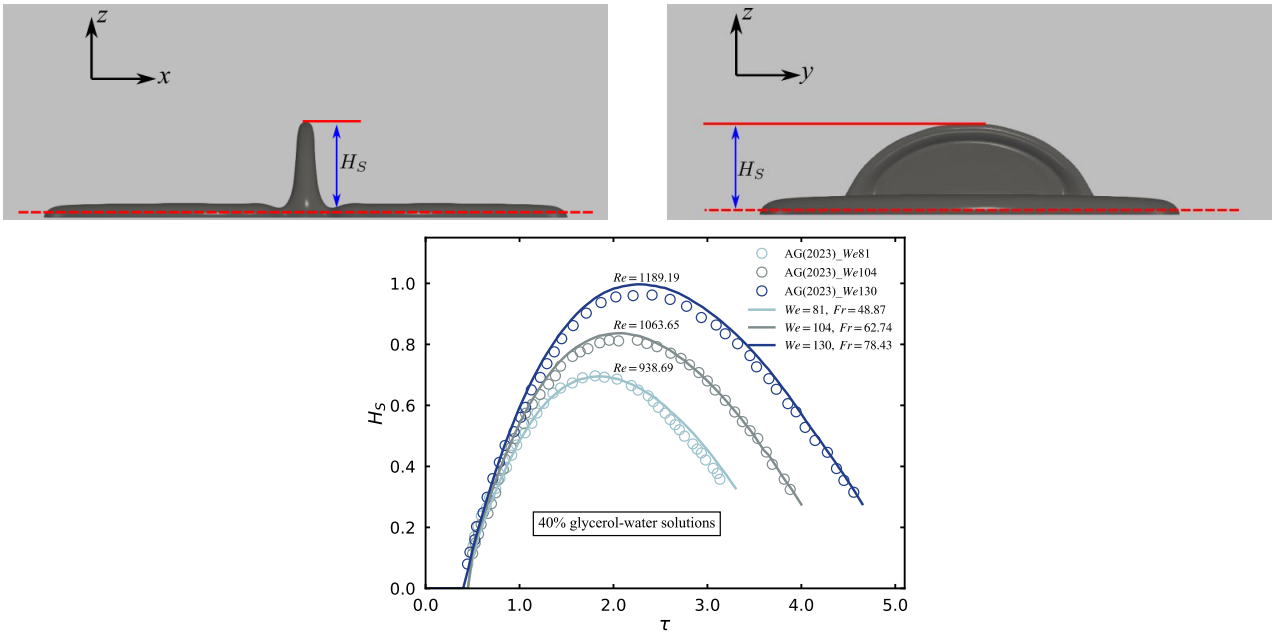

Figure 1. Sketch of central uprising sheet: (a) front view and (b) side view, and (c) the height comparison between experimental and numerical results. Note: points are experimental data from Goswami's (2023) thesis, lines are present results

Anjan Goswami, 2023, Impact of Multiple Droplets on Solid Surfaces. PhD thesis, Imperial College London.

CFD/015: Multimethod Analysis of Particle Transport in Pipe Flows - *Poster*

[1*]Bhardwaj, Akash; [2*]Brown, Joel ; [3*]Ma, Guowen; [4*] Romanzini-Bezerra, Grasiele; [5]Harlen, Oliver

[6]Hunter, Timothy; [7]Cunliffe, Christopher; [8]Spencer, Julian; [9]Borman, Duncan

[1]EPSRC Centre for Doctoral Training (CDT) in Future Fluid Dynamics, University of Leeds, UK, jxfz1202@leeds.ac.uk [2]EPSRC Centre for Doctoral Training (CDT) in Future Fluid Dynamics, University of Leeds, UK, mqhq8337@leeds.ac.uk [3]EPSRC Centre for Doctoral Training (CDT) in Future Fluid Dynamics, University of Leeds, UK, jbmzh4923@leeds.ac.uk [4]EPSRC Centre for Doctoral Training (CDT) in Future Fluid Dynamics, University of Leeds, UK, slcsr8458@leeds.ac.uk [5]School of Mathematics, University of Leeds, UK, o.g.harlen@leeds.ac.uk [6]School of Chemical & Process Engineering, University of Leeds, UK, t.n.hunter@leeds.ac.uk [7]United Kingdom National Nuclear Laboratory, UK, christopher.cunliffe@uknnl.com [8]United Kingdom National Nuclear Laboratory, UK, julian.spencer@uknnl.com [9]School of Civil Engineering, University of Leeds, UK, d.j.borman@leeds.ac.uk *Presenting Author

The transport of solid-liquid mixtures in pipes is a critical process in many industries, yet predicting flow behaviour remains a significant challenge. A comprehensive understanding of this phenomenon requires a multi-methods approach that integrates insights from numerical simulations, physical experiments, and analytical models. This work presents a combined investigation into particle-laden flows in pipes, utilising computational, experimental, and analytical methods to explore various aspects of the flow, including model fidelity and the prediction of critical flow transitions.

The study consists of four components. First, a 3D Computational Fluid Dynamics-Discrete Phase Model (CFD-DPM) was developed in ANSYS Fluent to assess model sensitivity. This DPM framework was validated against the benchmark experimental data from Alajbegovic *et al.* (1994), which involved the vertical upward flow of spherical ceramic particles with a uniform diameter of 2.32 mm, focusing specifically on the performance of the Saffman lift force model. Second, a CFD-Discrete Element Method (CFD-DEM) simulation was employed to investigate the water-particle flow, analysing both one-way and two-way coupling effects.

Third, an experimental study was carried out in a closed-loop pipe system, illustrated in Figure 1. The system contains an inclinable section, allowing tests at pipe angles of 0°, 5.0°, and 10.1°. The aim was to determine the Critical Deposition Velocity (CDV) for 0.379 mm spherical glass beads. Ultrasound Velocity Profiling (UVP) was used to collect data, and from the UVP signal amplitude, the sediment bed height (h/z) was estimated across a range of mean flow velocities for each pipe angle. CDV was then determined by extrapolating the bed height–mean velocity relationship to h/z→0. Finally, an analytical model, based on particle settling and turbulent suspension theory, was developed to predict CDV theoretically. The model showed good agreement with the experimental results.

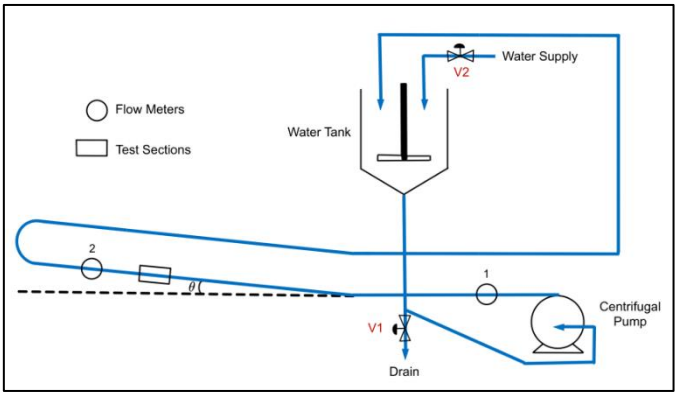

Figure 1. Diagram of the flow loop's main section used to perform the experiments.

Alajbegovi´c, A., Assad, A., Bonetto, F. and Lahey Jr, R. (1994), 'Phase distribution and turbulence structure for solid/fluid upflow in a pipe', International Journal of Multiphase Flow 20(3), 453–479.

CFD/016: CFD Study of Secondary Currents in Partially Filled Pipe Flows- *Poster*

[1*]Bose, Aniruddha; [2]Borman J, Duncan; [3]Hunter N, Timothy; [4]Spencer T, Julian; [5]Cunliffe J, Christopher

[1,2,3]University of Leeds, Leeds, LS2 9JT, UK, [4]United Kingdom National Nuclear Laboratory, Chadwick House, Birchwood Business Park, Warrington, Chesire, WA3 6AE, UK, [5]United Kingdom National Nuclear Laboratory, Havelock Rd, Workington, Cumbria, CA14 3YQ, UK

Pure liquid and particle laden flows are transported in partially filled pipes in different industries. Partially filled pipe flows are fundamentally different as compared to filled pipe flows because of the presence of secondary currents [1]. Secondary currents are the in-plane motion that generates because of the asymmetry in the pipe cross-section due to the presence of the air-phase. Secondary currents are shown to significantly affect the primary flow by modifying the streamwise velocity and the friction factor through the wall shear stress [1]. In this study, two different CFD approaches, one using the steady state single-phase Reynolds Averaged Navier Stokes (RANS) (with a slip condition at the pipe top wall to approximate the water free surface) and the other using a Volume of Fluid (VoF), air-water interface tracking multiphase model both with the Reynolds stress closure model are used to study primary and secondary flow components in a partially filled pipe flow. Results from both the studies are compared and contrasted and compared to established experimental results from the literature. Similar qualitative agreement is obtained between the results of the two studies but some of the structures and the quantitative values of different properties, like the velocity magnitude, Reynolds stress terms are found to be different. Velocity dip, whereby the maximum streamwise velocity occurs below the free surface (due to secondary currents), inner and outer secondary cells, etc are found to be present in the results of both the studies. The single-phase simulations were able to reproduce experimental results within a few percent deviation in a much shorter computational time as compared to the VoF.

Secondary current patterns in a filled single phase pipe flow were also compared to that in partially filled pipe flows by running a simulation in a semi-circular shaped pipe cross-section with no-slip boundary conditions at all the surfaces. Good agreement is found between all the CFD studies and the experimental results.

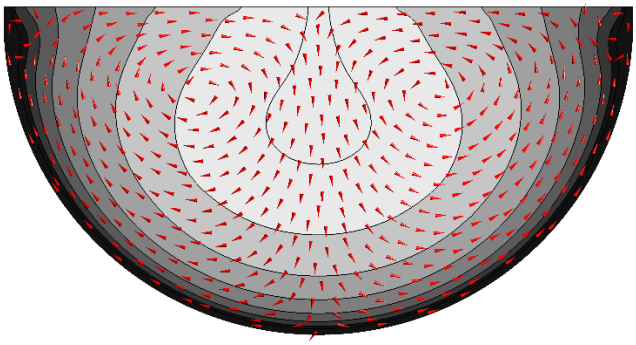

Figure 2. Streamwise velocity contour on the cross-section for a single-phase slip boundary condition pipe flow case. The in-plane motion is super-imposed on the contour.

[1] Liu, Yan and Stoesser, T and Fang, H, 2022, Effect of secondary currents on the flow and turbulence in partially filled pipes, Journal of Fluid Mechanics 938 pp A16

CFD/0017: CFD Simulation of Hydraulic Gear Pump

[1*]Babaeisarmadi, Morteza; [1]Ramos, Joao; [1,2] Mohamed, Mohamed

[1]University of South Wales, Llantwit Road CF37 1DL Pontypridd, UK

[2]Mechanical Engineering Department, Faculty of Engineering, South Valley University, Qena 83523, Egypt

morteza.babaeisarmadi@southwales.ac.uk. [2]joao.ramos@southwales.ac.uk. [3] mohamed.mohamed@southwales.ac.uk

Positive displacement pumps, particularly external gear pumps, are widely used in various industrial and mobile hydraulic systems due to their simple, efficient, and durable construction. However, cavitation remains a significant challenge, leading to performance degradation, material damage, noise, and vibrations. This study investigates the effects of rotational velocity on cavitation in an external hydraulic gear pump. The study examines the impact of two different rotational speeds on cavitation intensity, namely 1500 rpm and 3000 rpm. Using ANSYS Fluent, a 2-dimensional model was created, and a dynamic mesh is applied. Each full rotation is divided into 10,000 steps leading to a step time of 4 x 10^{-6} s and 2 x 10^{-6} s. The CFD study manages to replicate the cavitation creation locations quite accurately and in agreement with previous experimental results.

Keywords: *cavitation, gear pumps, external hydraulic gear pumps, fluid dynamics, computational fluid dynamics (CFD)*

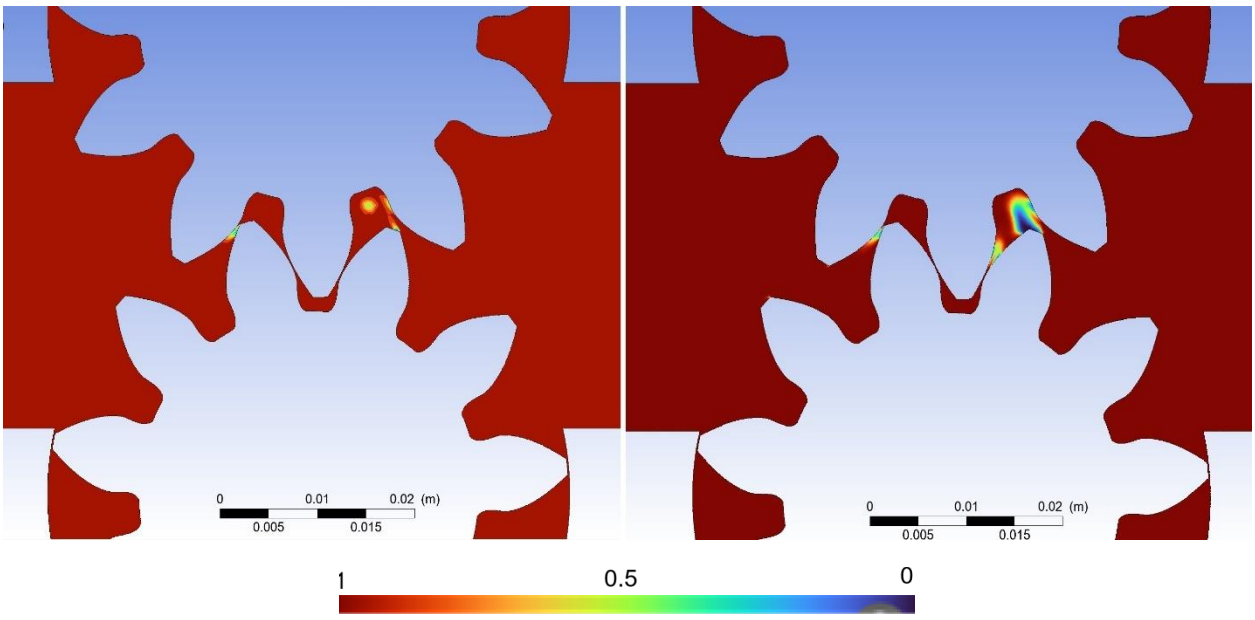

Figure 1. Screenshot of timestep from simulation showing the Volume Fraction contour at 1500 rpm (left) and 3000 rpm (right). Red represents 1 and blue represents zero. Simulation done using ANSYS Fluent.

CFD/018: URANS CFD Modelling of Perturbed Natural Circulation Loops with LES validation

[1*]John, Thomas; [1]Marshall, Deacon; [1]Davies, Heather; [2]Skillen, Alex; [1]Brown, Sophie; [1]Tunstall, Ryan; [1]Lewis, Patrick

[1]Rolls-Royce, Kings Place, 90 York Way, N1 9FX, London, United Kingdom, Thomas.John@Rolls-Royce.Com. [2]University of Manchester, Oxford Road, M13 9PL, Manchester, United Kingdom, alex.skillen@manchester.ac.uk. *Presenting Author

Natural Circulation (NC) can be used as an effective safety mechanism in nuclear reactors. However, due to the strong coupling between the flow and thermal fields, NC is inherently prone to instabilities such as flow oscillations, reversals, and stalls. This is particularly the case when the flow is subject to imposed perturbations, such as the injection of fluid at a different temperature to prevailing conditions in the loop. In terms of predictive modelling for nuclear reactors, 1D codes are typically relied on for pumped flow conditions. However, 1D methods can be unreliable for perturbed NC due to the 3D nature of the flow. We should therefore look to develop 3D Computational Fluid Dynamics (CFD) models for such predictions, however wide-scale CFD modelling is only realistically feasible when the Unsteady Reynolds-Averaged Navier-Stokes (URANS) approach for turbulence modelling is used, usually with an eddy-viscosity closure model. Such turbulence models include a range of assumptions and approximations, and as such must be carefully validated for any specific nuclear safety related application. Therefore, the question we wish to address is "*how reliable is URANS CFD for predicting flow rates in NC loops?*".

In this study, we perform URANS CFD simulations of a simple NC loop with transient step-changes in heater power and cold fluid injections. The geometry contains a primary heater and cooler, both positioned on the vertical legs of the loop, and a secondary cooler positioned on a corner of the loop. For validation of the URANS approach, we compare its predictions to Large Eddy Simulation (LES) results for the same cases. We also perform several sensitivity studies for the URANS modelling, in which the turbulent viscosity and turbulent diffusivity are varied, in order to further understand how the assumptions made in the URANS modelling affect the NC flow behaviour when perturbed. The results show that URANS CFD with the Standard $k-\epsilon$ (Two-Layer) turbulence model predicts the overall trend in mass flow rate well when compared to the LES. The frequency of flow oscillations matches well between the URANS and LES, but the amplitude of the oscillations for LES is higher than URANS in some cases. The trend in mass flow rate was not significantly affected by varying the turbulent viscosity and diffusivity. Overall, these results highlight that perturbed NC loops can be modelled with reasonable confidence by URANS CFD, and they provide insight into the response of NC loops subject to transient perturbations.

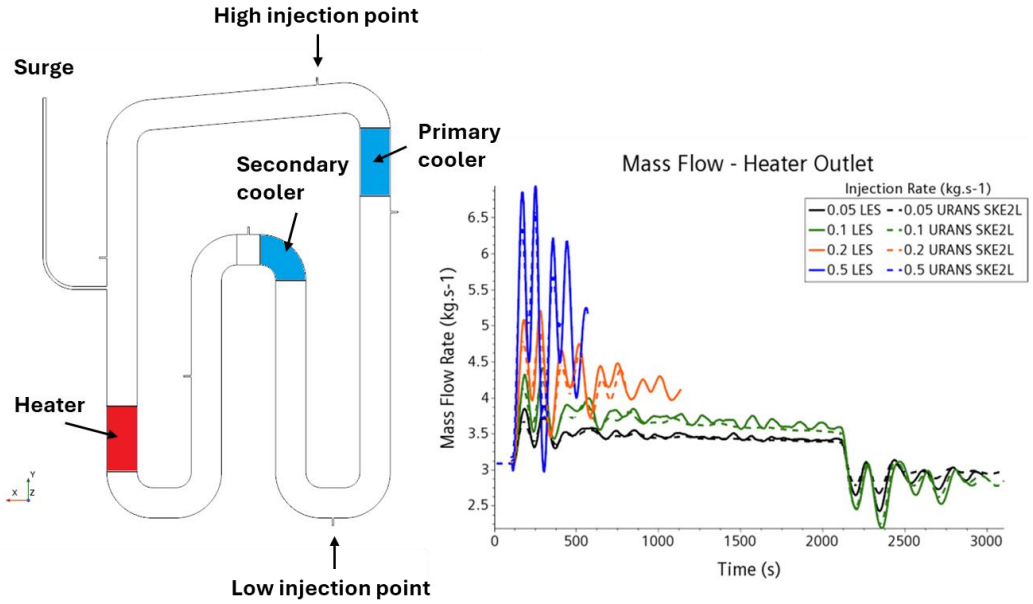

Figure 1. Left – NC loop geometry including heater/cooler positions and injection points. Right – LES and URANS results showing mass flow rate at the heater outlet vs time for NC with various high-point injection flow rates.

COM: Complex fluids

COM/001: Large Amplitude Oscillatory Shear (LAOS) for Protein-Pectin Crosslinking

[1,3*]Maklad, Osama; [2,3]Banergee, Bandita; [2,3]Vahid Baeghbali; [2,3]Parag Acharya

[1]*Centre for Advanced Manufacturing and Materials, University of Greenwich, London, UK.*

[2]*Natural Resources Institute, University of Greenwich, London, UK.*

[3]*Bezos Centre for Sustainable Protein, Imperial College London, London, UK*

*Presenting Author, o.maklad@gre.ac.uk

Protein-pectin crosslinked biopolymers are promising materials for food, pharmaceutical, and biomedical applications due to their tuneable rheological and structural properties. Large Amplitude Oscillatory Shear (LAOS) rheology provides critical insights into the nonlinear viscoelastic behaviour of these systems under deformation regimes relevant to processing and end-use conditions. In this study, we investigate the LAOS response of protein-pectin complexes formed via enzymatic, chemical, or physical crosslinking, analysing their strain-stiffening, shear-thinning, and network breakdown characteristics through Lissajous plots and Chebyshev harmonic decomposition. By correlating LAOS parameters (e.g., intracycle nonlinearities, harmonic distortions) with crosslinking density and bond type, we will reveal how molecular interactions dictate mechanical performance. Our results will demonstrate that LAOS effectively discriminates between crosslinking mechanisms and identifies optimal formulations for targeted texture or encapsulation properties. This work advances the design of protein-pectin hybrids for applications requiring precise control over nonlinear viscoelasticity.

Keywords: LAOS rheology, protein-pectin crosslinking, nonlinear viscoelasticity, biopolymer design, soft matter, food rheology

Ptaszek, P., 2014. Large amplitudes oscillatory shear (LAOS) behavior of egg white foams with apple pectins and xanthan gum. *Food Research International*, *62*, pp.299-307.

Wang, Y. and Selomulya, C., 2022. Food rheology applications of large amplitude oscillation shear (LAOS). Trends in Food Science & Technology, 127, pp.221-244.

Schreuders, F.K., Schlangen, M., Bodnár, I., Erni, P., Boom, R.M. and van der Goot, A.J., 2022. Structure formation and non-linear rheology of blends of plant proteins with pectin and cellulose. *Food Hydrocolloids*, *124*, p.107327.

COM/02: Yield stress fluids for advanced materials additive manufacturing

Rishav Agrawal,[a] Zhidong Luo,[a] Patrick Spicer[b] and **Esther García-Tuñón**[a,c,*]

[a]University of Liverpool, School of Engineering, Liverpool, United Kingdom
[b]School of Chemical Engineering, University of New South Wales, Sydney, Australia
[c]Materials Innovation Factory, University of Liverpool, United Kingdom

Abstract

Bridging materials discovery and advanced manufacturing relies upon successful fabrication of strategically designed hierarchical structures and composites. This places a high demand on materials' behaviour during processing. Developing robust formulations is key to expand the range of advanced materials (e.g. 2D and carbon based materials,[1, 2] perovskites, porous organic cages[3] and advanced ceramics[4] to name a few) that can be used in engineering solutions for energy and health applications.

Direct ink writing (DIW) is a versatile additive manufacturing technique that enables shaping bespoke advanced materials formulations. DIW feedstocks must meet different criteria to achieve "*printability*" via DIW, including *flowability*, *recoverability* and material strength and other assessable properties, e.g. *drawability*, or ability to *stretch*. These assessable properties have not been defined with symbols or dimensions, and cannot be directly measured;[5] however, they can be linked to measurable properties (e.g. "yield" stress, storage modulus, mutation times, etc).[2] DIW feedstocks are yield stress fluids (or elastic-viscous-plastic, EVP, materials) able to "yield" and flow through narrow nozzles (*flowability*) and to re-structure in short timescales to maintain the predesigned shape (*recoverability*). Once deposited the yield stress and storage modulus should be high to prevent the collapse or deformation of the printed structure (*material strength*). Understanding "yielding" of DIW feedstocks is critical for successful printing and final performance. However, it is known that not all yielding is the same, and that local structures and microscopic dynamics can be highly heterogeneous. Combining bulk measurements and direct visualization enable us to map local flows and structural heterogeneities, and to connect their evolution with bulk rheological properties.

We will present our latest findings bringing together rheology and microscopy to reconcile bulk and microscopic dynamic behaviours in yield stress fluids (YSF) for DIW. This talk will provide an overview of key outputs and unpublished research covering the design of bespoke formulations using liquid crystals and pH-responsive surfactants,[3, 4] and the characterization of their bulk and local dynamic behaviours.[1, 2, 6, 7]

REFERENCES:

1. García-Tuñón, E., et al., Physics of Fluids, 2023. 35(1).
2. Agrawal, R. and E. García-Tuñón, Soft Matter, 2024. 20(37): p. 7429-7447.
3. Ling, B., et al., Advanced Functional Materials, 2024: p. 2405320.
4. Jones, E., et al., Soft Matter, 2025. 10.1039/D4SM01473A (Advance article).
5. Reiner, M. and G.S. Blair, *Rheological terminology*. Chapter 9 in *Rheology*. 1967, Elsevier. p. 461-488.
6. Agrawal, R., et al., Journal of Non Newtonian Fluid Mechanics, 2025, 338 (105407).
7. Agrawal, R., P.T. Spicer, and E. García-Tuñón, Journal of Colloidal and Interface Science, 2025 (under review).

COM/003: Scale out of two-phase flows in small channels

*Olasinde, Malik; Angeli, Panagiota

ThAMeS Multiphase, Department of Chemical Engineering, University College London, UK

malik.olasinde.23@ucl.ac.uk. p.angeli@ucl.ac.uk. *Presenting Author

Modern and emerging technologies are sustained by critical metals; to secure their supply chains it is important to recover them from waste materials. The retrieval of critical metals from waste can be achieved with hydrometallurgical methods, where two-phase solvent extraction is a main operation. Small channel contactors have been shown to intensify solvent extractions. To overcome the low throughput of this system, numbering-up of the small channels has been proposed, where many channels are used in parallel, while maintaining the intensification advantages of the small channels [1, 2].

In light of the above, this study investigates the hydrodynamic characteristics of a scale out two-phase flow manifold consisting of five parallel small channels, which was designed based on a resistance network model [1]. The effects of flow rate, phase flow rate ratio, and fluid properties on the distribution in the channels are studied here.

Experimental Procedure

For the experiments, water and kerosene were used as the test fluids. Studies were carried out in the plug flow regime where significant mass transfer intensification has been found, while it can be easily modelled. To ensure plug flow, the phase volumetric flow rate of each phase and the phase volume ratio (Org/Aq) ranged from 0.01- 20 ml/min and 0.5 – 2 respectively. Based on the resistance network model, the diameters of the distribution, barrier and reaction channels (Figure 1) were designed to be 20 mm, 0.508 mm, and 2 mm, respectively, while the lengths of the barrier and reaction channels were 100 mm and 735 mm, respectively. The flow rates of the two-phases were measured by collecting the mixtures at the outlet of each test channel in measuring cylinders. A sensor setup consisting of a photodiode and LED was used for the characterisation of the hydrodynamic parameters of the plug flow; the results were validated against high-speed imaging.

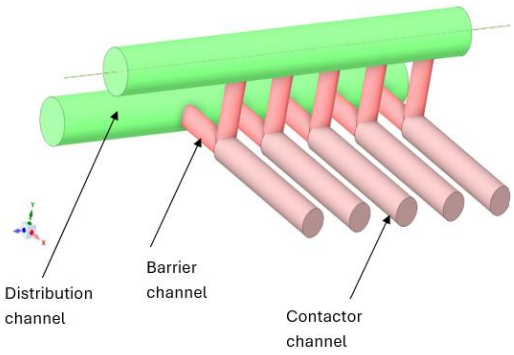

Figure 1. Schematic of the Scale-out manifold.

Results

In summary, the results revealed that the in gerneral flows were almost uniformly distributed among the channels, while the phase flow rate, phase ratio and viscosity were the main parameters that affect maldistribution. It can be concluded that the resistance network model can be used for the design of two-phase flow scale out manifolds. In the future, the manifold will be used for metal extraction studies.

References

[1] E. Garciadiego Ortega, D. Tsaoulidis, and P. Angeli, "Predictive model for the scale-out of small channel two-phase flow contactors," *Chemical Engineering Journal,* vol. 351, pp. 589-602, 2018, doi: 10.1016/j.cej.2018.06.020.

[2] C. Amador, A. Gavriilidis, and P. Angeli, "Flow distribution in different microreactor scale-out geometries and the effect of manufacturing tolerances and channel blockage," *Chemical Engineering Journal,* vol. 101, no. 1-3, pp. 379-390, 2004, doi: 10.1016/j.cej.2003.11.031.

COM/004: GNFFTy model predictions of 2D flow past a circular cylinder in the laminar vortex-shedding regime - *Poster*

[1]Geraghty, David; [2*]Poole, Robert J

[1]School of Engineering, University of Liverpool, UK; psdgerag@liverpool.ac.uk. [2] School of Engineering, University of Liverpool, UK; robpoole@liverpool.ac.uk. *Presenting Author

A recently proposed viscosity equation which incorporates flow-type, but is otherwise inelastic, the so-called GNFFTy model (Generalized Newtonian Fluid model incorporating Flow Type pronounced "nifty") [1] is tested in a complex flow. The results are collected in the computational solver, Ansys Fluent. We present predictions of this model in two-dimensional unsteady flow past a cylinder, i.e. in the laminar vortex-shedding regime, and compare to experimental results for dilute polymer solutions [2]. The GNNFTy model is shown to be able to capture many of the features observed experimentally including a stabilizing effect on the von Kármán instability, with the critical Reynolds numbers pushed to higher values than the Newtonian fluid. The value of this critical Reynolds number with respect to a non-dimensional parameter, defined by $\frac{\lambda U_\infty}{D}$, follows a linear change. Also, increasing this parameter leads to observing a reduction of the saturated vortex shedding frequency (Strouhal number). The increase in drag on the cylinder in the steady flow regime predicted by the GNFFTy model is also in good qualitative agreement with earlier classical experimental data [3]. As a result of raising the parameter $\frac{\lambda U_\infty}{D}$, the area of the wake region experiencing increases in viscosity, due to extensional flow between vortices, becomes larger. The distribution of molecular viscosity in the near wake region, as predicted by the model for a particular set of model parameters, is illustrated in Figure 1. The Figure shows regions of extensional flow experiencing an increase in viscosity.

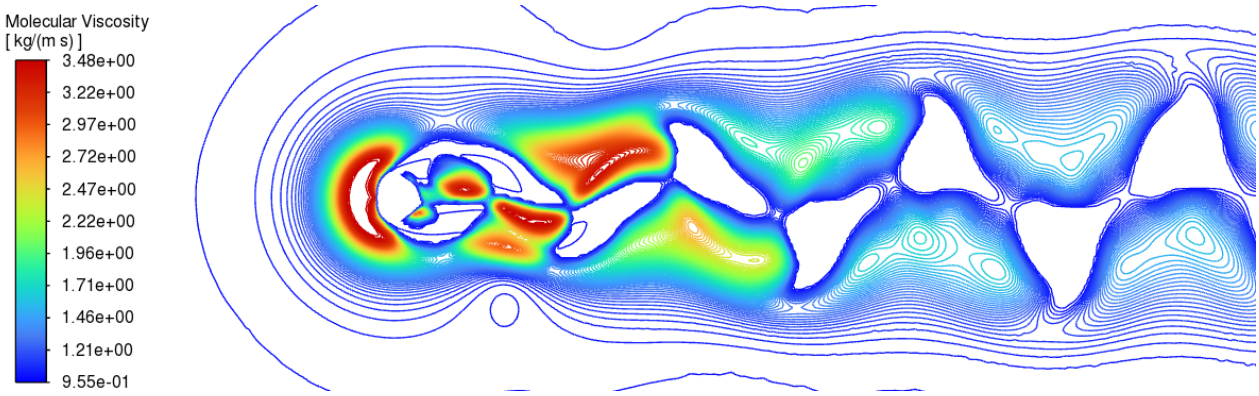

Figure 1. Plot of viscosity contours arising from 2D non-Newtonian flow around a circular cylinder, as predicted by the GNFFTy model. The particular model parameters for this flow are: $\frac{\lambda U_\infty}{D} = 20, Re = 100, \epsilon = 0.01$. *The contours are produced at a flow time of* $t = 120\ s$.

[1] Poole, R.J., 2024. On the use of the Astarita flow field for viscoelastic fluids to develop a generalised Newtonian fluid model incorporating flow type (GNFFTy). *Journal of Fluid Mechanics*, *987*, p.A2.

[2] Pipe, C.J. and Monkewtiz, P.A., 2006. Vortex shedding in flows of dilute polymer solutions. *Journal of non-newtonian fluid mechanics*, *139*(1-2), pp.54-67.

[3] James DF, Acosta AJ. The laminar flow of dilute polymer solutions around circular cylinders. *Journal of Fluid Mechanics*. 1970;42(2):269-288. doi:10.1017/S0022112070001258

COM/005: Steady parallel flows of dense granular suspensions

[1*]Watts, Jonathan; [1]Hewitt, Duncan

[1]Department of Applied Mathematics and Theoretical Physics, Centre for Mathematical Sciences, Wilberforce Road, Cambridge CB3 0WA, UK.

The rheology of dense non-Brownian suspensions is a problem with applications in biological, geophysical and industrial flows. There has been success in modelling their behaviour under steady simple shear using the family of "μ(J)" models, but it is known that these models are inadequate to describe inhomogeneous flows. For example, dense suspensions have been observed flowing below the locally-predicted yield stress apparent in the μ(J) models. In the case of dry granular flows, there has been success in reproducing this behaviour using nonlocal models, in which the stress response of a region of the flow depends on the flow in neighbouring regions. In this talk, we will explore a number of steady parallel dense suspension flows, with and without gravity, and investigate the predictions of μ(J) models and some nonlocal models, in particular suspension analogues of the Nonlocal Granular Fluidity and I-gradient models of granular rheology. We will compare these predictions to results from experiments and particle-based simulations.

COM/006: VISCOPLASTIC STOKES DRAG

[1*]Taylor-West, Jesse; [1]Hogg, Andrew

[1]School of Mathematics, University of Bristol, Woodland Road, Bristol, BS8 1UG, UK. *Presenting Author

We study the uniform flow of a Bingham fluid around two- and three-dimensional particles in the regime of slow creeping flow and relatively weak yield stress. In this regime, matched asymptotic expansions can be employed to match between a region close to the particle, where the equations reduce to those for Newtonian Stokes flow, and a far-field region where plasticity becomes significant and the problem reduces to that of a Bingham fluid driven by a point force at the origin (i.e. a viscoplastic Stokeslet). Thus, the methodology follows that of classical approaches to account for inertial effects in low-Reynolds-number flows around particles. A key difference to the inertial case is that, whereas the far field problem in the inertial case is governed by the linear ``Oseen" equation, for the viscoplastic case it is a fully non-linear viscoplastic flow problem, which requires direct numerical simulation. Employing this matched asymptotic approach, we calculate the drag force on the particle, neglecting terms at or above the order of the small Bingham number, Bi (the yield stress non-dimensionalised by a typical viscous stress). We explicitly consider the cases of a sphere, a circular cylinder and an elliptic cylinder. We further discuss the cases of a general three-dimensional particle and slender ellipsoids. For the three-dimensional flows the correction to the Newtonian drag scales with $Bi^{1/2}$, while for the two-dimensional flows around cylinders we obtain an algebraic relation between the drag and the Bingham number, the first three terms in an asymptotic expansion of which are at orders $1/\log(1/Bi)$, $\log(\log(1/Bi))/\log(1/Bi)^2$, and $1/\log(1/Bi)^2$, representing a slow asymptotic approach to the leading order prediction with decreasing Bingham number.

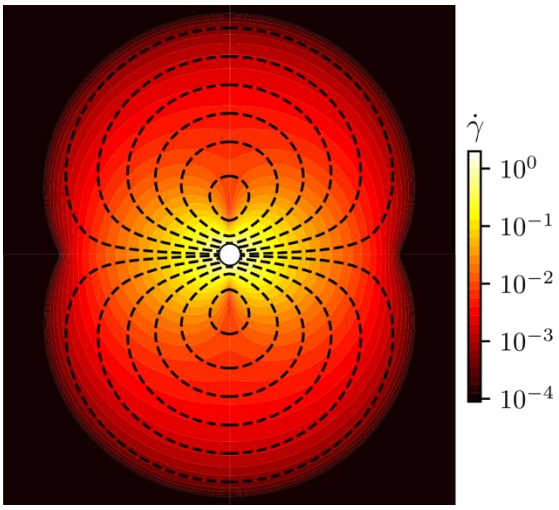

Figure 1. Streamlines (dashed) and strain-rate (color scale) for flow around a translating sphere in a Bingham fluid

COM/007: Modelling 3D printed rheologically complex materials using OpenFOAM - *Poster*

*Jackson, Chris; Harlen, Oliver; Read, Daniel; Jabbari, Masoud; Kay, Robert

EPSRC CDT in Future Fluid Dynamics

University of Leeds, LS2 9JT

sccjj@leeds.ac.uk

*Presenting Author

3D printing, is a layer-by-layer production method that reduces material waste compared to traditional techniques. The growing demand for higher-quality printed products with fewer defects has driven its rapid development in recent years. However, understanding how material properties influence printing behaviour remains a key challenge.

This work investigates the flow of non-Newtonian materials in extrusion-based 3D printing, where complex rheology plays a critical role. In particular, we consider the printing of high molecular polymers, where flow modifies the configuration of the polymer chains, leading to viscoelastic stress. Using the RheoTool library in OpenFOAM with a multiphase simulation approach, we compare the behaviour of a Newtonian fluid with a polymer melt (modelled using the Rolie-Double-Poly (RDP) constitutive equation). The comparison highlights the influence of viscoelasticity on the form of the printed strand, followed by an analysis of internal stress distributions that arise in the RDP flow.

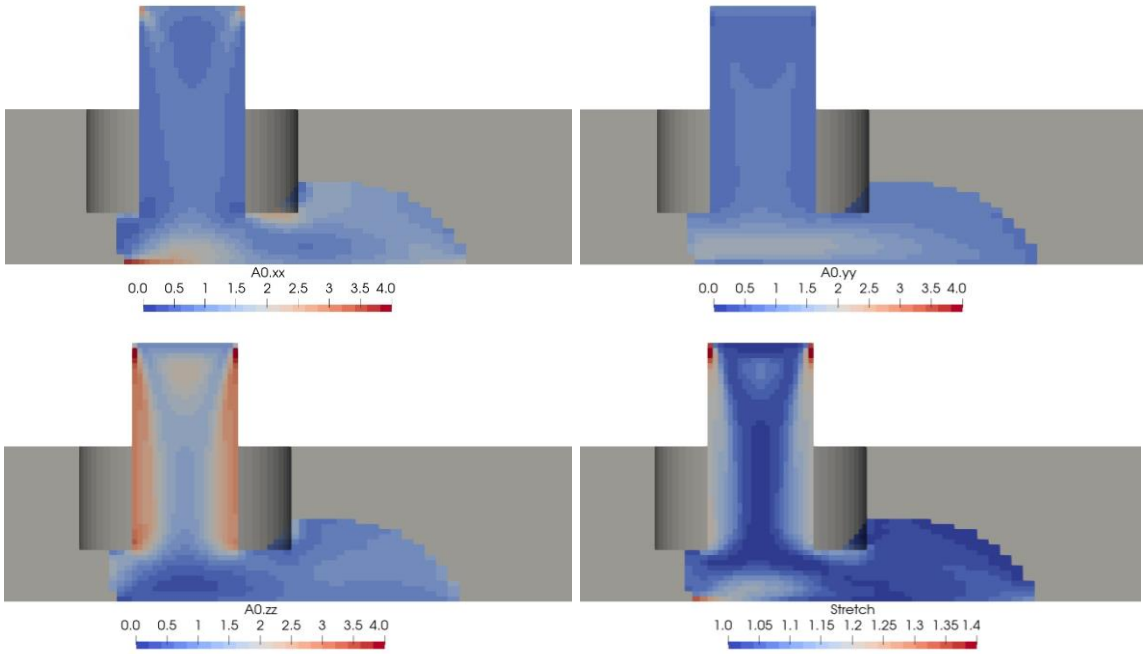

Figure 1. These are the results from an OpenFOAM simulation of the RDP flow. This shows the shape of the polymer strand and the polymer conformation for the RDP. They exhibit a combination of biaxial extension in the xy plane, along with the polymer chains aligned in the vertical z-direction in the nozzle.

COM/008: IMPACTS OF GEOMETRY ON VISCOELASTIC FRACTURE FIELDS

[1*]Sendula, Andrea; [2]Pegler, Sam

[1]University of Leeds, scase@leeds.ac.uk. [2]University of Leeds, s.pegler@leeds.ac.uk. *Presenting Author

Although fractures are typically associated with linear elastic materials, they can occur in various material rheologies. An example includes viscoelastic materials, which exhibit fluid-like flow and viscous dissipation. In such systems, disturbances can be governed by elastic or viscous behaviour, with different balances dominant over varying length scales. Thus, a key question arises: what happens when the characteristic length scales of the dominant balances are comparable to the length scale of the geometry?

In this study, we focus on a Kelvin-Voigt rheology, which provides a simple framework for the introduction of viscosity to an elastic material. We model steady-state crack propagation through a strip of finite thickness and examine the influence of geometry on the stress and strain fields within the viscoelastic material. We identify a dimensionless number, the fracture Deborah number, defined by the geometry, crack velocity, and material properties. Through a combination of numerical studies and asymptotic analysis of the governing equations, we explore how variations in the fracture Deborah number impact the disturbance around the crack.

Through our analysis, we identify two regimes. In the first, when the Deborah number is low and the impact of the boundaries is minimal, we observe a transition from viscously dominated flow close to the crack tip to elastic deformation further out, corresponding to the previously identified “viscoelastic trumpet” (de Gennes, 1996). In the second regime, when Deborah number is high, we uncover novel asymptotic structures. In this regime, we find a one-dimensional leading order flow, with higher order terms varying across multiple scales. In both regimes, we present the key asymptotic simplifications for an inner and outer deck and show their correspondence with the full numerical solution.

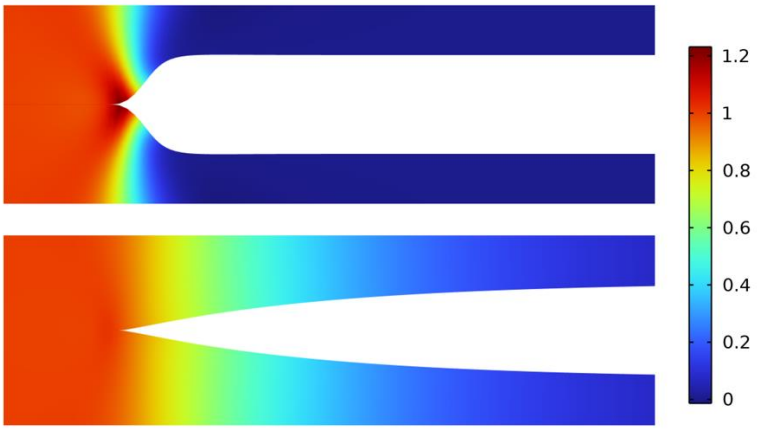

Figure 1. Strain fields, ε_{yy}, surrounding a crack for small D=0.25 (top image) and large D=4 (bottom image). The low Deborah number strain field resembles a linear elastic fracture, while the strain field for large Deborah number is significantly different and predominantly one-dimensional.

de Gennes, P. G. 1996 Soft Adhesives. Langmuir 12 (19), 4497–4500

COM/009: Dynamics of Confined Bubbles in Shear-Thinning Liquids: Toward Improved Photobioreactor Performance

[1*]Zhao, Runqi; [2]Kant, Pallav; [3]Anastasiou, Antonios; [4]Fonte, Cláudio P.

[1]Department of Chemical Engineering, The University of Manchester, Manchester M13 9PL, United Kingdom runqi.zhao@postgrad.manchetser.ac.uk. [2]Department of Mechanical and Aerospace Engineering, The University of Manchester, Manchester M13 9PL, United Kingdom pallav.kant@manchetser.ac.uk. [3]Department of Chemical Engineering, The University of Manchester, Manchester M13 9PL, United Kingdom antonios.anastasiou@manchester.ac.uk. [4]Department of Chemical Engineering, The University of Manchester, Manchester M13 9PL, United Kingdom claudio.fonte@manchester.ac.uk. *Presenting Author

The efficient cultivation of microalgae is crucial for sustainable bioresource production and CO_2 mitigation, yet photobioreactor performance remains limited at high cell concentrations. In particular, cultures exceeding 30 g/L exhibit pronounced shear-thinning behaviour, which significantly alters gas holdup and gas–liquid mass transfer rates. Moreover, such high biomass densities lead to severe light attenuation, reducing the effective light available to individual cells and thus limiting photosynthetic productivity. This study investigates the dynamics of gas bubbles rising through shear-thinning media under geometric confinement, as encountered in flat-panel photobioreactors. Experiments and computational fluid dynamics (CFD) simulations are conducted within a Hele-Shaw cell (~1 mm gap), representing a simplified 2D confined geometry. A validated numerical model accurately predicts bubble terminal velocities and shapes in Newtonian fluids across a range of bubble diameters. The model is extended to shear-thinning fluids assuming the Ostwald–de Waele rheological model, enabling systematic analysis of the effects of flow behaviour index, n, and consistency index, K, on confined bubble dynamics. Results reveal that shear-thinning markedly modifies bubble morphology and rising velocity, with implications for gas–liquid mass transfer. Preliminary experiments in model non-Newtonian fluids (Xanthan gum) support the numerical results. These findings contribute to the understanding of multiphase transport in non-Newtonian media and inform the design of intensified photobioreactors for high-density microalgal cultures.

COM/010: COLLECTIVE HYDRODYNAMICS OF LIVING FLUIDS AT LOW REYNOLDS NUMBERS

[1*]Raghuram, Srinivasan

[1]National Institute of Technology Karnataka, Surathkal, Mangaluru 575025. *Presenting Author

Coordinated motion of closely-packed, suspended swimming microorganisms on length scales (10 - 100 microns), much larger than their size (about 3 microns) is well known. The chemical energy stored in the microorganisms, drives their molecular motors, performing mechanical work on the fluid they are suspended to, causing fluid motion. This spontaneous motion of this *living fluid* can thus happen at equilibrium, in the absence of any imposed gradients! This self-propulsive mechanism of microswimmers produces a net force-dipole causing a long-range hydrodynamic disturbance field. This disturbance field induces stress in the complex fluid, influencing the motion of other microorganisms, resulting in their collective motion.

Bacterial cells, are of particular interest, especially, when they exhibit long periods of straight swimming, separated by much shorter tumbling events. The self-propulsive mechanism in the case of Escherichia coli or Basillus subtilis is using five or six flagella that are rotated by molecular motors. When the motors rotate counterclockwise (when seen from behind), the flagella, in the form of rigid, screw-shaped bundles, rotates to propel the bacterium in a nearly straight path. When one of the motor changes direction, the cell rotates chaotically (tumbles), due to unravelling of the bundle. The flagella produce propulsive force along the axis of rotation, while the drag force for slender bodies along the axis is twice as low compared to the drag force perpendicular to the axis, resulting in a net propulsive force on the cell-flagella unit. The behaviour and prediction of such complex living fluid flows is less understood and appropriate models need to be developed towards this end.

The characteristics of fluid motion can be inferred by performing an ensemble average of a detailed microscopic approach, where the microstructure of the interacting cells is modelled. In this case, the coupling between fluid stresses induced by the rotation of the swimmers and the swimming stresses can also be considered. An active swimmer thus induces stresses on the suspension due to the coupling of swimmer orientation, the fluid flow field and the self-propulsive action, which play pivotal roles in the stability/instability of the suspension. The present work aims at bridging the gap that exists between the findings from experimental observations and theory by using appropriate models for the boundary conditions in the problem.

COM/011: Capillary entry pressure of a hydrogel packing

[1*]Wei, Hangkai; [2]Paulin, Oliver; [1]Cuttle, Callum; [3]Hennessy, Matthew; [1]MacMinn, Chris

[1]Dept. Engineering Science, University of Oxford. [2]Max Planck Institute for Dynamics and Self-Organization. [3]University of Bristol. *Presenting Author

The capillary entry pressure of a porous medium is defined as the minimum pressure required for a non-wetting fluid to start invading the porous medium by displacing the wetting fluid, typically beginning at the largest pore. In rigid porous media, this pressure is governed by the properties of the two fluids and the pore structure, as described by the Young–Laplace equation. However, in soft porous media, the applied pressure can induce compression, reducing pore size and consequently increasing the capillary entry pressure. This mechanical-fluidic coupling challenges the conventional notion that capillary entry pressure is an intrinsic material property.

In this study, we employ both experiments and modeling to investigate the capillary entry pressure during a forced-drainage process of a soft porous medium composed of a packing of hydrogel beads (~1 mm in diameter), where the hydrogel beads themselves exhibit nanoscale porosity (~10 nm). Our results demonstrate that (i) capillary entry pressure increases as the porous medium undergoes compression due to applied pressure and (ii) this increase persists even after fluid invasion has commenced, which our model fails to predict even when accounting for deformation-dependent pore closure. Further investigation rules out pore-size distribution as the primary factor and instead identifies the poro-viscoelastic creep behavior of hydrogels—where the packing progressively compresses under sustained pressure—as the dominant mechanism governing this phenomenon.

ENV: Environmental flows (including coastal, riverine and urban fluid mechanics)

ENV/001: Propagation of Flood Model Uncertainty in Structural Design

[1*]Albuhairi, Danah; [2]Di Sarno, Luigi

[1]Department of Civil and Environmental Engineering, School of Engineering, The University of Liverpool, Liverpool L69 3BX, UK. Danah@liverpool.ac.uk

[2]Department of Civil and Environmental Engineering, School of Engineering, The University of Liverpool, Liverpool L69 3BX, UK. Luigi.Di-Sarno@liverpool.ac.uk

Flood hazard presents a growing global risk, particularly to communities and critical infrastructure. Among the most significant parameters influencing flood risk are depth and velocity, both of which directly inform engineering design and risk assessments. These parameters are typically derived from multi-stage hydrologic and hydraulic models, which are inherently embedded with aleatory and epistemic uncertainties. While recent studies have focused on reducing these uncertainties, a persistent gap remains between the probabilistic basis of flood models and their deterministic application in infrastructure design. This misalignment is especially problematic when hazard maps inform the design of high-consequence assets, as neglecting uncertainty can lead to both overdesign and catastrophic under-design. Critically, uncertainty affects all modelling contexts, including high-resource environments with access to advanced tools and data. However, in low-resource settings, this issue is exacerbated with the use of simplified or empirical methods due to capacity constraints. The absence of such information compounds the risk of misinformed design, especially where industrial or critical infrastructure is involved. To address this systemic issue, this study introduces a tiered classification framework for flood modelling, grounded in a state-of-the-art review of hydrologic and hydraulic methods. Hydrologic modelling tiers range from empirical flow estimates to probabilistic discharge simulations, while hydraulic modelling spans from indicative mapping to full hydrodynamic simulations based in governing flow equations. Drawing from this review, a decision matrix is developed to align model capabilities with the demands of structural design practice by evaluating the adequacy of the flood hazard parameters relative to engineering design thresholds. This alignment exposes key mismatches between modelling assumptions and the deterministic assumptions typically applied in design criteria. Where probabilistic outputs are available, the Propagated Uncertainty Index (PUI) is introduced to quantify the extent to which model uncertainty encroaches upon design thresholds, defined as the ratio of a flood parameter's confidence interval to its associated design value. The framework is demonstrated in a fluvial case study, illustrating how model fidelity, uncertainty treatment, and design implications interact in practice.

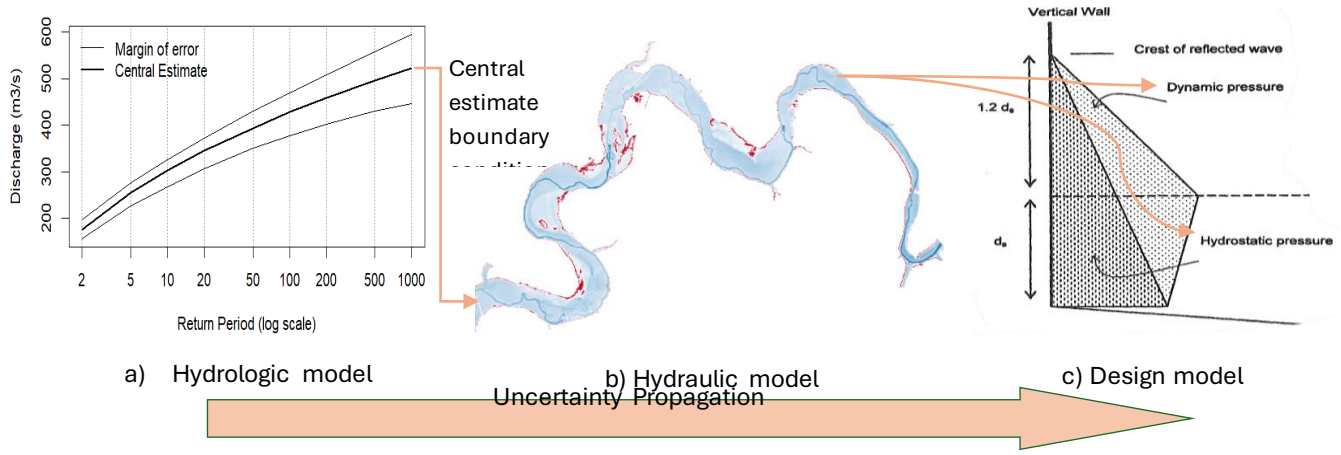

Figure 3. Standard flood modelling practice: deterministic chaining and unquantified uncertainty in design application.

ENV/002: SPH MODELLING OF RIVERINE FLOOD FLOW AT BRIDGE PIERS - *Poster*

[1*]Mogrovejo Villena, David Eduardo; [2]Majtan, Eda

[1]School of Engineering, University of Liverpool, Liverpool, UK, sgdmogro@liverpool.ac.uk

[2]School of Engineering, University of Liverpool, Liverpool, UK, eda.majtan@liverpool.ac.uk (Corresponding Author)

*Presenting Author

Bridges play a critical role in transportation infrastructure both in the UK and globally. In recent decades, climate change has increased the frequency and severity of flood events, leading to numerous instances of bridge damage and collapse. Previous research has extensively examined flood-related scour and substructure behaviour, while the effects of flooding on bridge superstructures have not been fully understood. The paper addresses this gap by aiming to quantify the flood-induced loads on bridge piers.

The numerical modelling of fluid-structure interactions (FSI) is complex due to the challenge of reproducing all relevant physics between fluid and structure, which requires a high level of temporal and spatial resolution. To overcome this difficulty, the FSI between the floating debris and water flow was simplified using one-way coupling where the floating debris was defined as a rigid body moving in relation to the fluid without consideration of the structure's response (Majtan et al., 2021). A two-way coupling method for a floating object in free surface flows was introduced using a mesh-based method (Wu et al., 2014). To overcome the drawbacks of the mesh-based approaches for the FSI between a floating object and fluid, a two-way coupling using the Smoothed Particle Hydrodynamics (SPH) method coupled with DEM was developed (Canelas et al., 2015). Although their work successfully simulated the two-way coupling between fluid and floating objects, the contact mechanics were not fully investigated. Their group recently developed a new DEM-based method with detailed contact modelling, called Project Chrono in DualSPHysics software (https://dual.sphysics.org/) coupling with the multiphysics library Project Chrono (Martínez-Estévez et al., 2023). The present research uses the DEM-P based on a penalty-based methodology where the structures are allowed to deform locally. A detailed parametric study on stiffness and contact properties was first performed. The developed method was then used to investigate riverine flood-induced hydrostatic, hydrodynamic and debris impact loads on bridge piers.

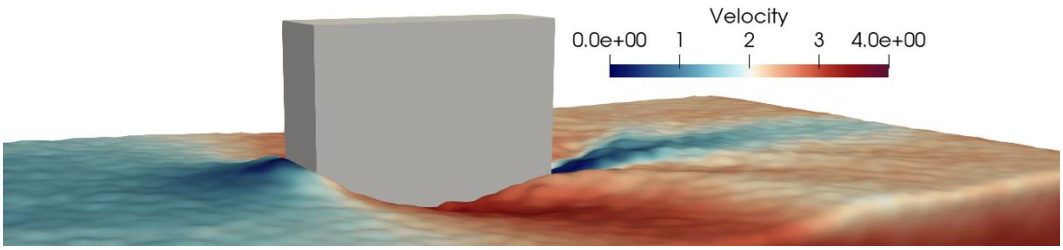

Figure 1. Riverine flood velocity distribution at a bridge pier without a cutwater (m/s)

Canelas, R. B., Domínguez, J. M., Crespo, A. J. C., Gómez-Gesteira, M., & Ferreira, R. M. L. (2015). A Smooth Particle Hydrodynamics discretization for the modelling of free surface flows and rigid body dynamics. *International Journal for Numerical Methods in Fluids*, *78*(9), 581-593. https://doi.org/https://doi.org/10.1002/fld.4031

Majtan, E., Cunningham, L. S., & Rogers, B. D. (2021). Flood-Induced Hydrodynamic and Debris Impact Forces on Single-Span Masonry Arch Bridge. *Journal of Hydraulic Engineering*, *147*(11), 04021043. https://doi.org/doi:10.1061/(ASCE)HY.1943-7900.0001932

Martínez-Estévez, I., Domínguez, J. M., Tagliafierro, B., Canelas, R. B., García-Feal, O., Crespo, A. J. C., & Gómez-Gesteira, M. (2023). Coupling of an SPH-based solver with a multiphysics library. *Computer Physics Communications*, *283*, 108581. https://doi.org/https://doi.org/10.1016/j.cpc.2022.108581

Wu, T.-R., Chu, C.-R., Huang, C.-J., Wang, C.-Y., Chien, S.-Y., & Chen, M.-Z. (2014). A two-way coupled simulation of moving solids in free-surface flows. *Computers & Fluids*, *100*, 347-355. https://doi.org/https://doi.org/10.1016/j.compfluid.2014.05.010

ENV/003: The role of mechanical weathering in microplastic transport: Effect of simulated river abrasion on settling velocity - *Poster*

[1*]O'Callaghan, Michael; [2]Bridgeman, John; [3]Ockelford, Annie

[1]University of Liverpool, mwaoc@liverpool.ac.uk; [2]University of Liverpool, John.Bridgeman@liverpool.ac.uk; [3]University of Liverpool, a.ockelford@liverpool.ac.uk

Microplastic contamination is ubiquitous, and with their main transport conduit being river systems there is a need to better understand the controls on their movement in order predict and remediate their transport. Microplastic transport deviates from conventional sediment transport due to the complex shape and variable densities of the microplastics (Horton and Dixon, 2018), which makes tracking their movement and fate difficult. Although predictive formulas have risen to address this challenge (Zhang and Choi, 2025), they are primarily based on data taken from pristine plastics. Further, adapted predictive models do not tend to account for the effects of weathering, especially by mechanical processes, on settling velocity (Alimi et al., 2022; Guo et al., 2024). Where abrasion processes are incorporated into models, they are typically included in tandem with other weathering mechanisms, such as UV ageing, where studies have shown that exposure to abrasive environments can lead to increasing sphericity as well as causing deformations on their surface (Bullard et al., 2022). Despite this, there is currently limited research on how this may impact microplastic transport and fate in the environment.

Through the development and evaluation of new methods of inducing microplastic mechanical degradation, 3mm PA (1.14 g/cm^3), PMMA (1.18 g/cm^3), and PS (1.05 g/cm^3) spheres were abraded over 10 minutes to 8 hours using a roller mixer, orbital shaker, and racetrack flume. The effect of this mechanical exposure was analysed morphologically through optical profilometry (Figure 1) and chemically through FT-IR analysis. Once weathered microplastic samples were dropped into a quiescent water column to measure their settling velocity. Results were compared with the measured settling velocities of smooth microplastic particles.

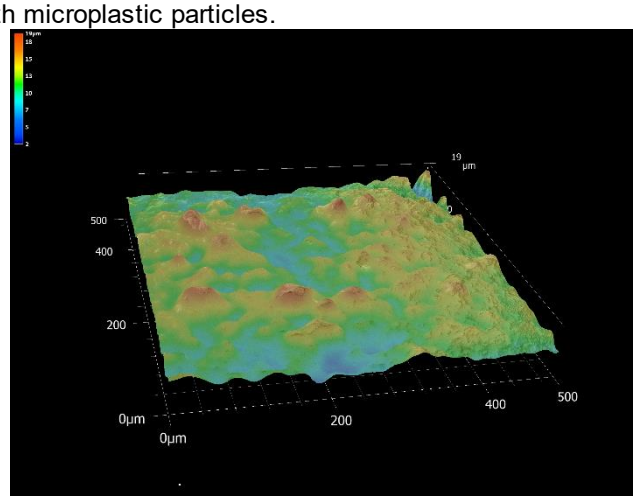

Figure 4 – 3D surface elevation of a polystyrene sphere rolled with sand for 8 hours.

Alimi, O.S., Claveau-Mallet, D., Kurusu, R.S., Lapointe, M., Bayen, S. and Tufenkji, N., 2022. Weathering pathways and protocols for environmentally relevant microplastics and nanoplastics: What are we missing?. *Journal of Hazardous Materials*, *423*, p.126955.

Bullard, J.E., Zhou, Z., Davis, S. and Fowler, S., 2022. Breakdown and modification of microplastic beads by aeolian abrasion. *Environmental science & technology*, *57*(1), pp.76-84.

Guo, M., Noori, R. and Abolfathi, S., 2024. Microplastics in freshwater systems: Dynamic behaviour and transport processes. *Resources, Conservation and Recycling*, *205*, p.107578.

Horton, A.A. and Dixon, S.J., 2018. Microplastics: An introduction to environmental transport processes. *Wiley Interdisciplinary Reviews: Water*, *5*(2), p.e1268.

Zhang, J. and Choi, C.E., 2025. Towards A universal settling model for microplastics with diverse shapes: Machine learning breaking morphological barriers. *Water Research*, *272*, p.122961.

ENV/004: DYNAMICS OF ATMOSPHERIC ROTORS

[1]*Rungta, Vartika; [2]Ross, Andrew; [3]Sheridan, Peter; [4]Vosper, Simon; [5]Khan, Amirul

[1]University of Leeds, scvr@leeds.ac.uk. [2]University of Leeds, School of Earth & Environment, a.n.ross@leeds.ac.uk. [3]Met Office, Exeter, peter.sheridan@metoffice.gov.uk. [4]Met Office, Exeter, simon.vosper@metoffice.gov.uk. [5]University of Leeds, Civil Engineering, a.khan@leeds.ac.uk. **Presenting Author

Lee-side turbulence in mountains can give rise to several extreme weather phenomena, one of which are **rotors.** They occur as a consequence of a temperature inversion and stable stratification of the atmosphere which leads to flow trapping and flow circulation about an axis parallel to the mountain ridge. These cause either hydraulic jumps and/or travelling rotor trains, both of which are hazardous to any low level flights due to a lower turbulence zone. The evolution and eventual decay of these rotors is difficult to predict, and pilots are often unaware of them before flying into them. Mount Pleasant Airfield (MPA) at the East Falkland Islands has been a site for the study of rotors for the last 3 decades primarily due to the location of an airfield immediately downstream of a mountain ridge. A high resolution (300m x 300m) forecast model and a higher resolution (50m) doppler LIDAR observations present a unique opportunity to sketch a life cycle of rotors as they form, reach a peak, and eventually decay. This research aims to utilize the rich dataset to first evaluate if the resolution of the model is enough to capture the variability of the winds, sketch a structural formation and decay of rotors using the LIDAR variability, and understand the Physics of rotors that can be applicable to mountain side turbulence everywhere around the world. The final goal of the research is to evaluate windows for safe flight during a rotor event so pilots can be safely informed.

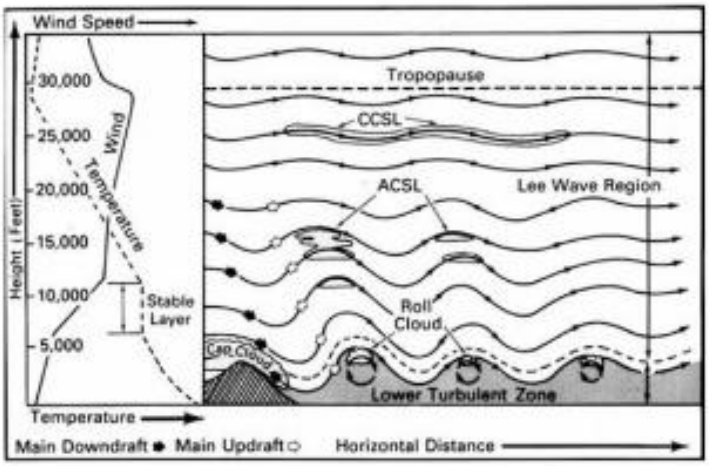

Figure 1. Schematic of a 2D rotor system showing trapped recirculating waves that rotate about an axis parallel to the ridge (in the lateral direction) as a consequence of flow trapping caused by stable statification and a temperature inversion in the atmosphere source: Hertenstein and Kuettner [2005]

Rolf Hertenstein and Joachim Kuettner. Rotor types associated with steep lee topography: influence of the wind profile. Tellus A, 57, 03, 2005. doi: 10.3402/tellusa.v57i2.14625.

ENV/005: EFFECTS OF BRIDGE PIERS ARRANGEMENT ON LOCAL SCOUR

[1] *Rasouli Pirouzian, Farid; [2] Majtan, Eda; [3] Wang,Yu

[1] School of Computing, Science & Engineering, University of Salford M5 4WT, UK, f.rasoulipirouzian@edu.salford.ac.uk

[2] School of Engineering, University of Liverpool L69 3GB, UK, eda.majtan@liverpool.ac.uk

[3] School of Computing, Science & Engineering, University of Salford M5 4WT, UK, y.wang@salford.ac.uk

* Rasouli Pirouzian, Farid

Scour, the localised erosion of soil surrounding foundations, is one of the major factors playing in the wide failure of infrastructures. Local scour can significantly reduce the stability and bearing capacity of bridge substructure leading to catastrophic consequence on lives and economy. For this reason, the challenge of scour must be effectively addressed for bridge design and assessments. However, due to the complicated multi-physical mechanisms involved in this engineering problem, deep understanding and knowledge in the scour faced in wide engineering projects and practices still remains of limitation. In this situation, numerical modelling plays an important and effective approach helping on estimating this complex multi-physics problem.

This study employs mesh-based finite volume method in open-source OpenFOAM software to investigate the performance of two configurations—two side-by-side and a cluster of four 3:2 rectangular cylinders—in reducing scour potential. The aim is to alter the flow around the piers to mitigate horseshoe vortices and downflow effects. Recommended models incorporating turbulence closures are used to predict bed shear stress for various pier arrangements. By reducing bed shear stress, these arrangements demonstrate their effectiveness in mitigating scour.

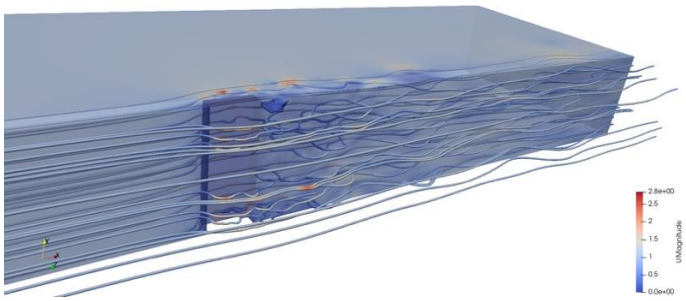

Figure 5. Velocity distribution with streamlines around a bridge pier (m/s)

Keywords: Scour, Bridge pier, Computational fluid dynamics, Erosion, Coastal infrastructure

ENV/006: INVESTIGATING FLOOD-INDUCED PRESSURES ON ARCH BRIDGES USING A WAVELET-BASED APPROACH

[1*]Majtan, Eda; [2]Rogers, Benedict D. and [3]Cunningham, Lee S.

[1]School of Engineering, University of Liverpool, Liverpool, UK, eda.majtan@liverpool.ac.uk

[2]School of Engineering, University of Manchester, Manchester, UK, Benedict.Rogers@manchester.ac.uk

[3]School of Engineering, University of Manchester, Manchester, UK, lee.scott.cunningham@manchester.ac.uk

*Presenting Author

Masonry arch bridges form a critical part of the UK's transport infrastructure, with over 50,000 such structures in service, many spanning rivers and watercourses. In recent decades, extreme flood events have caused significant damage and even collapse of several UK masonry arch bridges, including notable failures at Braithwaite Bridge (2009), Linton Bridge (2015), Tadcaster Bridge (2015) and Llanerch Bridge (2021), highlighting the urgent need to understand the effects of flood-induced load on historic masonry arch bridges. This study experimentally investigates the flood-induced effects on a single-span arch bridge with a specific focus on the transient hydrodynamic and impact pressures generated during extreme flood events. The 1:10 scaled Perspex bridge was located in the recirculating flume at the University of Manchester, with the dimensions of 4.88 x 1.22 x 0.61 m. To capture detailed flood-induced hydrodynamic and debris impact pressures on key structural components of arch bridges, the pressure sensors with less than 0.05% deviation in repeatability were accommodated on the arch barrel and front spandrel walls (Figure 1). The pressure sensors' range was −20 kPa and +20 kPa in relation to the expected negative pressure on the arch barrel, while the inner (sensing) diameter of the sensors was 25mm (Majtan et al., 2024). Raw data collected in hydraulic experiments are often influenced by noise due to interface disturbances in the testing environment. Selecting an effective signal processing technique is essential for accurately filtering this noise from the data. Flood-induced hydrodynamic and debris impact pressures and forces on structures are typically highly transient, where frequency-domain methods like Fast Fourier transform (FFT) is inadequate for capturing these unsteady signals. Following previous studies in scour monitoring (Fitzgerald et al., 2019), the present study employed the wavelet transform (WT). The wavelet signal analysis is divided into two as: continuous (CWT) and discrete wavelet transform (DWT). This study used the DWT based on its better spatial localisation. To achieve the highest accuracy in the detailed pressure-time histories, the Daubechies mother wavelet with different orders is examined.

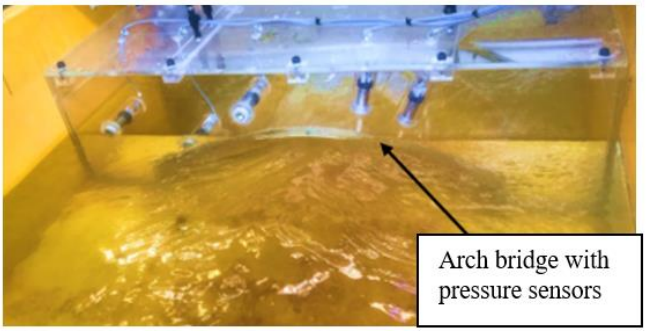

Figure 1. Pressure sensors on the arch barrel and front spandrel wall

Fitzgerald, P. C., Malekjafarian, A., Cantero, D., Obrien, E. J., & Prendergast, L. J. (2019). Drive-by scour monitoring of railway bridges using a wavelet-based approach. *Engineering Structures*, *191*, 1-11. https://doi.org/https://doi.org/10.1016/j.engstruct.2019.04.046

Majtan, E., S., C. L., & and Rogers, B. D. (2024). Riverine flow and floating wooden debris interaction with an arch bridge: flume experiments. *Journal of Hydraulic Research*, *62*(6), 542-559. https://doi.org/10.1080/00221686.2024.2437688

ENV/007: Experimental study of flow in a bottom-heated street canyon

[1,2*]Zhao, Chongyu; [1]Zhong, Shan; [1,2]Kang, Ximeng; [2]Topping, David

[1]Department of Mechanical, Aerospace and Civil Engineering, The University of Manchester, Manchester M13 9PL, UK

[2]Department of Earth and Environmental Sciences, The University of Manchester, Manchester M13 9PL, UK

chongyu.zhao@postgrad.manchester.ac.uk; shan.zhong@manchester.ac.uk; ximeng.kang@postgrad.manchester.ac.uk; david.topping@manchester.ac.uk

Buoyancy flow induced by a solar-heated bottom significantly influences the flow in street canyons, affecting the mechanisms of pollutant dispersion. Understanding this interaction is key to improving our knowledge of urban air quality dynamics. A series of experiments was conducted in a 0.9 m×0.9 m×5 m open-circuit suction wind tunnel. The wind speed was lower than 2 m/s, with the bottom temperature varied from room temperature to 200℃, to achieve a high Richardson number and maximize the influence of buoyancy flow. The height, width and length of the canyon were 10cm, 10cm and 90cm, which could be considered as two-dimensional. A streamlined leading edge ensured a laminar oncoming flow. 5400 snapshots of flow fields in the canyon were captured by the high-speed PIV at the frequency of 800Hz. The resolution of the high-speed Dantec SpeedSense 9070 camera was 1280×800 pixel^2. The multi-pass cross-algorithm with an interrogation window of 8×8 pixel^2 was used and led to a vector resolution of 0.8 mm. The effects of the buoyancy flow generated by the heated bottom can be clearly observed from both the time-resolved flow fields and the time-averaged flow fields, which weakens the downwards flow near the windward wall and strengthens the upwards flow near the leeward wall. Dynamic mode decomposition (DMD) method extracts and reconstructs dominate osillation flow components in the canyon to evaluate the effects of buoyancy flow in the frequency domain. λ_{ci} criterion and finite-time lyapnov exponent depict the time-resolved flow in the canyon well. The combined analysis revealed the formation and development of shear layers at the canyon top, internal circulation patterns, and the critical role of buoyancy flow in altering flow in the canyon.

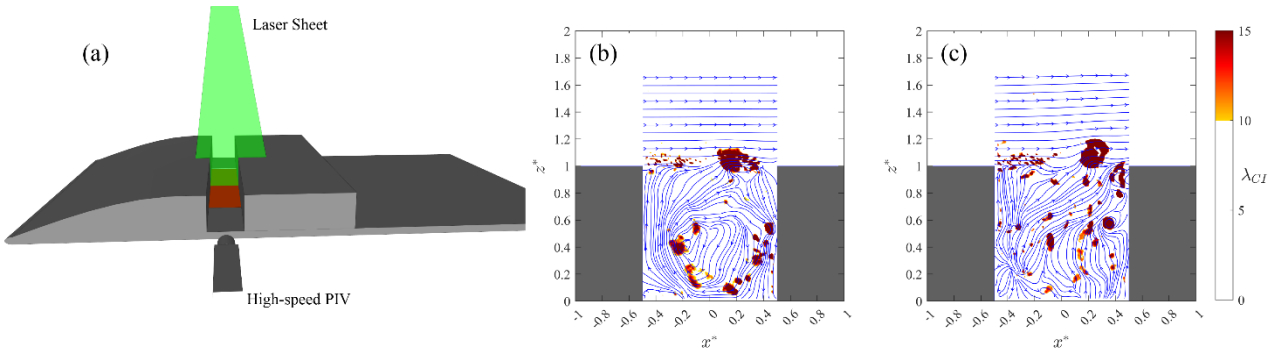

Figure 1. (a) Experimental setup. (b) Streamlines and contours of λ_{ci} on the central vertical plane for the 2D canyon without a heated bottom. (c) Same, with a heated bottom.

Bengana, Y., J.-Ch. Loiseau, J.-Ch. Robinet, and L. S. Tuckerman., 2019, Bifurcation Analysis and Frequency Prediction in Shear-Driven Cavity Flow. *Journal of Fluid Mechanics* 875: 725–57.

Callaham, Jared L., Steven L. Brunton, and Jean-Christophe Loiseau., 2022, On the Role of Nonlinear Correlations in Reduced-Order Modelling. *Journal of Fluid Mechanics* 938: A1.

ENV/008: Flow Regimes and Modal Dynamics in Urban Canyon Arrays under Varying Atmospheric Stability

[1*]Kang, Ximeng; [1] Rezaeiravesh, Saleh; [1]Zhao, Chongyu; [1]Topping, David; [1]Revell, Alistair

[1] Faculty of Science and Engineering, The University of Manchester, Oxford Road, Manchester, M13 9PL.
ximeng.kang@postgrad.manchester.ac.uk. *Presenting Author

Atmospheric stability plays a critical role in shaping urban airflow patterns and temperature distribution, directly influencing pedestrian comfort and air quality (Mei & Yuan 2022). Although extensive studies have investigated urban canyons, most have focused on parametric analyses or environmental performance, with relatively limited attention to the underlying fluid dynamics. On the other hand, fluid mechanics studies often rely on simple models—such as isolated cubes or 2D canyons—and are typically conducted under neutral stability condition, limiting their applicability to more realistic urban environments. This study advances the field by simulating a periodic domain composed of a 5 × 8 array of cubes using Wall-Resolved Large Eddy Simulation (WR-LES) at friction Reynolds numbers ($Re_\tau \approx 1400$–2000) under varying atmospheric stability conditions, characterized by different Richardson numbers. The simulations were validated and analyzed using modal decomposition methods—POD for energy perspective and DMD for frequency perspective. The results reveal two dominant modes: dynamics within the inner cavity and shear layer instability, consistent with previous findings (Callaham et al. 2022). Under unstable conditions, a new buoyancy-driven upward mode emerges. Notably, two distinct flow regimes—recirculation-dominated and upward-flow-dominated—are identified, alongside two temporal transition types: small-fluctuation-induced shifts and fully developed pattern transformations. This study also explores the connection between flow pattern transitions within the canyons and large-scale motions above the canyons.

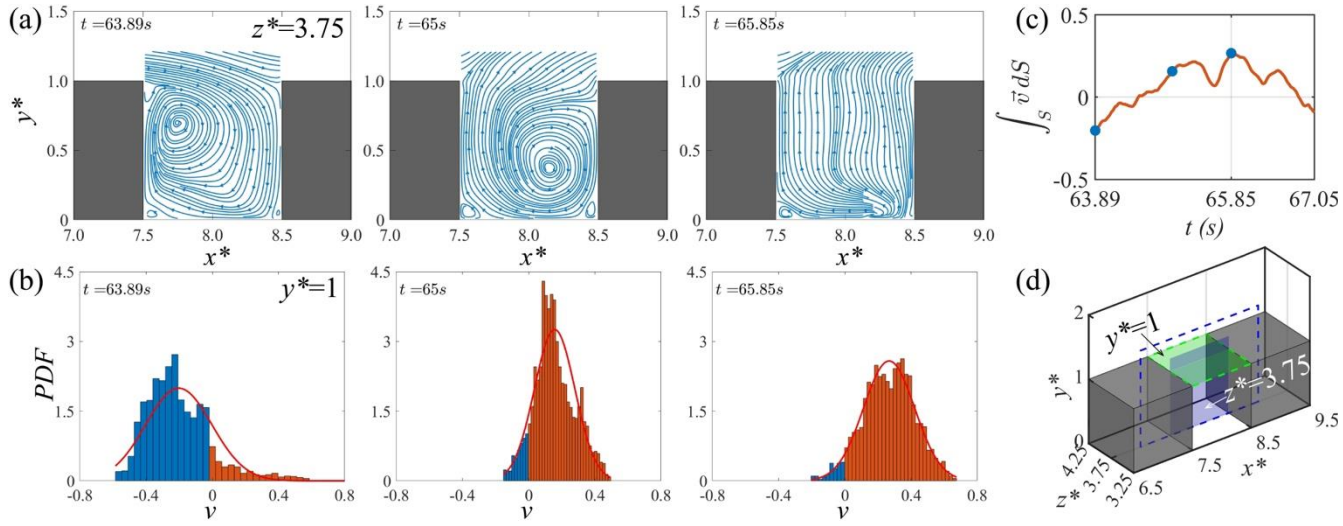

Figure 1. Temporal transition type T2: fully developed pattern transformations illustrated by (a) streamlines at the middle slice ($z^*= 3.75$) and (b) the probability density function (PDF) of the vertical velocity across the canyon top surface at $y^*= 1$, and the snapshots in (a) and (b) are selected from the time history of integrated vertical velocity over the canyon top shown in (c). Slice locations are indicated in (d).

Mei, S. and Yuan, C., 2022, Urban buoyancy-driven air flow and modelling method: A critical review. Built Environ. 230, 108708.

Taira, K., Brunton, S. L., Dawson, S. T. M., et al., 2017, Modal Analysis of Fluid Flows: An Overview. AIAA J. 55 (12) pp 4013–4041.

Callaham J. L., Brunton S. L., Loiseau J-C., 2022, On the role of nonlinear correlations in reduced-order modelling. J. Fluid Mech. 938:A1.

ENV/009: Waste Shells to Flood Control: A Numerical Study of Permeable Seashell Concrete Performance

[1*]Khajenoori, Leila; [2]Nasriani, Hamid Reza; [3]William, Karl S; [4]Anike, Emmanuel Ejiofor

[(1,2,3,4)] School of Engineering and Computing, University of Central Lancashire, Preston, UK

[1] lkhajenoori@uclan.ac.uk, [2] hrnasriani@uclan.ac.uk, [3]kswilliams@uclan.ac.uk, [4]eanike@uclan.ac.uk, [5]DKeller@uclan.ac.uk

As urban development accelerates and climate risks intensify, cities face increasing pressure to manage surface water sustainably. In the UK, the National Planning Policy Framework (NPPF) and its associated technical guidance state that priority should be given to sustainable drainage systems (NPPF, 2019) .
Permeable concrete is an alternative paving material that can effectively address growing environmental challenges by allowing rainwater to percolate into the ground and support urban SuDS. However, its environmental benefit is often diminished by the use of non-renewable aggregates. Consequently, several studies have investigated the substitution of natural aggregate with other materials, such as recycled aggregates, slag aggregates, and, more recently, seashells. (Gesoğlu et al., 2012; D. Nguyen et al., 2017; Tota-maharaj et al., 2017). The work described here involves evaluating the hydrological performance of a draining cast-in-place concrete pavement based on the substitution of aggregate with waste seashells. This concrete pavement offers a porous surface with a lower environmental impact and is also suitable for application of a low traffic load (Nguyen et al., 2017).

To assess the hydrological behaviour of this shell-based concrete pavement, a three-dimensional numerical model was developed using the Computer Modelling Group (CMG) software. The CMG software was chosen for its capability to simulate complex recovery processes and multi-physics, though it has not typically been used for rainfall and flood management applications. The simulated pavement structure consists of a shell-concrete surface layer, a granular subbase, and a compacted subgrade, incorporating real-world geometric dimensions and.l material parameters derived from laboratory tests and standards.The porosity and permeability parameters are the main evaluation criteria influencing the product's drainage capacity.

The model evaluated drainage performance, volumetric water content (VWC), and capillary pressure effects.

Results showed that the shell-based permeable concrete demonstrated excellent drainage capacity across all tested scenarios. VWC was not significantly affected by rainfall intensity but was highly sensitive to changes in capillary pressure, highlighting the critical role of pore pressure dynamics in system design. The shell-based pavement retained over 60% of rainfall and released it gradually, indicating strong flood mitigation potential. These findings support its application in high flood-risk zones and as a climate adaptation solution.

The applied numerical framework offers an efficient approach to evaluating pavement performance, thereby reducing the need for extensive field trials. This contributes to sustainable urban infrastructure design by promoting the use of low-impact materials and advanced simulation-based engineering.

Gesoğlu, M., Güneyisi, E., Mahmood, S. F., Öz, H. Ö., & Mermerdaş, K., 2012, Recycling Ground Granulated Blast Furnace Slag as Cold Bonded Artificial Aggregate Partially Used in Self-Compacting Concrete. Journal of Hazardous Materials. 235–236 pp 352–358.

Nguyen, D., BOUTOUIL, M., Sebaibi, N., Baraud, F., & Leleyter, L., 2017, Durability of Pervious Concrete Using Crushed Seashells. Construction and Building Materials. 135 pp137–150.

Tota-maharaj, K., Hills, C., & Monrose, J., 2017, Novel Permeable Pavement Systems Utilising Carbon-Negative Aggregate. NexGen Technologies for Mining and Fuel Industries (NxGnMiFu-2017), pp 683-696.

NPPF. (2019). National Planning Policy Framework. Ministry of Housing, Communities and Local Government. https://webarchive.nationalarchives.gov.uk/ukgwa/20210708211349/https://www.gov.uk/government/publications/national-planning-policy-framework--2

ENV/010: MICROPLASTIC FRAGMENTATION IN RIVER SYSTEMS: *Poster*

[1*]Ockelford, Annie; [2]Beaumont, Hazel.

[1*]Department of Civil and Environmental, University of Liverpool, Liverpool, UK. A.ockelford@liverpool.ac.uk. [2]School Engineering, unvierstiy of West of England, Bristol, UK.

Microplastic contamination of river sediments has been found to be pervasive at the global scale and responsive to plastic and sediment bed properties, the flow regime and the river morphology. The physical controls governing the storage, remobilization and pathways of transfer in sand bed rivers remain unquantified. This means it is not currently possible to determine the risks posed by microplastic contamination within these globally significant river systems.

Using controlled flume experiments we show that sand bed rivers can store up to 40% of their microplastic load within the sediment bed indicating that these environments can act as resilient sinks of microplastics. By linking bedform dynamics with microplastic transport characteristics we show that similarities exist between granular transport phenomena and the behavior, and hence predictability, of microplastic flux. Specifically, we demonstrate the inverse relationship between bedform celerity and microplastic retention within the bed can be used to predict microplastic flux. Further, we show that, in these environments, microplastic shape is more important than previously thought in controlling the fate of microplastics. Together, these findings are significant since they have important implications for the prediction and hence management of microplastic contamination in sand bed environments.

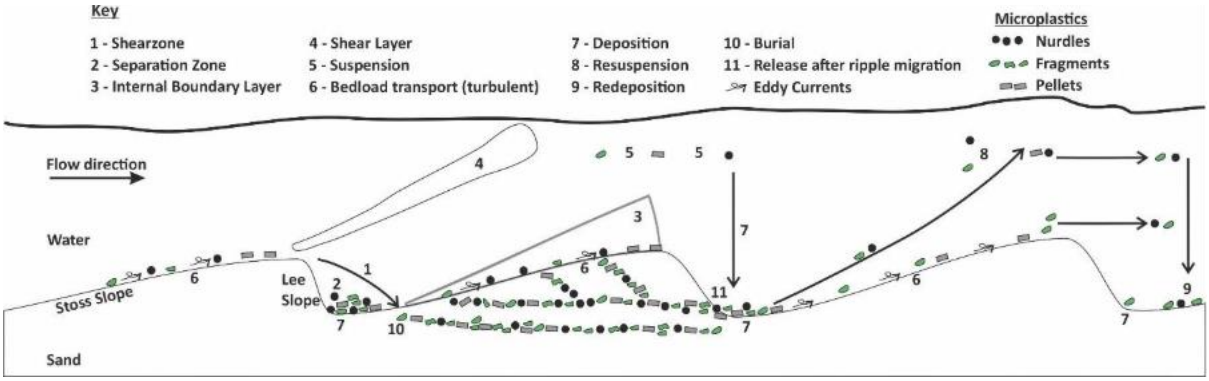

Figure 1. Schematic diagram displaying the different microplastic transport processes as seen in the flume experiments.Here points 1-4 link to interactions between bedform morphology flow dynamics, where points 1-2 are also the inter-ripple areas where microplastics tend to gather. Points 7, 10 and 11 indicate the bedform migration and trapping of microplastics within the sand bed.

GEO: GEOPHYSICAL FLOWS

GEO/001: Gravity current energetics in depth-averaged models

[1*]Skevington, Edward; [2*]Dorrell, Robert

[1]Loughborough University, e.w.skevington@lboro.ac.uk. [2]Loughborough University, r.m.dorrell@lboro.ac.uk. *Presenting Author

Gravity currents are a ubiquitous density driven flow occurring in both the natural environment and in industry. They include: seafloor turbidity currents, primary vectors of sediment, nutrient and pollutant transport; cold fronts; and hazardous gas spills. However, while the energetics are critical for their evolution and particle suspension, they are included in system scale models only crudely, so we cannot yet predict and explain the dynamics and run-out of such real-world flows. Herein, a novel depth-averaged framework is developed to capture the evolution of volume, concentration, momentum, and turbulent kinetic energy from direct integrals of the full governing equations. This novel model generalises two preexisting depth average frameworks. Models such as that proposed by Ellison & Turner (1959) include the effect of the vertical profiles through shape factors in equations describing volume, concentration, and momentum, but do not feature an energy equation. Conversely, models such as that proposed by Parker et al. (1987) assume a top-hat shape, where profiles are uniform over the current and discontinuously vanish above, but do include an equation for the turbulent kinetic energy in addition to the other three quantities. Our analysis allows for vertical profiles to be included in a model which describes the evolution of energy. For the first time, we show the connection between the vertical profiles, the evolution of the depth-averaged flow, and the energetics. We find that the new formulation can describe the full evolution of a shallow dilute current, with the accuracy depending primarily on closures for the profiles and source terms. Using the insights into energetics established, we propose an alternative modelling framework where gravitational potential energy is modelled rather than volume. We achieve a theoretical foundation for describing detrainment in particulate currents, the reduction in entrainment rate that is caused by particle settling. The resulting system of equations is equivalent in the case of top-hat profiles (Wells et al. 2010) but the generalisation to arbitrary profiles is substantially different and allows for entrainment to be robustly described in terms of turbulent statistics.

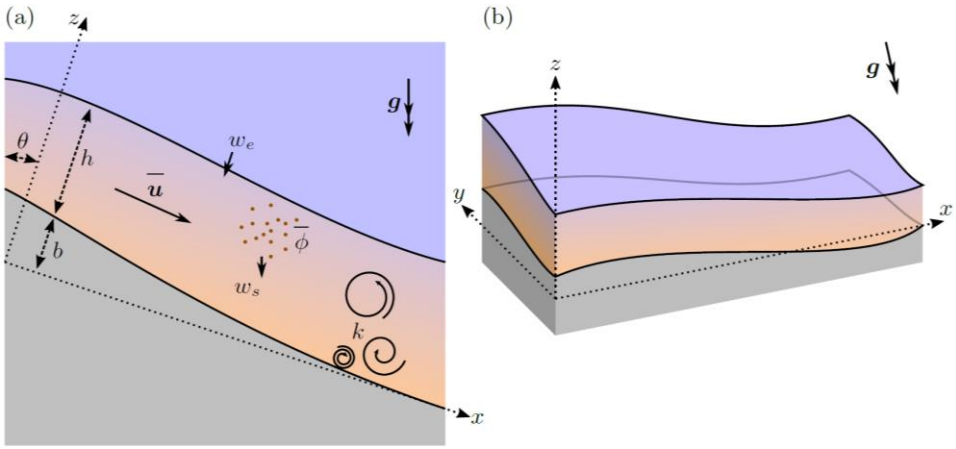

Figure 6: The configuration of the turbidity current, with the bed in grey, ambient in blue, and current in brown fading toward blue in the less concentrated upper regions. (a) A two-dimensional slice oriented with the vertical direction up. (b) A three-dimensional view oriented with respect to the coordinate system.

Ellison & Turner, 1959, Turbulent entrainment in stratified flows, *Journal of Fluid Mechanics* 6(3), pp 423-448

Parker, Garcia & Fukushima, 1987, Experiments on turbidity currents over an erodible bed, *Journal of Fluid Mechanics* 25(1), pp 123-147

Wells, Cenedese & Caulfield, 2010, The Relationship between Flux Coefficient and Entrainment Ratio in Density Currents, *Journal of Physical Oceanography* 40(12), pp 2713-2727

GEO/002: Echo State Networks for Nowcasting a Simplified Model of Atmospheric Convection

[1*]Nowakowska, Kasia; [1]Parker, Douglas; [2]Tobias, Steven; [1,3]Tomassini, Lorenzo

[1]University of Leeds, mm17ktn@leeds.ac.uk. [2]University of Edinburgh. [3]Met Office,UK. *Presenting Author

Echo State Networks (ESNs) are an adaptation of recurrent neural networks, specialised for time-accurate prediction of chaotic dynamical systems. ESNs utilise a unique reservoir framework, where a fixed, sparsely connected reservoir of nodes transforms the input into a high-dimensional space. This study explores the use of ESNs for short-term forecasting, or nowcasting, of atmospheric convection and storm initiation. Nowcasting refers to the current state of the weather and predictions for the near future, typically 0-6 hours ahead. Prediction of convective storms within this time frame is challenging. Traditional nowcasting has established methods which are effective at tracking the movement of convective cells, however predicting the initiation and decay of cells has proven more difficult.

This research investigates convective initiation by simulating a simplified model for moist convection known as the Rainy-Bénard model, which extends classical Rayleigh-Bénard convection. In this model, convective initiation is influenced by gravity waves, which play a role in the triggering and organisation of convection. Our objective is to evaluate the predictive capability of ESNs on this simplified model of convection and to enhance our understanding of gravity wave initiation. Our results demonstrate that ESNs trained on global parameters of the system exhibit good skill in predicting the timing of convective events.

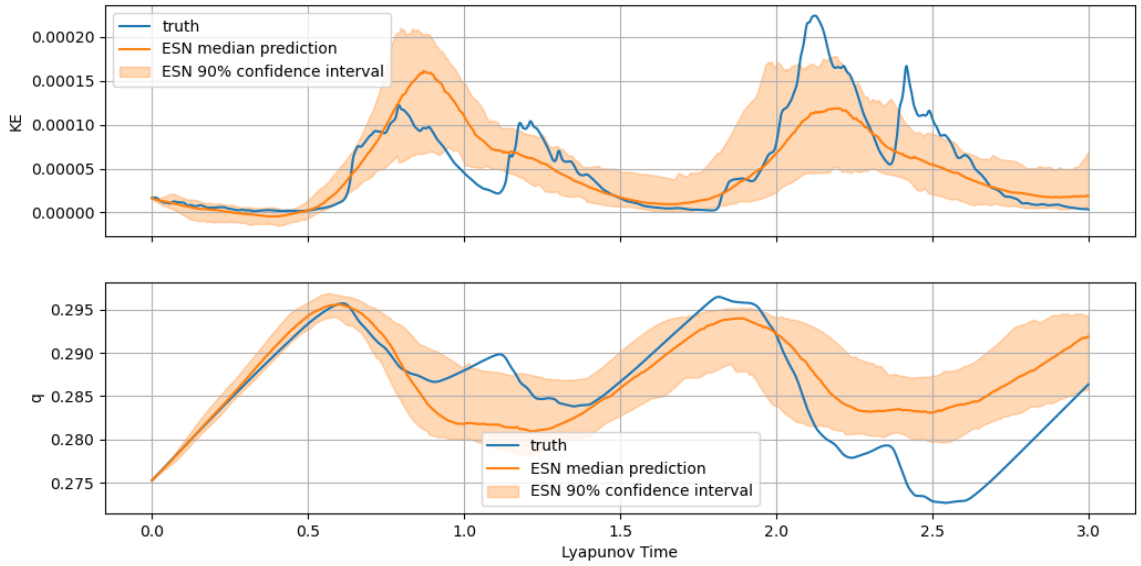

Figure 1. Prediction of global kinetic energy (KE) and moisture (q) using the Echo State Network. The blue line indicates the true global parameters from the Rainy-Bénard model, the orange line and the shaded region are the median prediction and the 90% confidence interval from 100 ensemble members, respectively.

GEO/003: Dynamics of rotating convection in the tangent cylinder

[1*]Kershaw, J K; [1]Davies, C.E; [2]Tobias, S, M; [1]Mound, J E,

[1]University of Leeds. [2]Edinburgh University. *scjkk@leeds.ac.uk

Understanding the flow dynamics of the electrically conducting liquid in Earth's outer core is a first step towards deciphering the mechanisms responsible for generating our planet's magnetic field. Numerical models rely on simplifying assumptions to capture the complex non-linear dynamics operating across extensive temporal and spatial scales. Complementary laboratory experiments, conducted in various curvilinear geometries, provide validation for theoretical predictions by offering easier access to certain parameter ranges, such as very low Ekman numbers, which are challenging to model numerically.

This talk presents an analysis of rotating convection specifically within the tangent cylinder region, utilizing data interpolated from spherical shell simulations onto cylindrical grids. Through examination of local force balances and kinetic and thermal transport properties, I highlight both similarities and differences compared to plane-layer convection bounded by sidewalls, as well as convection within the full spherical shell, focusing on the sidewall boundary and how its distinct dynamics shape the overall flow characteristics.

Finally, I address how these sidewall properties might be effectively reproduced or simplified within cylindrical models, both experimental and numerical. Establishing and validating these simplified boundary conditions can enhance the comparability of future studies, ultimately deepening our understanding of convective processes in the polar regions of planetary cores.

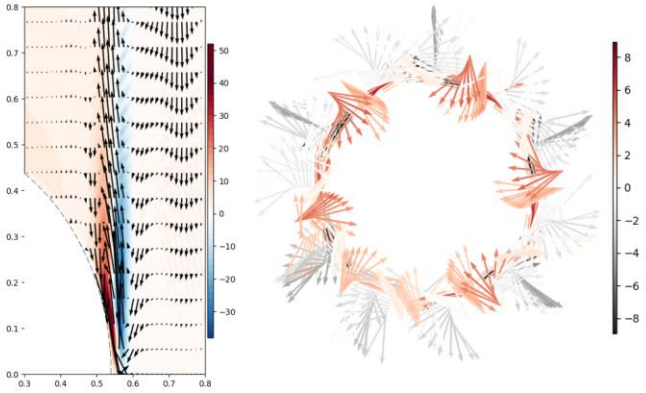

Figure 1. Slices of the tangent cylinder extracted from a spherical shell at Ek=1e-5, Ra=3.5e06. Left: Part of a meridional slice at the tangent cylinder sidewall, showing azimuthal average of velocity, coloured with potential vorticity. Right: horizontal slice with six modes at z=0.2, coloured by vertical velocity.

IND: Industrial applications (including microfluidics, mixing and 3D printing)

IND/001: The effects of adsorption on a particle-laden, sessile droplet undergoing one-sided evaporation

[1*]Sharp, Henry T.; [2,1]Wilson, Stephen K.; [1]Wray, Alexander W.

[1]Department of Mathematics and Statistics, University of Strathclyde, Livingstone Tower, 26 Richmond Street, Glasgow, G1 1XH, henry.sharp@strath.ac.uk, alexander.wray@strath.ac.uk

[2]Department of Mathematical Sciences, University of Bath, Claverton Down, Bath, BA2 7AY,

sw3197@bath.ac.uk

The evaporation of a sessile droplet is a phenomenon that appears in a variety of industrial applications, including inkjet printing and the production of biomarkers. In these applications, droplets contain suspended particles, and the deposition of particles onto the substrate is of considerable interest. In the case of a pinned droplet undergoing evaporation, the morphology of the deposit is determined by the competing effects of evaporation-driven capillary flow advecting particles towards the contact line and particle adsorption onto the substrate [1, 2, 3]. When an evaporating droplet is surrounded entirely by vapour, or when the vapour moves rapidly away from the surface of the droplet, the liquid and gas phases decouple, and the local evaporative mass flux depends solely on the liquid phase [4]. In this case, the associated thermodynamic disequilibrium at the liquid-gas interface drives evaporation and the local evaporative mass flux is described by the so-called "one-sided" model of evaporation [4, 5]. This is in direct contrast with the widely-studied case of diffusion-limited evaporation in which the local evaporative mass flux depends on the transport of vapour in the gas phase [6]. A mathematical model is formulated and analysed that predicts the concentration of suspended particles within a pinned, thin, particle-laden, axisymmetric, droplet undergoing one-sided evaporation incorporating particle adsorption onto the substrate. In particular, this model is used to predict the evolution of the mass of particles suspended within the droplet and adsorbed onto the substrate. Unlike in the absence of adsorption, in which all of the particles are advected to the contact line forming a coffee ring deposit, in the presence of adsorption, there is no coffee ring and all of the particles are adsorbed onto the substrate within the footprint of the droplet. The rate at which particles are adsorbed onto the substrate is governed by the Damköhler number, which gives a measure of the relative significance of the effects of adsorption compared to the effects of thermodynamic disequilibrium at the liquid-gas interface. It is shown that there exists a critical Damköhler number below which the particle concentration at the contact line is singular, and above which it is zero.

[1] Widjaja, E., Harris, M. T., AIChE Journal **54**(9), 2250–2260 (2008)

[2] Zigelman, A., Manor, O., Journal of Colloid and Interface Science **509**, 195–208 (2018)

[3] D'Ambrosio, H.-M., Wray, A. W., Wilson, S. K., Journal of Engineering Mathematics **151**(1) (2025)

[4] Burelbach J. P., Bankoff, S. G., Davis S. H., Journal of Fluid Mechanics **195**, 463–494 (1988)

[5] Murisic, N., Kondic, L., Journal of Fluid Mechanics **679**, 665–670 (2011)

[6] Wilson, S. K., D'Ambrosio, H.-M., Annual Review of Fluid Mechanics **55**, 481–509 (2023)

IND/002: Design and Integration of a Vortex T-Mixer Stopped-Flow Device for Time-Resolved SAXS at Synchrotron Beamlines

[1*]Soroor, Mostafa; [2]Terrill, Nick J.; [3]Tyler, Arwen I. I.; [4]Kapur, Nikil

[1]EPSRC CDT in Fluid Dynamics, School of Computer Science, University of Leeds, UK, scmso@leeds.ac.uk. [2]Diamond Light Source, Harwell Science and Innovation Campus, UK, nick.terrill@diamond.ac.uk. [3]School of Food Science and Nutrition, University of Leeds, UK, A.I.I.Tyler@leeds.ac.uk. [4]School of Mechanical Engineering, University of Leeds, UK, N.Kapur@leeds.ac.uk. *Presenting Author

Time-resolved small-angle X-ray scattering (TR-SAXS) is a powerful technique for probing rapid structural changes in biomedical systems, such as protein folding and nanoparticle self-assembly, on millisecond timescales. Stopped-flow devices are widely used for this purpose, enabling precise mixing of reactants just before X-ray exposure. However, existing systems often require large sample volumes and high flow rates, making them less suited for beamline use with limited or sensitive samples. To address these limitations, this work presents the design and development of a beamline-compatible stopped-flow device that enables low-volume, low-deadtime operation while maintaining transparency to the X-ray beam. The device is based on a vortex T-mixer, with its geometry optimised through computational fluid dynamics (CFD) simulations carried out in COMSOL Multiphysics. A Design of Experiment approach was used to evaluate 24 configurations, identifying the optimal geometry for rapid mixing and short flow paths. The final mixer achieved mixing indices greater than 0.96 within 5 mm of first fluid contact at Re > 200. Experimental validation was carried out on the synchrotron beam using X-ray transmission measurements (KBr–water), yielding a deadtime of 3.4 ms. This result confirm the system's ability to achieve fast and effective mixing, with the sample reliably delivered to the beam within a well-defined timeframe. The device uses less than 25 µl of sample per shot and supports TTL triggering for synchronisation with beamline data acquisition. It has been successfully used in TR-SAXS experiments at both the I22 beamline at Diamond Light Source and the ID02 beamline at ESRF, including studies on lipid nanoparticles and AdhE spirosome dynamics. These developments advance dynamic reaction monitoring by providing a more precise, efficient, and adaptable platform for time-resolved experiments, with broad applicability across structural biology, soft matter, and nanomaterials research.

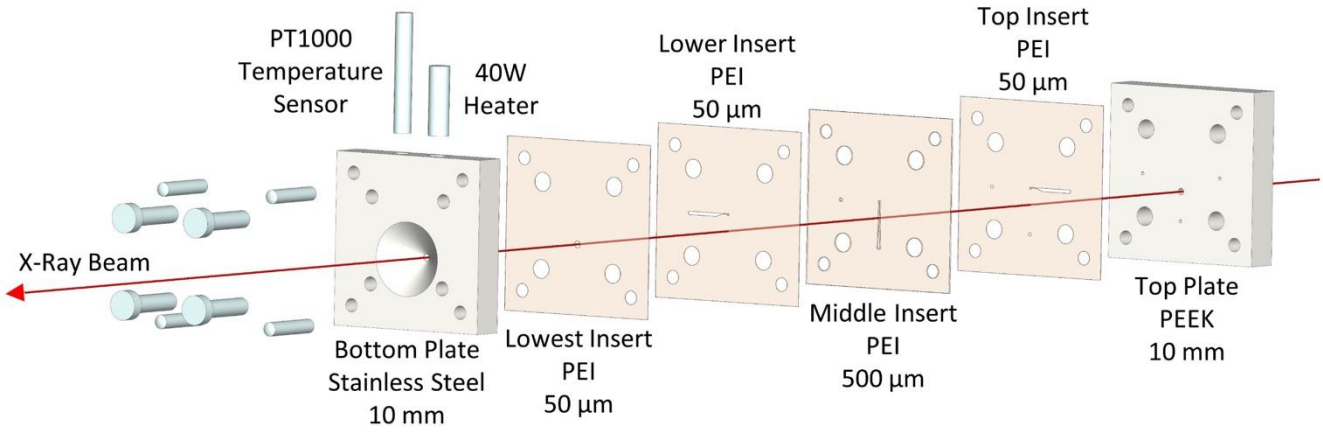

Figure 1. Schematic of the layered microfluidic device and instruments developed for the novel stopped-flow application.

IND/003: Effects of viscoelasticity and shear-thinning on the inertial instability in a T-channel geometry

[1*]Hill, Rebecca J.; [2]Davoodi, Mahdi; [3]Haward, Simon J.; [4]Fonte, Claudio P.; [5]Poole, Robert J.

[1]School of Engineering, University of Liverpool, Brownlow Hill, Liverpool, UK. psrhill@liverpool.ac.uk.

[2]Schlumberger Cambridge Research, High Cross, Madingley Road, Cambridge, UK. mdavoodi@slb.com.

[3]Micro/Bio/Nanofluidics Unit, Okinawa Institute of Science and Technology Graduate University, Okinawa, Japan. simon.haward@oist.jp.

[4]Department of Chemical Engineering, The University of Manchester, Oxford Road, Manchester, UK. claudio.fonte@manchester.ac.uk.

[5]School of Engineering, University of Liverpool, Brownlow Hill, Liverpool, UK. robpoole@liverpool.ac.uk. *Presenting Author

The T-channel geometry—two planar inlet streams of square cross section that join and turn through 90 degrees, into a single rectangular outlet stream—serves as a fundamental microfluidic configuration for enhancing fluid mixing. At sufficiently high Reynolds number, flows in this geometry encounter an instability where the flow breaks symmetry and transitions to a steady but asymmetric state, known as the engulfment regime. This regime dramatically improves mixing quality and therefore understanding the instability and how we may control of considerable practical importance to an array of industries. In this study, we use numerical simulations to investigate how viscoelasticity and shear-thinning influence the onset of this instability. Using a finite-volume method, we simulate three different non-Newtonian fluid models: Oldroyd-B, Oldroyd-A, and Giesekus and the generalised-Newtonian Carreau model. Parameters are selected such that the Giesekus and Carreau models have approximately matched shear-viscosity profiles.

For a Newtonian fluid, the critical Reynolds number for the onset of engulfment is approximately 139, consistent with experimental and numerical results from the literature. In comparison, the Oldroyd-B model shows a reduction in the critical Reynolds number, indicating a destabilisation of the flow. In contrast, the Oldroyd-A model shows a delayed transition, suggesting a stabilisation of the flow. Using a zero-shear-rate viscosity, both the Giesekus and Carreau models initially appear to lower the critical Reynolds number. However, when we account for their shear-thinning behaviour using the fully developed wall-centreline viscosity (which better reflects local flow conditions), both models exhibit a stabilising effect like the Oldroyd-A model. We attribute these observations to the development of secondary Dean-type flows in the outlet channel, caused by the curvature of the flow, in combination with inertia, as it navigates the 90-degree turn. In the constant-viscosity models studied, the onset of instability corresponds to a threshold in the strength of these secondary flows.

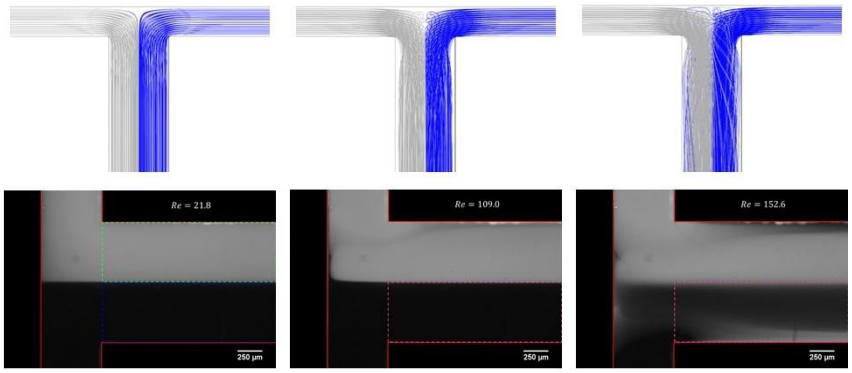

Figure 1. Visual comparison of experimental images with sreamlines from the Newtonian simulations for the symmetric stratified (Re~21.8), symmetric vortex (Re~109.0) and asymmetric engulfment (Re~152.6) regimes.

Kockmann, N., et al., *Proc. SPIE.* 4982, 319 (2003).

Poole, R. J., et al., *Chemical Engineering Science.* 104, 839 (2013).

IND/004: THE EFFECT OF FIN GEOMETRY ON BUBBLE NUCLEATION AND GROWTH CHARACTERISTICS IN PIN-FIN EVAPORATORS

[1*] Hasnain Raja Fakhar Ul; [2]Chakraborty, Bhaskar; [3] Anastasios Georgoulas; [3] Eddie Blanco-Davis;

[3] Guangming Zhang; [1] Manolia Andredaki

[1] School of Civil Engineering and Built Environment, Liverpool John Moores University, Liverpool, UK

[2] School of Architecture Technology and Engineering, University of Brighton, Brighton, UK

[3] School of Engineering, Liverpool John Moores University, Liverpool, UK

Micro-pin-fin evaporators have emerged as promising alternatives to conventional multi-microchannel heat sinks for high-power density electronic cooling applications. This study investigates the effect of fin geometry on bubble nucleation and growth characteristics in micro-pin-fin evaporators using an enhanced Volume of Fluid (VOF) computational framework with a novel random nucleation model. The applied numerical approach addresses critical limitations in traditional artificial seeding methods by implementing a stochastic nucleation site selection based on local thermal conditions. In more detail, this enhanced VOF method that is implemented in the framework of OpenFOAM CFD Toolbox incorporates a random nucleation model that selects potential nucleation sites using a non-biased random number generator, where vapor seeds are initiated stochastically when local wall temperatures exceed thermodynamically derived activation temperatures based on the Clausius-Clapeyron and Young-Laplace equations. This approach captures the natural variability of nucleation processes, providing superior realism compared to deterministic pre-defined nucleation site models.

Numerical simulations are conducted for various pin-fin geometries including circular, square, and triangular cross-sections with different aspect ratios and surface arrangements. The investigation covers a range of operating conditions relevant to electronic cooling applications. Grid independence studies ensure adequate resolution of thin liquid films and interface dynamics with mesh sizes down to 2 µm.

Results demonstrate that fin geometry significantly influences the bubble nucleation characteristics and growth patterns. Circular pin-fins promote uniform nucleation distribution and stable bubble growth, while sharp-edged geometries (square and triangular) create localized hot spots that intensify nucleation activity but may lead to vapour accumulation. The random nucleation model reveals that surface topology affects nucleation site activation probability, with corner regions and fin-base interfaces showing preferential bubble initiation.

This investigation provides fundamental insights into bubble dynamics in micro-pin-fin providing significant insight on the complex interfacial dynamics during the transient stages of two-phase flow development within micro-pin-fin evaporators. The enhanced VOF methodology with random nucleation modelling offers a robust framework for future investigations of phase-change heat transfer in complex microstructures.

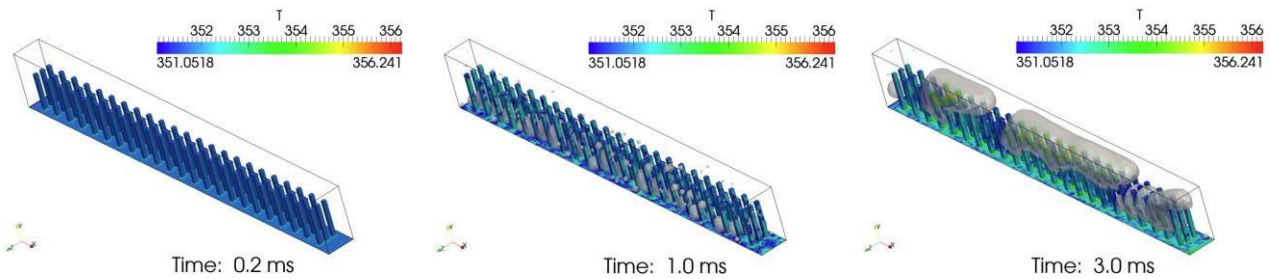

Figure 1. Two-phase flow development within a micro-pin-fin evaporator with rectangular pin fins during saturated flow boiling of Ethanol at 1atm

IND/005: Propeller Wake Propagation within a Model Cooling Duct of a Hydrogen-Electric Aircraft

[1*]Bryce-Smith, T; [2]Buxton, O.R.H; [2]Papadakis, G; [2]Steiros, K.

[1]Department of Aeronautics, Imperial College London, London SW7 2AZ, UK; tb1416@ic.ac.uk *Presenting Author.

[2]Department of Aeronautics, Imperial College London, London SW7 2AZ.

The unsteady flowfield of a square duct immersed in propeller wake was characterised at two advance ratios (J) using planar particle image velocimetry. Results show the ingestion and propagation of unsteadiness within cooling ducts typical of novel hydrogen-electric propeller aircraft propulsion systems. Two discrete structures, a root vortex and a portion of the vortex sheet, were ingested, creating a heterogenous flowfield within the entrance region characterised by a shear flow and skewed instantaneous velocity profile. Unsteady motions at the blade passing frequency are dominant through the first ten duct widths, typical of a nacelle's length scale, which decay into incoherent motions. A novel reenergising mechanism of energy at the blade passing frequency is observed. Results imply that this mechanism is highly sensitive to design variables (e.g. number of propeller blades) and to changing propeller settings (e.g. advance ratio) across the mission profile. Additionally, results highlight the importance of unsteady measurements when considering propulsive system flows, especially when motions at coherent frequencies in the bulk flow may lead to increased time-averaged heat transfer yielding improved cooling or conversely, may lead to local overcooling that could damage a fuel cell.

IND/006: Visualisation of Multi-Scale Desorption Dynamics in Clay-Coated Microfluidic channels: Optimising Recovery Strategies for Valuable Contaminants

[1*]Razaghi, Negar; [2]Mousavi Nezhad, Mohaddeseh

[1]School of Engineering, The University of Warwick, Coventry, UK. Negar.Razaghi@warwick.ac.uk.

[2]School of Engineering, The University of Liverpool, Liverpool, UK. M.Mousavi-Nezhad@liverpool.ac.uk

*Presenting Author

Recovering valuable water contaminants is a cornerstone of sustainable water management, addressing environmental challenges, resource scarcity, and promoting sustainable resources management and circular economy principles. Among various techniques for contaminant sequestration and recovery, sorption-desorption methods stand out for their operational simplicity, cost-effectiveness, and high efficiency, while minimising harmful by-products during both removal and recovery processes. While sorption processes have been extensively studied, desorption dynamics remain underexplored despite their importance in recovering and recycling valuable substances. Traditionally, dynamic sorption-desorption processes are studied using column experiments with effluent and solid surface analysis, nevertheless these methods do not provide direct in-situ observation of pore-scale solid-fluid interactions. Moreover, studying pore-scale interfacial processes in geomaterials is challenging due to the opacity and heterogeneity of them. Overcoming these challenges demands innovative, multidisciplinary approaches to visualize and analyse these processes.

We developed a streamlined surface modification technique to functionalize PDMS microfluidic channels with transparent synthetic smectite clay (Laponite), creating geomaterial micromodels that replicate the physicochemical properties of clay-rich porous media. The fabrication process involves plasma treatment of PDMS surfaces followed by dry powder coating and controlled heat treatment, resulting in stable, randomly distributed clay aggregates that form interconnected porous networks upon hydration. Using fluorescein as a model sorbate, we conducted systematic desorption experiments across different flow rates while maintaining laminar flow conditions. Fluorescence microscopy enabled continuous monitoring of concentration changes within both inter-aggregate flow pathways (micron-scale pores) and intra-aggregate domains (nanometer-scale pores), revealing multi-scale transport mechanisms previously inaccessible through conventional column studies.

Our results demonstrate that desorption behavior exhibits dependencies on the intricate interplay between flow dynamics and porous geometry. Higher flow rates accelerate overall desorption kinetics but do not necessarily improve recovery efficiency. Lower flow rates extend equilibration times while potentially reducing residual concentrations at exhaustive desorption. Significantly, porous structures with different pore size distributions respond distinctly to identical flow conditions, with smaller pores creating concentration gradients that drive readsorption phenomena manifested as local peaks in desorption profiles. The study reveals quasi-irreversible sorption characteristics, with residual fluorescent compounds persisting even after extensive flushing, indicating strong physicochemical affinity between sorbate and clay surfaces. Initial rapid desorption from larger inter-aggregate pores transitions to slower, diffusion-limited release from smaller intra-aggregate domains, highlighting the importance of multi-scale transport processes. This work provides the first direct pore-scale visualization of flow-coupled desorption in clay-rich media, offering fundamental insights for designing efficient water filteration systems and optimizing flow conditions for contaminant recovery.

IND/007: TOWARDS A LAGRANGIAN CFD MODEL FOR AEROSOL RESUSPENSION IN TURBULENT FLOW

[1*]Duthou, Nicolas; [2]Gambaruto, Alberto

[1]School of Engineering Mathematics and Technology, University of Bristol, nicolas.duthou@bristol.ac.uk.

[2] School of Engineering Mathematics and Technology, University of Bristol, alberto.gambaruto@bristol.ac.uk. *Presenting Author

Aerosol resuspension is a key vector for introducing particles into the atmosphere and is driven by a wide range of natural and other external forces capable of detaching particles from surfaces. Its impact spans diverse fields - including industry, ventilation, healthcare, farming, transportation, and nuclear safety - yet it remains underrepresented in aerosol transport and dispersion modelling due to a lack of understanding of the complexity of its underlying physics. Several mechanistic, probabilistic, and semi-empirical models have already been developed, but are constrained by simplistic assumptions, sometimes resulting in significant discrepancies between predicted and observed data, thus limiting their predictive accuracy and applicability.

This research aims to further understand the dynamics of aerosol resuspension by developing a high-resolution CFD-based model that captures the fundamental physics more comprehensively than current approaches. Specifically, we investigate how aerodynamic forces, variability in particle-surface adhesion and morphology affect rolling or sliding thresholds and influence resuspension rates under realistic atmospheric conditions. The model is implemented in Siemens Simcenter StarCCM+ v2302, employing a three-dimensional Lagrangian approach with six-degree-of-freedom (6 DoF) particle displacement within turbulent flow (Stokes regime, Re ≈ 1). Particular emphasis is placed on near-surface interactions, integrating Dynamic Fluid-Body Interaction (DFBI), boundary layer theory and turbulent eddy behaviour, detailed contact mechanics, and adhesive/repulsive force distributions to maximise the completeness of the model. The framework is designed to be flexible, accommodating a broad range of particle sizes, shapes, surface topologies, and flow boundary conditions, thereby enabling the simulation of complex, real-world scenarios. Currently, the model features operational boundary layer and contact mechanics modules, supporting variable particle morphologies being re-entrained on flat surfaces. Significant challenges were encountered while accurately modelling particle-surface contact with suitable mesh and temporal resolutions, quantifying the forces influencing detachment, and limiting the evolving computational costs associated with high-fidelity simulations.

Once completed, the model will be validated against experimental trajectory and detachment rates data and benchmarked against established Eulerian resuspension models. Ultimately, improving the capabilities for the prediction of aerosol resuspension addresses a critical health and safety concern as it helps anticipate hazards and supports better risk mitigation strategies for harmful aerosols in the environment.

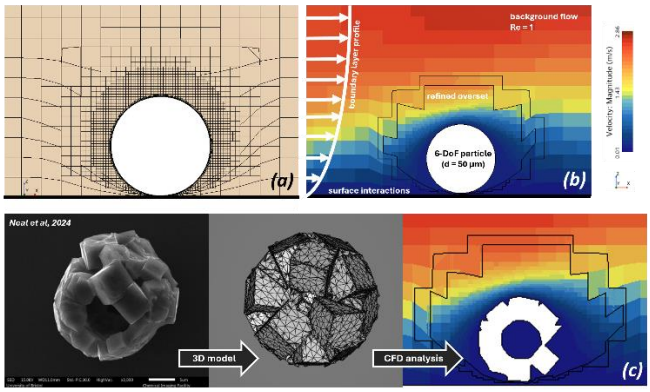

Figure 1. Example meshing (a) and flow resolution (b) around a spherical particle on a flat surface. Current model developments include the ability to evaluate different particle morphologies, e.g. NaCl "raspberry-shaped" crystals modelled from real-life into the software (c).

Neal, E et al., 2024, *A novel approach to resuspend particles of controlled morphologies in a 3D printed wind tunnel*. Aerosol Science and Technology. 58 (12) pp 1389–1404.

Gelain, T., Ricciardi, L., and Gensdarmes, F., 2020. *Implementation of a particle resuspension model in a CFD code: Application to an air ingress scenario in a vacuum toroidal vessel*. Proceedings of the ASME 2020 International Conference on Nuclear Engineering (ICONE28), V001T03A003. American Society of Mechanical Engineers.

IND/008: Erosion of cohesion-less sediment beds by submerged impinging jets: Impact of particle size

[1*]Mohamadiyeh, Ahmad; [2]Peakall, Jeffery; [3]Fairweather, Michael; [4]Barnes, Martyn; [5]Hunter, Timothy

[1]*University of Leeds, School of Computer science, Leeds LS2 9JT, United Kingdom, scamm@leeds.ac.uk*

[2] *University of Leeds, School of Earth and Environment, Leeds LS2 9JT, United Kingdom, j.peakall@leeds.ac.uk*

[3] *University of Leeds, School of Chemical and Process Engineering, Leeds LS2 9JT, United Kingdom, m.fairweather@leeds.ac.uk*

[4] *Sellafield Ltd, Birchwood, Warrington, WA3 6GR, United Kingdom, martyn.g.barnes@sellafieldsites.com*

[5] *University of Leeds, School of Chemical and Process Engineering, Leeds LS2 9JT, United Kingdom, t.n.hunter@leeds.ac.uk*

Impinging jets are implemented in mixing and erosion processes across various industries, with one relevant application being nuclear waste management. At Sellafield Ltd, for instance, impinging jets are employed to remotely erode and maintain nuclear waste in suspension within highly active storage tanks (HASTs). This process is crucial for preventing the formation of stubborn sediment beds and the development of radioactive hotspots, which can pose significant challenges and damage the tanks. One key factor influencing erosion by impinging jets is the properties of the particles involved. This study focuses on examining the effect of particle size on erosion by a submerged liquid jet, as well as determining the size limits in erosion modeling. Soda-lime glass spherical particles were used in this study as inactive simulants for the cohesionless nuclear particles present in HASTs. Five particle grades with median sizes ranging from 650 µm to 35 µm were investigated. The experimental setup comprises an impinging jet tank fed by a pump that draws water from a freshwater supply tank. The jet nozzle is interchangeable, enabling tests with various diameters and corresponding velocities. Ultrasonic Velocity Profiling (UVP) was used to measure and scan the crater profiles. The UVP probe, attached to a traverse via an arm, moved across the crater to capture these measurements. Additionally, a camera positioned beneath the tank recorded the jet's clearing effects. A few LiDAR measurements were also conducted to obtain 3D reconstructions of the craters. Alongside the commonly used erosion parameter, E_c, a new parameter is proposed, providing an alternative approach for modelling the erosion of cohesion-less particles. The new parameter is based on the critical shear stress of the particle bed rather than particle size. It was derived from a force balance at the crater interface and normalised by the jet height. The new parameter was able to capture the transition to cohesive behaviour observed in the smallest particles.

IND/009: Quantifying stick-slip motion of droplets on chemical patterns

[1*]Creasy, Nick; [2]Pradas, Marc

[1]The Open University nick.creasy@open.ac.uk. [2]The Open University marc.pradas@open.ac.uk. *Presenting Author

Controlling droplet transport and localisation on solid surfaces is important for many technologies, such as microchemical reactors, liquid-repellent surfaces, and micro-printing. Consequently, considerable effort has been devoted to designing solid surfaces that control wetting and droplet's contact area and/or direct droplet's motion. A key aspect here is the concept of stick-slip contact line motion, which arises because of impurities on the surface.

In this work, we study droplets that are subjected to external, slow time-dependent variations, such as evaporation and condensation, to quantify the emergence of stick-slip motion. We consider a two-dimensional droplet that is slowly evaporating on a smooth chemical pattern. Under these conditions, it has recently been shown that the motion and shape of the droplet is quantified in terms of a hierarchy of bifurcations. By gradually decreasing the smoothness of the pattern, we describe the emergence of stick-slip mechanisms in terms of bifurcation transitions. We present our most recent research into the emergence of stick phases and slip phases, and related computational results based on a diffuse interface model which display good agreement.

IND/010: Liquid-liquid dispersions in milli scale symmetric confined impinging jets: effect of viscosity

*Duan, Cong; Angeli, Panagiota

[1]Department of Chemical Engineering, University College London, UK *Presenting Author

This research aims to understand the formation of dispersion of two immiscible liquids and the behaviour of the resulting dispersions in symmetric confined impinging jets (CIJs) with dual opposing outlets. Confined Impinging jets find applications as intensified small-scale contactors. A combined methodology, utilizing high-speed imaging experiments and Computational Fluid Dynamics (CFD) simulations, was employed to analyse the complex phenomena involved in dispersion formation for varying flow rates, dispersed phase fractions, and fluid viscosities. A flow pattern map was developed based on different flow rates and dispersed phase fractions. CFD simulations, integrating Volume-of-Fluid (VOF) and Discrete-Phase-Model (DPM) approaches, were employed to understand the droplet formation mechanisms at the impingement zone and to predict the drop size distributions (DSDs) downstream from the inlet. These simulations revealed that droplet formation is initiated by the breakup of ligaments generated from a thin liquid sheet in the impingement zone. Experimental results from high-speed imaging, analysed using an in-house post-processing code, provided data on droplet size distributions. The continuous phase was a 10% w/w glycerol-water mixture, and the dispersed phase was either kerosene or silicone oil with viscosities 2.04 mPa·s and 50 mPa·s respectively. Jet velocities ranged from 0.034 m/s to 16.6 m/s, with dispersed phase volume fractions varying between 0.02 and 0.98.

Key findings indicate that DSDs follow a log-normal distribution when the dispersed phase has low viscosity, a result also found by the CFD simulations. However, at higher dispersed phase viscosities, the DSD transitions to a bimodal distribution, attributed to increased dampening effects on the instabilities which cause the ligament breakup. The velocity profiles at the impinging zone can be referred to in Figure 1(a). The disintegration of the ligaments, the process of which is indicated in Figure 1(b), is found to be controlled by different modes of break-up events involving filament stretching and wave growth. Compared to asymmetric CIJs (single outlet), symmetric CIJs produce dispersions with smaller droplet sizes and larger specific interfacial areas, particularly at high energy dissipation rates, making them preferable for high-throughput manufacturing and extraction separation processes.

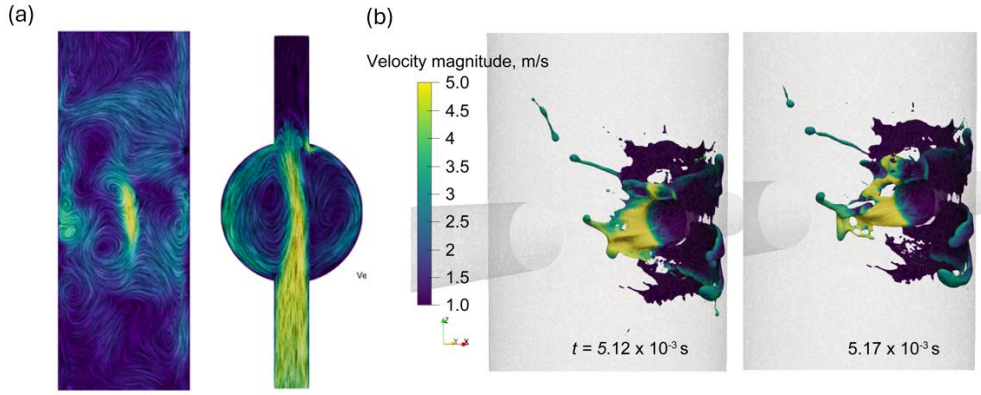

Figure 1. (a) Representations of velocity profiles on two planes (perpendicular to inlets and outlet flow axis) with a visualisation of stream lines using surface line-integral convolution; (b) Contours of liquid-liquid interface corloured with velocity magnitude, capturing the evolution of break-ups of the liquid filaments..

IND/011: EVAPORATION OF A RIVULET ON AN INCLINED PLANAR SUBSTRATE

[1*]Tomczyk, Fryderyk; [2]Wilson, Stephen, K.; [3]Wray, Alexander, W.

[1]Department of Mathematics and Statistics, University of Strathclyde, Livingstone Tower, 26 Richmond Street, Glasgow G1 1XH, United Kingdom, fryderyk.tomczyk.2019@uni.strath.ac.uk [2]Department of Mathematical Sciences, University of Bath, Claverton Down, Bath BA2 7AY, United Kingdom, sw3197@bath.ac.uk [3]Department of Mathematics and Statistics, University of Strathclyde, Livingstone Tower, 26 Richmond Street, Glasgow G1 1XH, United Kingdom, alexander.wray@strath.ac.uk *Presenting Author

The effects of uniform evaporation on the shape and length of a rivulet on an inclined substrate are investigated. Specifically, a mathematical model for the steady gravity-driven flow of a thin rivulet [1,2,3] on an inclined planar substrate undergoing uniform evaporation is derived and analysed for a rivulet with either a fixed semi-width (Figure 1(a)) or a fixed contact angle (Figure 1(b)). Specifically, we determine the variation of the rivulet length, footprint area, and volume with the problem parameters. In particular, it is found that pendant rivulets only exist when their initial semi-width is below a critical value, and that the maximum possible dimensionless length of a sessile rivulet with fixed semi-width occurs in the limit of large semi-width and is given by

$$\frac{\bar{\beta}^3 \sin\alpha}{3J\,|\cos\alpha|^{3/2}},$$

where $\bar{\beta}$, α and J are the dimensionless initial contact angle, the inclination angle of the substrate and the dimensionless evaporative flux, respectively.

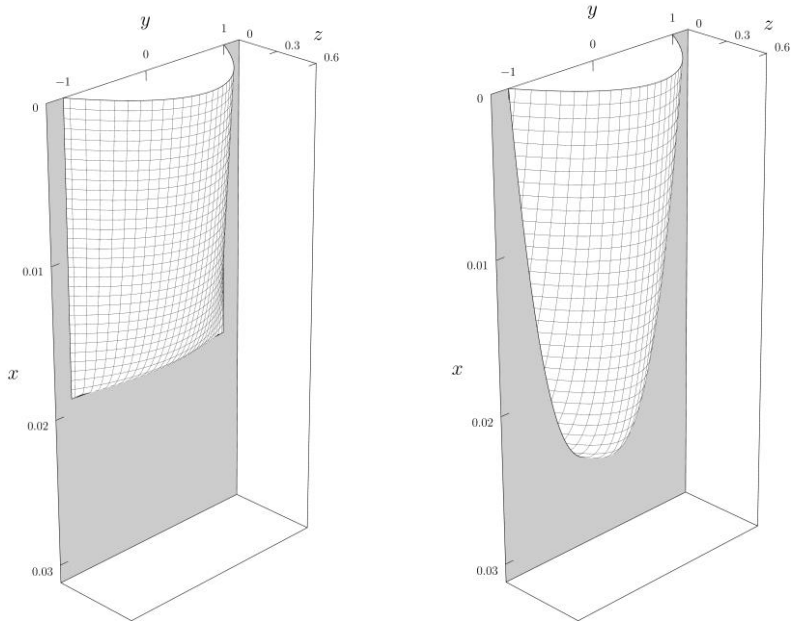

(a) *(b)*

Figure 1. A uniformly evaporating rivulet with (a) fixed semi-width and (b) fixed contact angle on a vertical substrate.

[1] Duffy, B. R., Moffatt, H. K., 1995, Flow of a viscous trickle on a slowly varying incline. Chem. Eng. J. 60, 141. pp 141.

[2] Alshaikhi, A. S., Wilson, S. K., Duffy, B. R., 2021, Rivulet flow over and through permeable membrane. Phys. Rev. Fluids 6, 104003.

[3] Paterson, C., Wilson, S. K., Duffy, B. R., 2013, Pinning, de-pinning and re-pinning of a slowly varying rivulet, Euro. J. Mech. 41, pp 94.

IND/012: Theoretical analysis of Stokes flow through a sharp-cornered cross-slot

[1*]Ji, Xintong; [2]Wilson, Helen; [3]Luca, Elena

[1]Department of Mathematics, University College London, Gower Street, London WC1E 6BT, UK. (xintong.ji.22@ucl.ac.uk) [2]Department of Mathematics, University College London, Gower Street, London WC1E 6BT, UK. (helen.wilson@ucl.ac.uk) [3]Climate and Atmosphere Research Center, The Cyprus Institute, Nicosia 2121, Cyprus. (e.louca@cyi.ac.cy) *Presenting Author

A cross-slot (or cross-channel) is a flow geometry with four 'arms'. The inflow comes from two opposite (horizontal as default) 'arms' and the outflow goes away from the other two opposite (vertical as default) 'arms'. A slow flow through this geometry produces a pattern with reflectional symmetry and produces a good approximation to a pure planar extension near the stagnation point at the centre. As an important example of microfluidic flow, it plays a great role in mixing process in chemical engineering as well as chip manufacturing in material and electronic engineering.

We consider the flow of a viscous fluid through a two-dimensional cross-slot geometry with sharp corners. The problem is analysed using the Unified transform method in the complex plane, providing a quasi-analytical solution which can be used to compute all the physical quantities of interest. This study is a novel application of this method to a truly complex geometry featuring multiple sharp corner singularities and multiple inlets and outlets. Our approach offers the advantage of resolving unbounded domains, as well as providing quantities of interest, such as the velocity and stress profiles, and the Couette pressure correction, from the solution of low-order linear systems. Our results agree well with existing literature, which has largely used truncated bounded geometries with rounded or curved corners.

IND/013: Research overview of the Multiphase Fluid Flow In Nuclear systems (MULTIForm) Facility

[1*]Hunter, Timothy; [1]Baker; Alastair; [1]Rumney, Jacob; [1]Harbottle, David; [1]Fairweather, Michael

[1]School of Chemical and Process Engineering, University of Leeds. *Presenting Author: t.n.hunter@leeds.ac.uk.

The University of Leeds is proudly home to one of the largest academic groups of nuclear engineering researchers within the UK, where multiphase flows are instrumental to much of the work we do. Research within the Nuclear Engineering Group (NEG) encompasses the whole of the fuel cycle, from characterising bubbly reactor flows and investigation of new molten salt designs, to intensified separators and the transportation of nuclear wastes. Additionally, with the UK's push to renew its nuclear power enabling its ambitious Net Zero goals, this is a critical time for nuclear engineering. To support our nuclear mission, both for new reactors and to ensure the safe disposal of legacy wastes, Leeds has established the Multiphase Fluid Flow In Nuclear systems (MULTIForm) suite, as part of the UK's National Nuclear Users Facility (NNUF). Herein, we will present a research overview of current investigations in nuclear waste flows within the hydrotransport loop (Fig. 1) and initial studies of flow accellerated corrosion within our molten salt reactor loop. Importantly, these loops serve as test beds for new flow sensors (e.g., noninvasive ultrasonic systems) as well as provide high fidelity validatation data for CFD simulations, using stereo particle image velocitmetry (PIV) and laser Doppler anenometry (LDA). In particular, an innovative bored quartz test cell has been designed that significantly mittigates curvature effects at the pipe walls.

Figure 1. Image of the hydrotransport pipe loop, as part of the MULTIForm facility.

IND/014: Oldroyd-A vs. Oldroyd-B: analytical equivalence of planar incompressible flows - Poster

[1*]Hill, Rebecca J; [2]Hillebrand, Fabian.; [3]Davoodi, Mahdi.; [4]Haward, Simon J.; [5]Shen, Amy Q.; [6]Poole, Robert J.; [7]Varchanis, Stylianos.

[1]School of Engineering, University of Liverpool, Brownlow Hill, Liverpool, UK. psrhill@liverpool.ac.uk.

[2]Micro/Bio/Nanofluidics Unit, Okinawa Institute of Science and Technology Graduate University, Okinawa, Japan. fabian.hillebrand@oist.jp.

[3]Schlumberger Cambridge Research, High Cross, Madingley Road, Cambridge, UK. mdavoodi@slb.com.

[4]Micro/Bio/Nanofluidics Unit, Okinawa Institute of Science and Technology Graduate University, Okinawa, Japan. simon.haward@oist.jp.

[5]Micro/Bio/Nanofluidics Unit, Okinawa Institute of Science and Technology Graduate University, Okinawa, Japan. amy.shen@oist.jp.

[6]School of Engineering, University of Liverpool, Brownlow Hill, Liverpool, UK. robpoole@liverpool.ac.uk.

[7]Centre for Computational Biology, Flatiron Institute, New York, USA. svarchanis@flatironinstitute.org. *Presenting Author

In his seminal 1950 paper, Oldroyd argued that for a constitutive equation to be properly formulated, the time derivatives need to be evaluated in a frame that moves with the material – whether that is a rotation, a translation or a deformation. In doing so he provided two possible invariant forms of the Jeffreys model, case “A”, which uses a lower convected derivative, and case “B”, which uses an upper convected derivative. Oldroyd then showed how, despite “at first sight these might appear to be trivially different generalisations", in rotational Couette flow one model (the “Oldroyd-B") can give rise to the Weissenberg effect of rod climbing whilst the other (the “Oldroyd-A") does not. This is because, despite both models exhibiting a constant shear viscosity, the Oldroyd-B model gives $N_1 > 0$ and $N_2 = 0$ whereas the Oldroyd-A gives $N_1 = -N_2$.

The Oldroyd-B model has since become standard for simulating viscoelastic fluids such as dilute polymer solutions and has become the default constitutive relation in many studies of elastic flow phenomena. In contrast, the Oldroyd-A model - formulated in the same foundational work - has seen limited use. While Oldroyd-B describes the affine deformation of line-like microstructures (e.g. polymers), Oldroyd-A is more naturally associated with the deformation of surface-like entities (e.g. elastic discs or films).

In this work, we prove analytically that under planar, incompressible flow conditions, the Oldroyd-A and Oldroyd-B models yield identical velocity and total stress fields when evaluated at the same Reynolds and Weissenberg numbers. This equivalence is demonstrated across multiple benchmark flows and follows from a simple in-plane rotational symmetry between the models. These results suggest that many findings based on the Oldroyd-B model can be directly extended to flat-disc suspensions and related materials. This has important implications for modelling elastoinertial instabilities in quasi-2D flows, and prompts a reconsideration of the Oldroyd-A model as a physically meaningful and computationally relevant alternative.

Oldroyd, J.G., *Proceedings of the Royal Society, Series A,* **200**, 523 (1950).

Frohlich, A., Sack, R., *Proceedings of the Royal Society, Series A,* **185**, 415 (1946).

Hinch, J., Harlen, O.G., *Journal of Non-Newtonian Fluid Mechanics*, **298**, 104668 (2021).

INS: Fluid dynamic instabilities, transition and turbulence

INS/001: Interfacial Study of Surfactant-Assisted Evaporation within the Porous Media using Lattice Boltzmann Modelling

[1*]Bello, Ayomikun; [1]Kharaghani, Abdolreza; [1]Tsotsas, Evangelos

[1]Institute of Process Engineering, Otto von Guericke University, Universitatsplatz 2, 39106 Magdeburg, Germany *Presenting Author

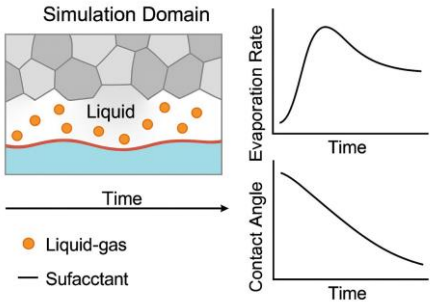

Evaporation within porous media is a fundamental phenomenon relevant to numerous industrial and environmental processes such as soil drying, fuel cell operation, energy storage, and food preservation. While traditional models address capillary forces, vapor diffusion, and thermodynamic effects, they often oversimplify interfacial phenomena, particularly in the presence of surfactants. Surfactants are amphiphilic molecules that significantly influence liquid-gas interfaces by dynamically altering surface tension and wettability. This study presents a modeling framework using the Lattice Boltzmann Method (LBM) integrated with a surfactant transport equation to investigate the coupled dynamics of evaporation, wettability, and Marangoni flows in porous media.

Our multiphase LBM framework, implemented on a D3Q19 lattice, simulates evaporation from a porous domain populated with randomly distributed solid obstacles. The gas-liquid interface is initialized based on a sharp density gradient, while the surfactant is concentrated at the interface. Our key findings demonstrate a multi-stage evaporation process governed by dynamic interfacial feedback. Initially, surfactants accumulate at the liquid-gas interface, reducing interfacial tension and enhancing evaporation. This process is driven by steep surfactant concentration gradients that initiate Marangoni flows, redistributing surfactant and homogenizing interfacial properties. As gradients diminish, evaporation slows, revealing a temporal offset between peak surfactant concentration and the decline in evaporation rate. This phase offset suggests a feedback mechanism where interfacial stabilization lags behind surfactant saturation.

Simulations comparing porous media with and without solid obstacles highlight how geometric complexity influences flow path formation, surfactant transport, and evaporation uniformity. Obstacles introduce tortuosity and local curvature variations, disrupting capillary pathways and surfactant redistribution. Consequently, evaporation becomes spatially heterogeneous, particularly in regions with surfactant depletion or contact line pinning.

This study fills in critical gaps in evaporation modeling by explicitly coupling surfactant dynamics with interfacial physics. The LBM-surfactant framework offers a platform for investigating complex drying mechanisms in porous structures, which provide a foundation for optimizing surfactant-based drying methods and can be extended to applications such as enhanced oil recovery, heat pipes, and pharmaceutical drying systems. Future work will extend this model to include more complex wetting heterogeneities and non-equilibrium phase transitions across multiple spatial scales.

INS/002: Turbulent wake resonance via oscillation of a solid plate

[1*] Gao, Xiangyu; [2] Steiros, Kostas

[1] Department of Aeronautics, Imperial College London, London, UK. xiangyu.gao23@imperial.ac.uk

[2] Department of Aeronautics, Imperial College London, London, UK. k.steiros@imperial.ac.uk

It has long been appreciated that periodic forcing of a bluff body wake can induce significant alterations to both the large-scale (vortex shedding) structures and to the mean-flow wake topology. These effects are greatly accentuated at particular forcing frequencies which induce 'flow-resonance': For instance, Tokumaru and Dimotakis [1] demonstrated that when a cylinder in a uniform stream undergoes forced rotary oscillation at its natural vortex shedding frequency, body drag drops sharply, accompanied by a transformation of the momentum-deficit profile downstream of the cylinder (typical of wakes) into a momentum-excess profile (typical of jets). Unfortunately, the physics of this remarkable 'flow-resonance' phenomenon remain obscure. This work aims to answer two questions. Firstly, is the wake-jet transition exclusive to rotating cylinders, or can it be found in other types of oscillatory movements which are relevant to offshore floating structures, e.g., dynamic tilting of bluff bodies? Secondly (and more importantly), what is the cause of this phenomenon – in particular, can it be linked to the formation of near wake vortical structures?

To answer the above questions we conducted an extensive series of wind tunnel measurements of the turbulent wake of an oscillating solid disk, actuated via a robotic arm. Our experiments tested a parameter space that spanned amplitudes of 5°,10°,and 20° disk oscillation and six Strouhal numbers (characteristic oscillation frequencies) ranging from 0.047 to 0.23. In all cases the tunnel velocity was set to 2.95m/s, leading to a fully turbulent Reynolds number of 39000. The measurements were comprised of high-speed Particle Image Velocimetry at various downstream streamwise planes.

Our key-findings can be summarized as follows. First, the oscillatory titling of the disk performed at a frequency very close to that of the natural vortex shedding, produced downstream mean velocity profiles which resembled a jet, i.e., flow resonance was indeed observed. This jet flow started appearing approximately 5 disk diameters downstream of the body. Second, the cause of this phenomenon was found to be linked to the formation of a 'reverse Karman street', i.e., a vortex street which is identical to the regular Karman one, except from the fact that the vortices rotate in the opposite direction. Such 'reverse' Karman streets are known to exist in the wake of oscillating airfoils [2], but have not been hitherto observed in the wake of bluff bodies. The presentation will discuss in detail the above flow physics, and how they differ from the 'off-resonance' conditions.

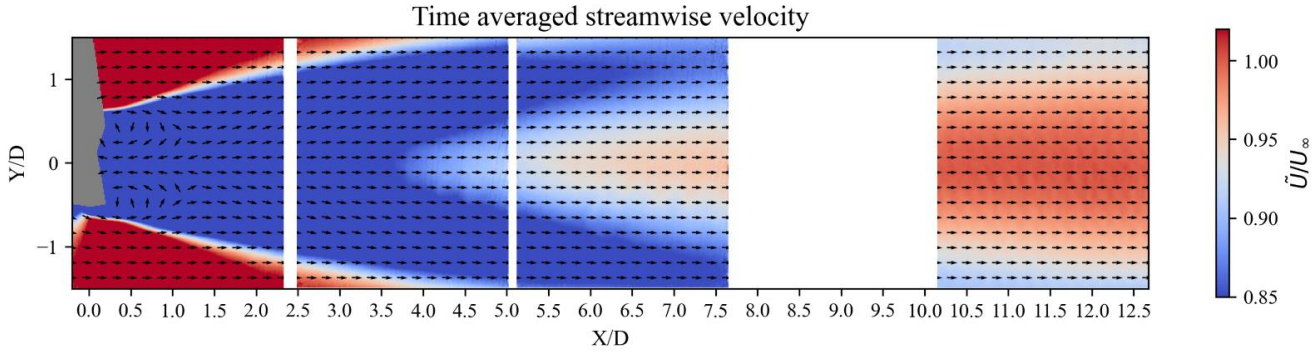

Figure 1. Time-averaged streamwise velocity, normalized with the free stream velocity for the St = 0.186 and amplitude 20 degrees case. The arrows show the time-averaged velocity vectors.

References

[1]. Tokumaru, P.T. and Dimotakis, P.E. (1991), Rotary oscillation control of a cylinder wake, Journal of Fluid Mechanics, 224, pp. 77–90.
[2]. Koochesfahani, M.M. (1989), Vortical patterns in the wake of an oscillating airfoil, AIAA Journal, 27(9), pp. 1200–1205

INS/003: OPTIMAL BODY FORCE FOR HEAT TRANSFER IN TURBULENT VERTICAL HEATED PIPE FLOW

[1]Chu, Shijun; [2]Marensi, Elena; [3*]Willis, Ashley P.

[1,3]School of Mathematical and Physical Sciences, University of Sheffield, schu3@sheffield.ac.uk, a.p.willis@sheffield.ac.uk

[2]School of Mechanical, Aerospace and Civil Engineering, University of Sheffield, e.marensi@sheffield.ac.uk . *Presenting Author

The vertical heated-pipe arrangement is widely used in engineering applications, as the buoyancy can help drive the flow. When buoyancy, measured by parameter C, is weak, shear-driven turbulence in the flow enhances the transport of heat from the wall to the bulk. For intermediate C, turbulence collapses and the heat transfer drops substantially. At large C, buoyancy-driven turbulence slowly leads to a recovery of the heat transfer.

In this work, the influence of a body force on the heat transfer is examined for each of the above regimes. Supposing that the magnitude of the force is limited, an optimisation procedure is applied to determine an optimal spatial structure for the force. This is found to be in a form that induces axially-aligned rolls in all cases, but the radial position of the roll-forcing and the optimal number of pairs of rolls is dependent on the flow regime (figure 1). Interestingly, the force can both stabilise or destabilise the flow (laminarise or induce chaotic flow), and inducing time-dependent flow does not necessarily lead to an enhancement of the heat transfer.

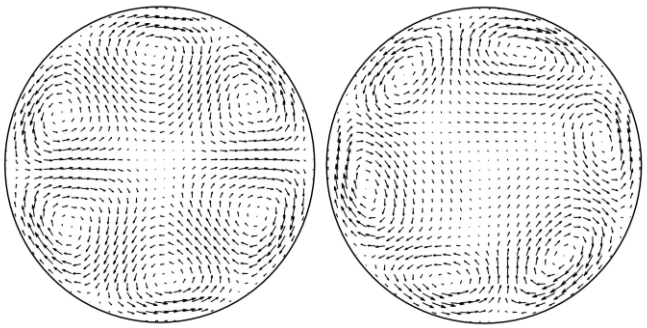

Figure 1. Optimised body force for heat transfer at C=1, Re=3000, assuming (left) laminar and (right) turbulent flow conditions. C measures the ratio of the buoyancy force to the laminar axial pressure gradient force, and Re is the Reynolds number.

INS/004: TURBULENT-TURBULENT TRANSIENTS IN LOW-REYNOLDS-NUMBER PULSATING FLOWS

[1*]Onasanya, Tobi; [1]Taylor, Phil; [1**]Seddighi, Mehdi; [2]Thijssen, Dick

[1]School of Engineering, Liverpool John Moores University, Liverpool L3 3AF, UK; O.Onasanya@2021.ljmu.ac.uk; M.Seddighi@ljmu.ac.uk; P.S.Taylor@ljmu.ac.uk

[2]School of Sport and Exercise Sciences, Liverpool John Moores University, Liverpool L3 5AF, UK; D.Thijssen@ljmu.ac.uk

*Presenting Author

** Corresponding Author

Understanding the detailed flow structure of blood in arteries - where pulsatility and low Reynolds numbers dominate - is crucial for understanding the onset of vascular diseases. This study uses direct numerical simulations to investigate flow behaviour and underlying transition processes in low-Reynolds-number pulsatile turbulent regimes. Simulations were performed at an amplitude of 1 and within the intermediate- and low-frequency regimes of l_s^+ = 16 and 26, across a range of mean bulk Reynolds numbers, Re_b = 2000, 3100, 4200, 5240 and 6275. Whereas the pulsating flow at Re_b= 2000, and l_s^+ = 16, relaminarised after a few cycles, the pulsating flow at other Reynolds numbers and frequencies exhibits a multistage turbulent–turbulent transition process, closely resembling the multistage response observed in non-periodic acceleration and also intermediate- and low-frequency pulsation at the highest Reynolds number, Re_b = 6275. The transition process includes five distinct stages: Residual Decay (I), encompassing frozen turbulence production but the attenuation of turbulent structures persisting from the prior deceleration phase; Pre-transition (II), characterised by the growth and elongation of streamwise velocity streaks. While turbulent energy production remains frozen, the perturbation field follows a self-similar laminar profile confined between the periodic quasilaminar and non-periodic extended Stokes solutions; Transition (III), characterised by the instability and subsequent breakdown of these streaks, accompanied by the formation of new turbulent spots, often extending into deceleration; Post-transition (IV), occurring only if transition concludes before the end of the acceleration period, with near-wall Reynolds stresses stabilising whilst there is a continuing growth of these components in the core of the flow; and Turbulence Decay (V), marked by a gradual decay of the Reynolds stresses, driven by the breakdown of streamwise velocity streaks and the diminishing of vortical structures across the domain. As mean bulk Reynolds number is reduced, the onset of the transition stage is delayed. Notably, transition can still occur even if it begins during the decelerating phase of the cycle.

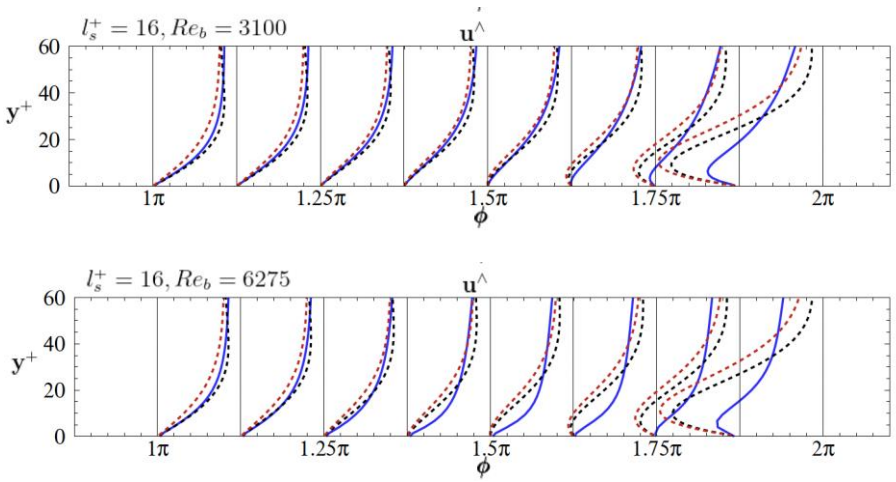

Figure 1. Growth of the perturbation velocity with time for Re_b = 3100 and 6275; (solid blue) cases; (black dashed-line) quasilaminar solution to Stokes second problem; (red dashed line) extended laminar solution to Stokes first problem.

INS/005: Large Eddy Simulation of Wake Dynamics Behind Multi-Scale Porous Patches

[1]Higham, J.E. ; [2*]Marjoribanks, T.

[1]Department of Geography and Planning, School of Environmental Sciences, University of Liverpool, Liverpool L69 7ZT, UK. [2] School of Architecture, Building and Civil Engineering, Loughborough University, Loughborough, UK. *J.E. Higham

Previous experimental studies have demonstrated that the wake dynamics behind multi-scale porous patches, composed of square cylinders arranged in fractal-like configurations, exhibit complex nonlinear interactions driven by flow separation, bleed flow, and multi-scale instabilities. These investigations, utilizing Particle Image Velocimetry (PIV) and modal decomposition techniques such as Proper Orthogonal Decomposition (POD) and Dynamic Mode Decomposition (DMD), revealed that patch configuration significantly influences shedding frequencies, turbulence kinetic energy (TKE) distribution, and wake momentum thickness. To further elucidate the intricate physics governing these flows, we present results from high-fidelity Large Eddy Simulations (LES) of flow past the same multi-scale porous patches. The LES approach resolves fine-scale turbulent structures and provides detailed insights into the spatiotemporal evolution of coherent and incoherent flow features. Our simulations confirm experimental observations of protracted wakes and modulated shear layers due to bleed flow, while offering new perspectives on the role of vortex interactions and energy transfer across scales. Notably, the LES results highlight the impact of patch porosity distribution on the near-wake turbulence production and the downstream decay of element-scale perturbations. These findings enhance our understanding of flow dynamics in natural and engineered systems, such as aquatic vegetation and urban canopies, and underscore the potential of LES as a tool for optimizing turbulence control strategies. This work bridges experimental and computational approaches, paving the way for advanced modeling of multi-scale flow phenomena.

Higham, J. E., and W. Brevis. "Modification of the modal characteristics of a square cylinder wake obstructed by a multi-scale array of obstacles." *Experimental Thermal and Fluid Science* 90 (2018): 212-219.

Higham, J. E., et al. "Modification of modal characteristics in wakes of square cylinders with multi-scale porosity." *Physics of Fluids* 33.4 (2021).

Higham, J. E., et al. "Modification of modal characteristics in wakes of square cylinders with multi-scale porosity." *Physics of Fluids* 33.4 (2021).

INS/006:Spin-Up and Spin-Down Flow Instabilities in Cylinders - Poster

[1*]Bartle, Ellen; [2]Beaume, Cédric; [3] Kapur, Nik; [4] de Boer, Greg

[1]University of Leeds LS2 9JT, sceab@leeds.ac.uk

[2]University of Leeds LS2 9JT, c.m.l.beaume@leeds.ac.uk

[3]University of Leeds LS2 9JT, n.kapur@leeds.ac.uk

[4]University of Leeds LS2 9JT, g.n.deboer@leeds.ac.uk

*Presenting Author

Several areas of academia and industry, ranging from projectile dynamics (Wedemeyer, 1964) to food processing (Goto, 2023), seek to deepen their understanding of fluid behaviour within bounded rotating systems. Despite their practical relevance, the transient flows that emerge in such configurations remain poorly understood, due in part to a lack of targeted studies examining the onset and development of instabilities.

The present study focuses on the impulsive spin-up and spin-down flows, of a Newtonian fluid, in bounded cylinders. In the impulsive spin-up case, a stationary cylinder filled with a fluid, initially at rest, is suddenly set into rotation, while in the impulsive spin-down case, a rotating cylinder containing a fluid in solid-body rotation is abruptly stopped. While geometrically simple, these setups generate complex flow structures driven by viscous boundary layer dynamics, redistribution of angular momentum, and the onset of instabilities (Greenspan, 1968; Benton, 1974). Analytical techniques are employed alongside high-order numerical simulations to investigate the criteria for the development of these instabilities. Starting from the Navier–Stokes equations expressed in cylindrical coordinates under the assumption of axisymmetry, expressions for the azimuthal velocity are derived in unbounded cylinders and in cylinders bounded by rigid walls. A parametric study involving the aspect ratio is conducted to explore the influence of the geometry and show how bounded system flows asymptotically approach the behaviour of unbounded systems as the aspect ratio increases. The investigation is then extended to three-dimensional simulations using spectral methods tailored for cylindrical geometries (Boroński & Tuckerman, 2007a, 2007b). This methodology enables a detailed examination of boundary layer evolution of intricate flow structures and of the onset of instabilities. This combination of analytical and numerical approaches allows the identification of the spatial structure of the vortical modes developing near the side and the end walls, thereby providing the criteria for instability in impulsive spin-up and spin-down flows within rotating cylinders.

Wedemeyer, E. H. (1964). The unsteady flow within a spinning cylinder. *Journal of Fluid Mechanics, 20*(3), 383–399. https://doi.org/10.1017/S002211206400129X

Goto, S., Horimoto, Y., Kaneko, T., Oya, K., Sugitani, Y., Aritsu, S., Yoshida, M., Ohyama, H., Eguchi, K., Kukimoto, S., Matsuyama, K., Nishimura, T., Fukuda, K., & Onoda, K. (2023). Precessing cylinder as high-shear-rate mixer: Application to emulsification. *Physics of Fluids, 35*(3), 035139. https://doi.org/10.1063/5.0139991

Greenspan, H. P. (1968). *The theory of rotating fluids*. Cambridge University Press.

Benton, E. R., & Clark, A., Jr. (1974). Spin-up. *Annual Review of Fluid Mechanics, 6*, 257–280. https://doi.org/10.1146/annurev.fl.06.010174.001353

Boroński, P., & Tuckerman, L. S. (2007a). Poloidal-toroidal decomposition in a finite cylinder. I. Influence matrices for the magnetohydrodynamic equations. *Journal of Computational Physics, 227*, 1523-1543. https://doi.org/10.1016/j.jcp.2007.08.023.

Boroński, P., & Tuckerman, L. S. (2007b). Poloidal-toroidal decomposition in a finite cylinder. II. Discretization, regularization and validation. *Journal of Computational Physics, 227*, 1544-1566 https://doi.org/10.1016/j.jcp.2007.08.035.

INS/008: The Formation of Large-Scale Vortices on Jupiter and Saturn

[1]Nicholls, Rhiannon; [2]Kersalé, Evy; [2]Hughes, David; [3]Davies, Chris

[1]EPSRC CDT in Fluid Dynamics, University of Leeds, Leeds LS2 9JT, United Kingdom. scramn@leeds.ac.uk *Presenting Author

[2]School of Mathematics, University of Leeds, Leeds LS2 9JT, United Kingdom

[3]School of Earth and Environment, University of Leeds, Leeds LS2 9JT, United Kingdom

Within the wide array of atmospheric circulation patterns seen across the solar system, polar vortices are an almost universally observed planetary-scale phenomenon. Recent missions to Jupiter and Saturn have offered satellite images of their polar regions with unparalleled detail. These images have unveiled unexpected structures. At Jupiter's Northern pole, there exists a cluster of vortices, with a central vortex at its core, surrounded by eight vortices of similar size. A similar arrangement is present at Jupiter's Southern pole, featuring six surrounding vortices. In contrast, both polar areas of Saturn display a sizable central vortex encircled by numerous smaller vortices. Notably, Saturn's Northern hemisphere boasts a unique feature: a zonal "hexagonal" westerly jet encompassing the vortex.

These captivating observations raise numerous questions about their origins. One conceivable hypothesis suggests that these vortex formations originate from the rotational convection within the layered outer zones of the planets, where properties such as viscosity and density undergo significant changes with increasing planetary radius. This research aims to attain a thorough comprehension of the instabilities arising from rotating stratified convection, with a particular emphasis on a simplified model of two-layer convection in rotation.

INS/010: Behaviour of upper edge trajectories in pipe flow

[1*]Bennett, Robert; [2]Duguet, Yohann; [3]Willis, Ashley; [4]Marensi, Elena

[1]School of Mechanical, Aerospace and Civil Engineering, University of Sheffield, Sheffield S1 3JD, UK. rcbennett1@sheffield.ac.uk [2]Laboratoire Interdisciplinaire des Sciences du Numérique–LISN-CNRS, Université Paris-Saclay,

F-91400 Orsay, France. duguet@lisn.fr

[3]School of Mathematics and Statistics, University of Sheffield, Sheffield S3 7RH, United Kingdom. a.p.willis@sheffield.ac.uk

[4]School of Mechanical, Aerospace and Civil Engineering, University of Sheffield, Sheffield S1 3JD, UK. e.marensi@sheffield.ac.uk *Presenting Author

Recent novel experiments and simulations [1,2] have presented a range of methods to completely suppress turbulence in shear flows by temporarily increasing the turbulent kinetic energy. This points to the dynamical systems idea of the "*upper edge*" [3], a boundary in phase space that separates higher-energy flows which relaminarise from lower-energy flows within the basin of attraction of turbulence (which stands in contrast to the well-studied "*lower edge*" that separates perturbations to laminar flow too small to trigger turbulence from those which are large enough). However, this perspective has yet to receive significant investigation, and much about the behaviour of trajectories on the upper edge is unknown. We study this effect with well-resolved direct numerical simulations of pipe flow using the open-source code Openpipeflow [4]. In order to track trajectories within the upper edge, we perform bisections between higher-energy initial flows which relaminarise and lower-energy flows which lead to turbulence (see below figure). We use nonlinear adjoint optimisation methods in order to refine the bisection process and investigate how close in phase space the upper edge approaches the turbulent attractor. In doing so, we study the differences in flow structures between turbulent flows and high-energy flows which relaminarise. Through these bisections we observe that trajectories on the upper edge are transient and rapidly approach the lower edge. To quantify this behaviour, we compute the average time taken for upper edge trajectories to approach the lower edge, and discuss potential implications for flow control.

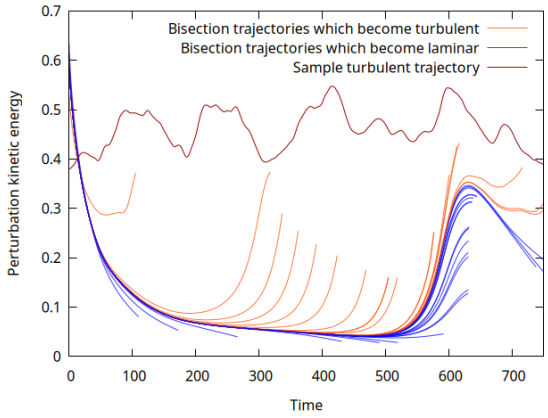

Figure 1: Kinetic energy of the perturbation to laminar flow versus time for a variety of trajectories at Re = 3,000. The red trajectory is a sample turbulent flow; the orange and blue trajectories represent trajectories found in the bisection of an upper edge trajectory which either became turbulent (orange) or relaminarised (blue). Though initially higher in energy than turbulence, the upper edge trajectory shadowed in the bisection was found to transiently approach a travelling wave embedded in the lower edge.

Bibliography

[1] Kühnen, J., Song, B., Scarselli, D., Budanur, N. B., Riedl, M., Willis, A. P., Avila, M., and Hof, B. (2018). Destabilizing turbulence in pipe flow. Nature Physics, 14(4), 386-390.

[2] Marensi, E., Ding, Z., Willis, A.P. and Kerswell, R.R. (2020). Designing a minimal baffle to destabilise turbulence in pipe flows. Journal of Fluid Mechanics, 900.

[3] Budanur, N. B., Marensi, E., Willis, A. P., and Hof, B. (2020). Upper edge of chaos and the energetics of transition in pipe flow. Physical Review Fluids, 5(2), 023903.

[4] Willis, A. P. (2017). The openpipeflow navier–stokes solver. SoftwareX 6, 124–127.

INS/011: Streamwise vortices in the entrance region of a circular pipe

[1*]Richards, Benjamin L.O.; [1]Marensi, Elena; [1]Ricco, Pierre

[1]School of Mechanical, Aerospace and Civil Engineering, The University of Sheffield, S1 3JD, UK; blorichards1@sheffield.ac.uk *Presenting Author

Despite extensive research on transitions to turbulence in fully developed pipe flow, relatively little is known about transitional flow in the entrance region [1]. Disturbances present at the pipe inlet enter the flow and are ultimately responsible for turbulent motion downstream. Here, we investigate the nonlinear evolution of free-stream disturbances in the entrance region of a circular pipe using the mathematical framework developed in [2]. Disturbances are assumed to be low-frequency and intense enough to give rise to nonlinear interactions inside the pipe, necessitating the use of the nonlinear unsteady boundary-region equations. A single pair of vortical modes of opposite azimuthal wavenumbers entering near the pipe mouth is used to model the disturbances. Matched asymptotic expansions are employed to construct appropriate initial conditions and the resulting initial-boundary value problem is solved numerically by a marching procedure in the streamwise direction. Particular focus is given to the identification of vortices in the entrance region and the effect of disturbances with high degrees of azimuthal symmetry. Common measures to identify vortex cores (pressure minimum, λ_2, Q-criterion) (see, e.g. [3]) are found to align better as nonlinear effects become stronger (figure 1). The dominant terms in the boundary region equations are considered in order to investigate the nature of these vortices. The effect of disturbances with short azimuthal wavelengths is found to confine vortices towards the pipe wall and shift the location of maximum velocity growth upstream compared with disturbances of lower order azimuthal symmetry.

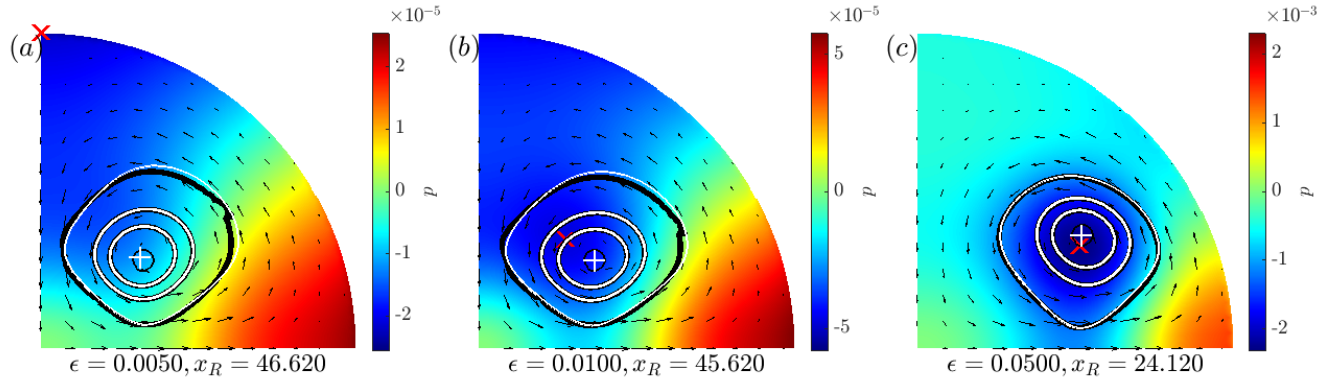

Figure 1. Quarter-pipe contours of pressure with cross-flow velocity components (shown as arrows) at streamwise locations of maximum instantaneous streamwise velocity. ϵ denotes the free-stream disturbance amplitude and x_R the distance from pipe mouth in units of pipe radius. Black and white contour lines denote lines of constant λ_2 and Q respectively. Red crosses indicate pressure minima, white crosses indicate Q maxima (which overlap with λ_2 minima, shown as small black circles). The pressure minimum is found at the pipe wall for ϵ = 0.005 and moves closer to the extremal points of the other criteria as nonlinear effects increase. In all cases, the inlet disturbances have 2-fold rotational symmetry and the subsequent flow largely maintains this symmetry, allowing to focus just one quarter of the pipe.

[1] I.J. Wygnanski and F.H. Champagne. On transition in a pipe. Part 1. The origin of puffs and slugs and the flow in a turbulent slug. J. Fluid Mech., 59:281–335, 1973.

[2] K. Zhu and P. Ricco. Nonlinear evolution of vortical disturbances entrained in the entrance region of a circular pipe. J. Fluid Mech., 998:A19, 2024.

[3] J. Jeong and F. Hussain. On the identification of a vortex. J. Fluid Mech., 285:69–94, 1995.

INS/012: From internal waves to turbulence in a stably stratified fluid

[1*]Rodda, Costanza; [2]Clement, Savaro; [2]Vincent, Bouillaut; [2]Pierre, Augier; [2]Joel, Sommeria; [2]Thomas, Valran; [2]Samuel, Viboud; [2]Nicolas, Mordant

[1]Imperial College London c.rodda@imperial.ac.uk [2]Universite' Grenoble Alpes. *Presenting Author

We report on the statistical analysis of stratified turbulence forced by large-scale waves. The setup mimics some features of the tidal forcing of turbulence in the ocean interior at submesoscales. Our experiments are performed in the large-scale Coriolis facility in Grenoble, which is 13 m in diameter and 1 m deep. Four wave makers excite large-scale waves of moderate amplitude. In addition to weak internal wave turbulence at large scales, we observe strongly nonlinear waves, the breaking of which triggers intermittently strong turbulence at small scales. A transition to strongly nonlinear turbulence is observed at smaller scales. Our measurements are reminiscent of oceanic observations. Despite similarities with the empirical Garrett and Munk spectrum that assumes weak wave turbulence, our observed energy spectra are rather to be attributed to strongly nonlinear internal waves.

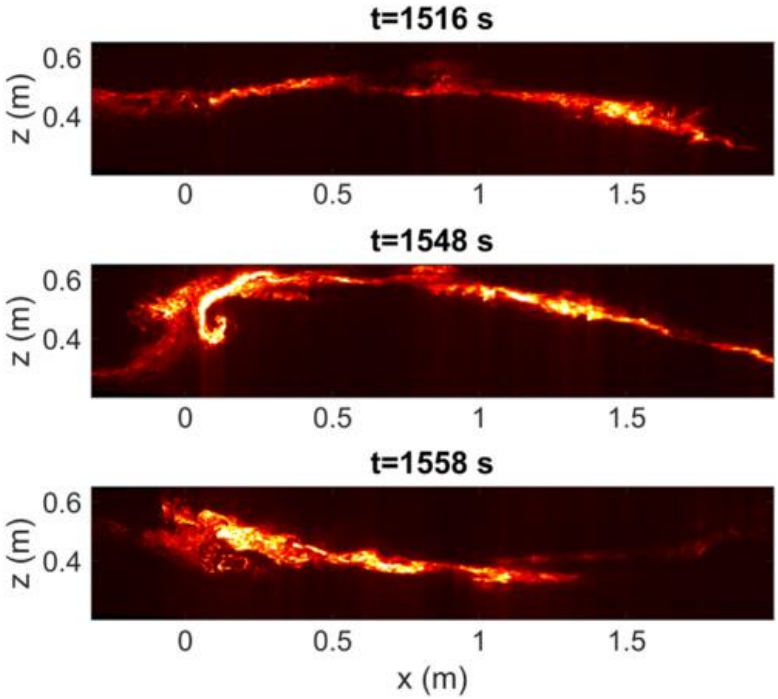

Figure 1. Snapshots in a vertical plane of a volumetric laser scan of a fluorescent dye layer showing an overturning internal wave.

Costanza Rodda, Clément Savaro, Vincent Bouillaut, Pierre Augier, Joël Sommeria, Thomas Valran, Samuel Viboud, Nicolas Mordant. "From Internal Waves to Turbulence in a Stably Stratified Fluid", Phys. Rev. Lett., 131(26).

Costanza Rodda, Clément Savaro, Géraldine Davis, Jason Reneuve, Pierre Augier, Joël Sommeria, Thomas Valran, Samuel Viboud, Nicolas Mordants. "Experimental observations of internal wave turbulence transition in a stratified fluid." Phys. Rev. Fluids, 7(9

INS/013: Breakdown to turbulence in high-enthalpy boundary layers

[1*]Ala, Teja; [1]Sandham, Neil D.

[1]Boldrewood Innovation Campus, University of Southampton, SO16 7QF. *Presenting Author: t.ala@soton.ac.uk

Transition from laminar to turbulent flow in hypersonic boundary layers critically affects surface heat flux and skin friction, especially under high-enthalpy conditions where chemical and vibrational nonequilibrium effects are significant. Accurate transition prediction must account for these effects, which influence both the base flow and the evolution of instabilities. This study combines Direct Numerical Simulations (DNS) and Implicit Large Eddy Simulations (ILES) to examine the growth and nonlinear breakdown of Mack's second-mode instabilities in chemically frozen flows subject to different thermal excitations. While linear instability has been extensively studied, the breakdown to turbulence under varying thermal states remains less explored. Post-shock flow conditions were defined behind a sharp wedge flying at Mach 10 and 36 km altitude. Four cases were considered based on two wedge angles (producing post-shock Mach numbers of 6 and 8) and two isothermal wall temperatures (1200 K and 1800 K). Simulations were run under three thermal states: calorically perfect gas (CPG), thermal equilibrium (TEQ), and thermal nonequilibrium (TNE), each representative of a different streamwise region along the wedge. Linear Stability Theory (LST) identified the dominant 2D Mack mode in each case, and a spanwise-varying wall forcing was applied to excite second-mode instabilities. Results show that transition onset is highly sensitive to the thermal state: CPG and TEQ cases transition earlier and show steeper gradients in skin friction and heat flux. In contrast, TNE delays transition. DNS and ILES results for the TNE case align closely, predicting the same onset location. These findings underline the importance of modelling the base flow thermal state correctly. Omitting thermal nonequilibrium can lead to premature transition predictions and overestimated surface heating. For robust transition forecasting in hypersonic boundary layers, thermal models must reflect the actual relaxation state of the flow.

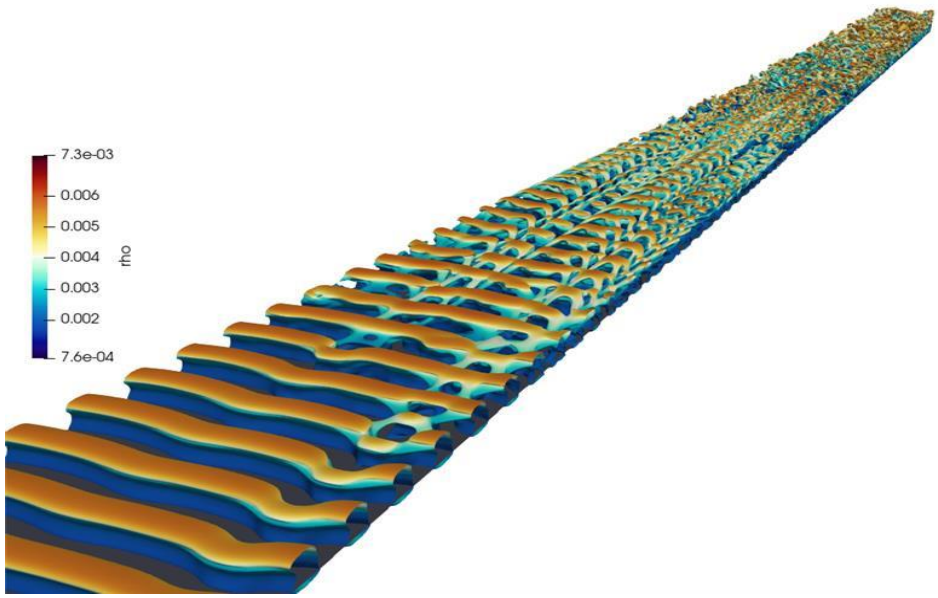

Figure 1. Oblique view of Q-criterion isosurfaces coloured by density in the Mach 6 (Tw = 1800 K, TNE). Only a subsection of the domain is shown to highlight the emergence and evolution of coherent vortical structures.

INS/014: Experimental study on the effects of Couette component on Poiseuille flow in a square duct geometry using laser doppler velocimetry

Oliver F. King[1]*, Jonathan M. Dodds[2], Christopher J. Cunliffe[2], Eann Patterson[1], Steve Graham[2], Robert J. Poole[1]

[1] School of Engineering, University of Liverpool, Liverpool L69 3GH, United Kingdom
[2] United Kingdom National Nuclear Laboratory, Workington CA14 3YQ, United Kingdom
*presenter, sgoking@liverpool.ac.uk

Couette–Poiseuille flow represents a fundamental fluid dynamic scenario characterized by simultaneous pressure-driven flow (Poiseuille component) and boundary-driven flow (Couette component).

There is a lack of comprehensive understanding of turbulence control in pressure-driven flow with moving walls in the current literature. Prior research on similar configurations was mainly based on numerical approaches, with limited experimental validation. Owolabi et al. (2019) analysed laminar flow in a square duct and explained the significant role of wall motion in the flow profile but did not include the consideration of turbulent conditions in their study. Thurlow et al. (2000) analysed Couette–Poiseuille flow in a planar duct where wall motion created significant changes in the velocity profiles. The research of Thurlow et al. (2000) was based on low relative wall speed experiments, in which slight decreases in near-wall turbulence were observed without considering the effects of high relative wall motions.

In an effort to address the current gap in knowledge, the current research investigates experimentally the effects of a moving wall (Couette component) with a substantial relative speed on the production of turbulence in pressure-driven water flow through a square duct using the technique of laser Doppler velocimetry (LDV) measurements. Velocity and turbulence intensity profiles were measured in the vertical and in the horizontal duct cross-section at different wall velocities in comparison with the centreline flow velocity. It was observed that the reduction in turbulence intensity near the moving wall is significant, especially for wall velocity close to the centreline flow velocity. This mitigation of turbulence is attributed to the removal of mean shear as a turbulence production mechanism caused by the moving wall.

Thurlow, E.M. and Klewicki, J.C. (2000) 'Experimental study of turbulent Poiseuille–couette flow', Physics of Fluids, 12(4), pp. 865–875. doi:10.1063/1.870341.

Owolabi, B.E., Dennis, D.J. and Poole, R.J. (2019) 'Entry length requirements for two- and three-dimensional laminar couette–Poiseuille flows', Journal of Fluids Engineering, 141(12). doi:10.1115/1.4043986.

INS/015: Real-world turbulence effects on the aerodynamic sensitivity of an Ahmed body

[1*]Taramasco, Jacob; [1]Ng, Henry; [1]Poole, Rob; [1]Cadot, Olivier

[1]School of Engineering, University of Liverpool, Liverpool L69 3GH

Nowadays, there are major concerns on addressing the aerodynamic performance of vehicles that perform in realistic conditions. These conditions typically differ considerably to those that have been historically used within wind tunnel testing and are found in most wind tunnels today. Studies by Wordley and Saunders (2008,2009) and Saunders and Mansour (2000) show how typical wind tunnel measurements differ significantly to the incoming flow automobiles would face when comparing the turbulence inhomogeneities and intensities. All 3 studies measured turbulence intensities significantly higher than the typically low (<1%) turbulence intensities found in most automotive wind tunnels around the world (Wordley and Saunders, 2008). The highest measured turbulence intensity was 16% with the lowest being greater than 1%.

Over the past decade, most fundamental studies address the physics of the recirculation region at the base of the vehicle with clean inflow conditions. The effects of real-world effects on this region are scarcely explored, with a handful of studies on the effects of the recirculating flow dynamics and how this effects the overall drag. Burton et al. (2021) and Cadot et al. (2020) studied the effects of the turbulent intensity on the wake switching rate on an Ahmed body but achieved somehow opposite conclusion.

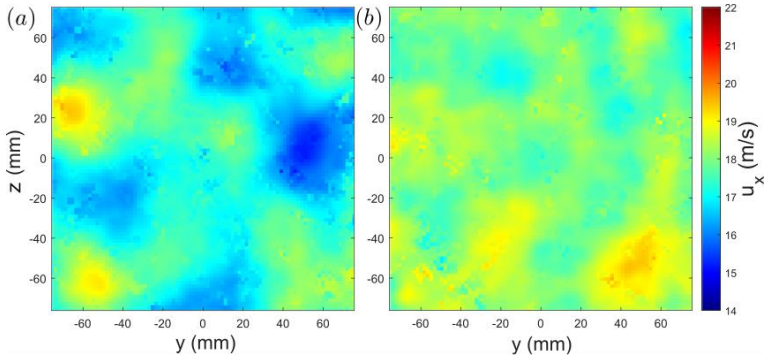

Figure 1: Velocity snapshots of the turbulent freestreams in a transversal plane measured above the force balance location with (a) full squared mesh grid 20mm bars and solidity 42.2% and (b) clean tunnel with no installed grid

This research aims to use the varying turbulence fields to better understand the drag and pressure characteristics of a taller-than-wide square-back Ahmed body, at variable body attitudes. Elevated freestream turbulence intensities are achieved via a bespoke set of turbulence generating grids of variable bar diameter and aperture. The tested model is the same as studied by Fan et al. (2022).

Example results from a grid characterisation study are shown in Figure 1 for 20mm diameter bars and solidity of 42.2%. At the UK fluids conference, the effects on the physics of the flow around the Ahmed body will be presented for varying turbulence intensities.

Wordley, S. & Saunders J., 2008, On-Road Turbulence. *SAE International Journal of Passenger Cars-Mechanical Systems.* 117 (6) pp 341-360

Wordley, S. & Saunders J., 2009, On-Road Turbulence: Part 2. *SAE International Journal of Passenger Cars-Mechanical Systems.* 118 (6) pp 111-137

Saunders J. & Mansour R., 2000. On-Road and Wind Tunnel Turbulence and its Measurement Using a Four-Hole Dynamic Probe Ahead of Several Cars. *SAE International Journal of Passenger Cars-Mechanical Systems.* 109 (6) pp 477-49

Burton D., Wang S., Smith D. T., Scott H. N., Crouch T. N. & Thompson M. C., 2021. The influence of background turbulence on Ahmed-body wake bistability. *Journal of Fluid Mechanics.* 926

Cadot O., Almarzooqi M., Legeai A., Parezanovic V. & Pastur L., 2020. On three-dimensional bluff body wake symmetry breaking with free-stream turbulence and residual asymmetry. *Comptes Rendus. Mechanique.* 348 (6-7) pp 509-517

Fan Y., Parezanovic V. & Cadot O., 2022. Wake Transitions and steady z-instability of an Ahmed body in varying flow conditions. *Journal of Fluid Mechanics.* 942 ppA22

INS/017: Magnetoconvection in a rapidly rotating fluid layer - Poster

[1*]Jackson, Oliver; [2]Kersalé, Evy

[1]University of Leeds, scorj@leeds.ac.uk. [2]University of Leeds, E.kersale@leeds.ac.uk.

Large scale coherent vortices have been observed in striking images of the polar regions of Jupiter and Saturn. One theoretical explanation for these structures is that they emerge because of deep convection, strongly influenced by rotation. This project considers the crucial influence of magnetic fields and stratification, with the specific aim of understanding the mechanism that determines the depth to which the vortices extend. As a first step, using linear stability analysis we make the Boussinesq approximation and investigate the stability of a rotating layer, heated from below and subject to a uniform magnetic field. The relative magnitudes of the Taylor number characterising rotation strength and Chandrasekhar number characterising magnetic field strength can be split into three regimes: magnetic field dominant, fields co-dominant and rotation dominant. We determine the onset of steady and oscillatory modes and compare the transition between regimes at high Taylor numbers as magnetic field strength is increased. The analysis reveals that the transition boundaries differ significantly between the two modes. This work provides a foundation for the analysis of the analogous case under the anelastic approximation, which aims to capture the effects of fluid stratification present in planetary atmospheres. Our findings offer insights into the role of magnetic fields and rotation in the underlying fluid dynamics within the polar atmospheres of Jupiter and Saturn.

INS/018: Data-driven dynamical modelling of noise generation by a mixing layer

[1] Zhou, Dao; [2*] Wang, Zhong-Nan

[1] University of Birmingham (dxz324@student.bham.ac.uk) [2] University of Birmingham (z.n.wang@bham.ac.uk). *Zhou, Dao

Noise, identified by WHO as the second largest environmental pollution, can cause both auditory and non-auditory health issues [1]. Turbulent shear flow is a major source that is responsible for the noise of land and air vehicles. Growing evidence suggests that coherent structures within turbulent shear flows are highly correlated to the generation of sound. Linear models are used to predict the coherent structures as instability waves, but tend to underestimate the noise generation, as nonlinear dynamics of coherent structures, such as intermittency, can play a key role in radiating sound [2]. The research in this paper aims to model the nonlinear dynamics of coherent structures in a mixing layer and identify their roles in noise production. The Sparse Identification of Nonlinear Dynamics (SINDy) is used to derive the physics-constrained reduced-order model (ROM) from LES data to capture the key nonlinear dynamics in the low-dimensional basis provided by Proper Orthogonal Decomposition (POD), shown in Figure 1. An improved eddy viscosity closure is proposed to consider the energy transfer between the resolved and truncated modes. Moreover, stability analysis methods based on the reduced-order model will be employed to elucidate the critical role of nonlinear effects in sound radiation. The acoustic field will be obtained by solving the Acoustics Perturbation Equation with reduced-order modeled sources, offering insights into the relationship between the nonlinear dynamics of coherent structures and noise generation.

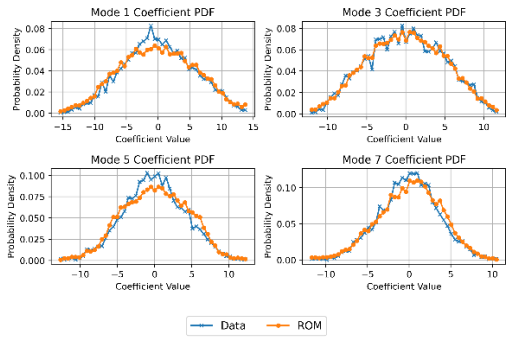

(a) *Probability density functions (PDFs) of the coefficients of the four leading POD modes (Blue line: LES, orange line: ROM).*

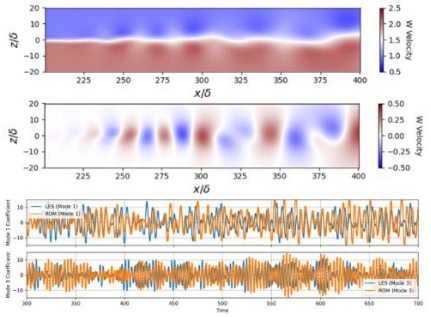

(b) *Reconstructed instantaneous velocities and predicted temporal evolution of the coefficients of the two leading POD modes (Blue line: LES, orange line: ROM) (bottom) from the reduced-order model.*

Figure 1. ROM-based prediction of nonlinear dynamics of coherent structure in a mixing layer.

[1] M. Basner, W. Babisch, A. Davis, M. Brink, C. Clark, S. Janssen, and S. Stansfeld. Auditory and non-auditory effects of noise on health. Lancet, 383(9925):1325–1332, 2014.

[2] P. Jordan and T. Colonius. Wave packets and turbulent jet noise. Annual Review of Fluid Mechanics, 45(1):173–195, 2013.

INS/021: Avian Flapping Flyer Response to Discreet Gusts

[1*]Proe, Charles; [2]Shepard, Emily; [3]Celik, Alper

[1,2,3] Faculty of Science and Engineering, Swansea University Bay Campus, Fabian Way, Swansea, UK

[1]2015531@swansea.ac.uk. [2]e.l.c.shepard@swansea.ac.uk, [3]alper.celik@swansea.ac.uk.

Development of UAV's (Unmanned aerial vehicles) and UAM (Urban air mobility) vehicles has highlighted opportunities for a wide range of emerging technologies, ranging from fast acrobatic drones to the air taxis, covering diverse applications and sizes. Many of these vehicles are envisaged to operate in built up urban areas to provide most economic benefit. Large buildings such as factories and skyscrapers produce a wide range of unsteady airflows which can in turn affect a wide range of different sized aircraft. Since their primary operational environment will be turbulent, it is imperative that we understand effective ways to reject gusts and turbulence to ensure that drones can safely and efficiently operate in urban environments. To address this challenge, we are employing a bio-inspired approach to understand how pigeons (Columba livia) reject 1-cosine gusts. Specifically, we assess their body movements under gust conditions using motion capture equipment. Using tools such as PCA and PRC (Principal component analysis, Phase response curve), we identify how the body movements of the pigeons evolve throughout the gust encounter, and quantify its impact on the flapping cycle. We have also examined the pigeons' response under varying gust magnitudes, frequencies and flight conditions, such as climbing and level flight, to understand how the gust response-rejection strategies change. Importantly, this type of in-depth study has not been previously conducted on this flapping style, which is comparable to rotorcraft, which make up the vast majority of UAV's and UAM vehicles. Our preliminary results indicate that gust encounters during upstroke induce a delayed response but has less significant impact on phase change compared to gust encounters in downstroke. Through this comprehensive approach, we aim to gain a deeper insight into pigeons' gust rejection strategies, informing the design of future aircraft to effectively operate in complex environments.

INS/022: Instability-Induced Vortex Collisions and Wake intrainment in Floating offshore Wind Turbines

[1*]Shahrokhi, Ava; [2]Seddighi, Mehdi, [3]Al Awaj, Belal

[1,2,3] Liverpool John Moores University, Liverpool, UK, L33AF

[1]a.shahrokhi@ljmu.ac.uk , [2] m.seddighi@ljmu.ac.uk, [3] b.a.alawaj@2024.ljmu.ac.uk , *Presenting Author

Floating offshore wind turbines (FOWTs) operate in highly unsteady flow environments where platform motion, wind shear, and low ambient turbulence collectively alter wake dynamics. A critical factor influencing turbine performance and structural integrity is the development of near-wake instabilities—particularly tip-vortex breakdown, wake distortion, and vortex interactions. Among these, unsteady vortex collisions and pairing instabilities can induce three-dimensional flow structures that significantly impact energy transport, turbulence production, and the spatial evolution of the wake (Fang et al., 2020).

This study investigates the role of instability-induced vortex collisions in shaping the near- and far-wake structure of offshore wind turbines. Particular emphasis is placed on the nonlinear evolution of tip vortices and their pairwise interaction—commonly known as leapfrogging—which can result in complex unsteady behaviour. The instability mode becomes significant when adjacent helical vortex filaments are close enough to exert mutual induction, initiating vortex pairing. This pairing instability is a precursor to vortex distortion, core merging, and eventual breakdown. It enhances turbulent mixing and facilitates the transport of kinetic energy across the wake shear layer, accelerating wake recovery and impacting downstream turbine inflow conditions (Li et al., 2022; Liu et al., 2017).

The simulations employ an unsteady Reynolds-Averaged Navier–Stokes (URANS) approach with a turbulence model capable of capturing shear-layer instabilities and vortex-induced turbulence. ANSYS Fluent is used for numerical modelling, with dynamic mesh techniques applied to unstructured grids. User-defined functions (UDFs) are developed to introduce platform motion, track vortex structures, and compute vortex interaction metrics. The computational domain is designed to resolve both near- and far-wake features, with special attention to vortex stretching, leapfrogging behaviour, and the amplification of instability modes.

The outcomes of this study will provide novel insights into the instability-driven dynamics of FOWT wakes. By improving our understanding of vortex interactions and wake mixing, the findings aim to support more accurate wake models, inform optimal turbine spacing, and contribute to the fatigue-load management and power stability of next-generation offshore wind farms.

References

Dong, J. & Vire, A., 2021. Comparative analysis of different criteria for the prediction of vortex ring state of floating wind turbines. *Renewable Energy,* Volume 163, pp. 882-909.

Fang, Y., Duan, L., Zhao, Y. & Yang, H., 2020. Numerical analysis of aerodynamic performance of a floating offshore wind turbine under pitch motion. *Energy,* Volume 192.

Liu, Y. et al., 2017. Establishing a fully coupled CFD analysis tool of floating offshore wind turbine. *Renewable Energy,* Volume 112, pp. 280-301.

Sivalingam, K., Steven, M. & Singapore Wala, A. A., 2018. Numerical Validation of Floating Offshore Wind Turbine Scaled Rotors for Surge Motion. *Energies,* p. 2578.

INS/023: LOCAL SHORT-WAVELENGTH ANALYSIS OF CENTRIFUGAL AND MCINTYRE INSTABILITIES IN VISCO-DIFFUSIVE SWIRLING FLOWS

[1*]Kirillov, Oleg N.; [2]Mutabazi, Innocent

[1]Department of Mathematics, Physics, and Electrical Engineering, Northumbria University, Newcastle upon Tyne, UK; Email: oleg.kirillov@northumbria.ac.uk. [2]LOMC UMR-6294 CNRS, Université Le Havre Normandie, Normandie Université, Le Havre, France; Email: innocent.mutabazi@univ-lehavre.fr. *Presenting Author

An analytical theory is presented for linear, local, short-wavelength instabilities in swirling flows, in which axial shear, differential rotation, radial thermal stratification, viscosity, and thermal diffusivity are all taken into account. The simultaneous inclusion of these physical effects is considered both timely and essential for the accurate modelling of swirling flows encountered in natural and industrial contexts. A geometrical optics approach is applied to the Navier–Stokes equations, coupled with the energy equation, leading to a set of amplitude transport equations. From these, a dispersion relation is derived, capturing two distinct types of instability: a stationary centrifugal instability and an oscillatory, visco-diffusive McIntyre instability. Instability regions corresponding to different axial or azimuthal wavenumbers are found to possess envelopes in the plane of Azimuthal Reynolds number (Re) and axial Grashof number (Gr), which are explicitly determined using the discriminants of polynomials. In light of the established relationship between envelopes of curve families and parametric optimisation, it is concluded that the envelopes correspond to curves of critical values of physical parameters, thereby providing a method to obtain compact, closed-form criteria for the onset of instability. The derived analytical criteria are validated for a swirling flow modelled by a cylindrical, differentially rotating annulus with axial flow induced by a radial temperature gradient combined with vertical gravity – baroclinic Couette flow (BCF). These criteria unify and extend, to viscous and thermodiffusive differentially heated swirling flows, the Rayleigh criterion for centrifugally driven instabilities, the Ludwieg–Eckhoff–Leibovich–Stewartson (LELS) criterion for isothermal swirling flows, and the Goldreich–Schubert–Fricke (GSF) criterion for non-isothermal azimuthal flows.

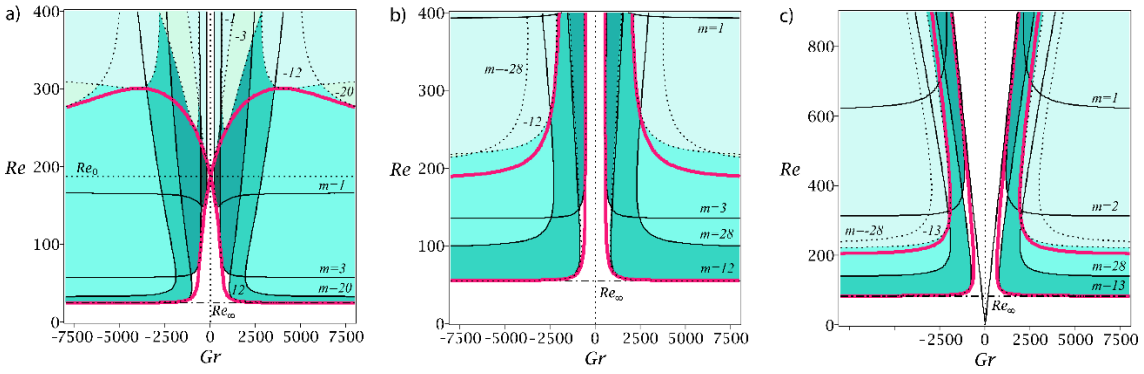

Figure 1. Greenish domains of centrifugal instability bounded by (black lines) neutral stability curves for BCF with η = 0.8, Pr = 5.5, γ =0.0004, $k_r = 4\sqrt{2}$. Panels (a–c) show the curves parameterized by the azimuthal wavenumber m, for (a) Rayleigh unstable (μ = 0), (b) modified Rayleigh line (μ ≈ 0.63935), (c) Rayleigh stable (μ = 0.8). Thick red curves indicate the envelope with horizontal asymptotes Re = Re∞: (a) ≈ 24.66, (b) ≈ 55.13, (c) ≈ 83.99. In (a), envelope branches intersect at Re = Re_0 ≈ 187.14. Oblique black lines in (c) represent the visco-thermodiffusive extension of the LELS and GSF criteria. Computations are performed at the mean geometric radius $r_g = \sqrt{\eta} / (1 - \eta)$.

Kirillov, O.N. & Mutabazi, I. 2017, Short wavelength local instabilities of a circular Couette flow with radial temperature gradient, *J. Fluid Mech.,* 818 319-343.

Kirillov, O.N. & Mutabazi, I. 2024, Unification theory of instabilities of visco-diffusive swirling flows, *Phys. Rev. Fluids*, 9 124802.

Kirillov, O.N. 2025, Geometrical optics stability analysis of rotating visco-diffusive flows, *Mathematics*, 13 382.

Kirillov, O.N. & Mutabazi, I. 2025, Instabilities in visco-thermodiffusive swirling flows, *J. Fluid Mech.*, subm, arXiv:2502.00773v1.

OTH: OTHER TOPIC

OTH/001: DYNAMIC DROPLET FRICTION ON LIQUID-LIKE SURFACES

[1*]McHale, Glen; [2]Chen, Jinju; [1]Wells, Gary G.; [1]Barrio-Zhang, Hernán;

[1]Janahi Sara; [1]Wang, Yaofeng; [1]Ledesma-Aguilar, Rodrigo

[1]The University of Edinburgh, glen.mchale@ed.ac.uk. [2]Loughborough University.

Frictional forces resisting droplet motion often appear to be separate to surface wettability and liquid adhesion. Here we show such friction arises from a simple combination of the surface heterogeneity and the normal adhesive force [1]. Our alternative to the Kawasaki-Furmidge equation [2,3] allows the contributions to the friction to be separated into a product involving the surface wettability (normal adhesion) and hysteresis (heterogeneity) of the surface thereby providing insight into the design of surfaces slippery to liquids. Using tilt angle experiments on low (c50-SOCAL) and high (SOCAL) dynamic friction liquid-like surfaces [4], we confirm the dependence of the coefficient of droplet-on-solid kinetic friction on system parameters [5]. We find the ratio of frictional force, F_f, to the normal component of the surface tension force, F_N, for the moving droplet is directly proportional to the difference, $\Delta\theta=(\theta_f - \theta_b)$, in the front and back dynamic contact angles. The experimentally determined constant of proportionality, k/π, is $k=0.785\pm0.002$ in excellent agreement with the value of $k=\pi/4\approx0.785$ of our theoretical model for a droplet moving with a circular contact area. We also show a molecular kinetic theory (MKT) type model [6] can describe the non-linear velocity-force relationship. Our findings provide a fundamental understanding of droplet-on-solid friction, wettability and liquid adhesion.

Acknowledgement. The authors acknowledge financial support from the UK EPSRC (grant EP/V049348/1).

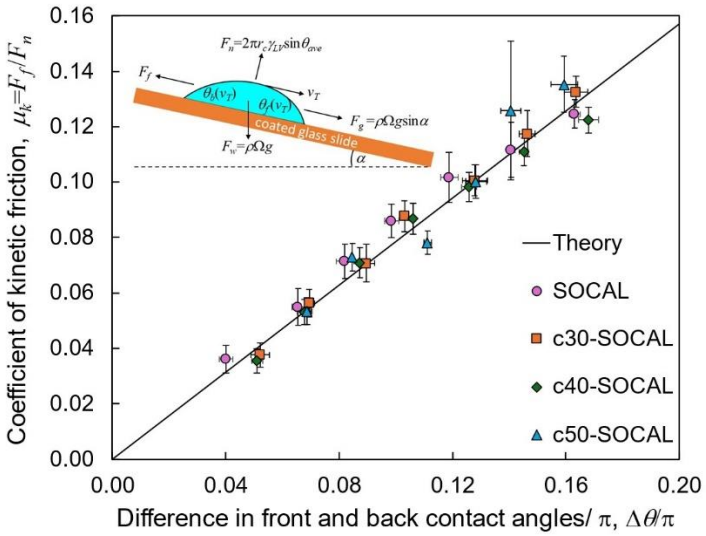

Figure 1. Measurement of forces and droplet shape to determine the coefficient of kinetic friction. Inset shows experimental arrangement.

[1] McHale, G., Gao, N., Wells, G.G., Barrio-Zhang, H., Ledesma-Aguilar, R., 2022, *Langmuir* 38 (14) pp 4425-4433.

[2] Kawasaki, K., 1960, *J. Colloid Sci.* 15 (5) pp 402-407.

[3] Furmidge, C.G.L., 1962, *J. Colloid Sci.* 17 (4) pp 309-324.

[4] Wang, L., McCarthy, T.J., 2016, *Angew. Chemie Int. Ed.* 55 (1) pp. 244-248.

[5] McHale, G., *et al.*, 2025, To be submitted.

[6] Blake, T.D., Haynes, J.M., 1969, J. Colloid Interf. Sci. 30 (1) pp. 421-423.

OTH/002: Using sub-sonic vibrating flow fields for micro particle collection

[1*]Ansu Sun, Joseph Meredith, Prashant Agrawal

[1]Smart Materials and surfaces Laboratory, Faculty of Engineering and Environment, Northumbria University, Newcastle upon Tyne, NE1 8ST, United Kingdom. a.sun@northumbria.ac.uk

Particle enrichment and sorting play a crucial role in industries such as healthcare, food, and energy, where precise control over particle size is essential for quality and safety of product. Current large scale technologies like filtration and centrifugation, often lack precision, while microscale technology, though highly accurate, are costly and limited in throughput. Achieving an optimal balance between efficiency, scalability, and precision in particle enrichment processes remains a significant challenge, particularly for both soft and hard microparticles used in industrial and biomedical applications.

In this study, we present a technique relying on fluid flow gradients induced by low-frequency oscillations to collect microparticles. Different strategies are introduced to control the spatial and temporal flow field gradients in a liquid to drive particles to specific regions in the flow field. This method can also be used to control the second order flow fields, that aids in stabilising the motion of particles towards the collection region. Our experimental findings are further validated through finite element numerical simulations.

This energy-efficient, scalable technique has the potential to advance particle enrichment technologies across multiple industries while also unlocking new opportunities in bio-medical diagnostics and therapeutic development.

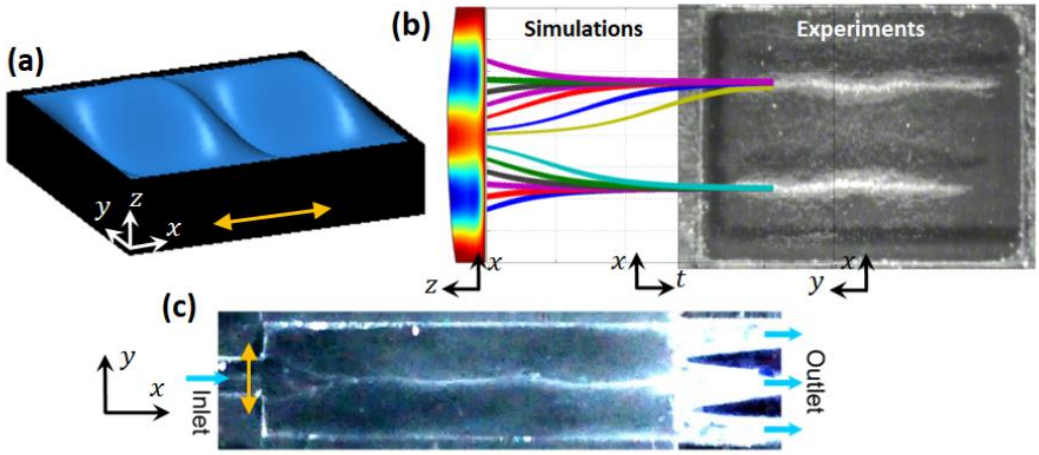

Figure 1: (a) Capillary wave depiction in a chamber vibrating in the x-direction; (b) Particle collection position as obtained in simulations (COMSOL and MATLAB) and experiments. The experiments show polystyrene particles (diameter 30 µm), vibrated via an electromagnetic shaker at 2V amplitude and 220 Hz frequency; (c) Collection of 5 µm silica particles in an open channel.

Acknowledgment

The authors would like to thank funding support from Northumbria University and EPSRC grant EP/W037718/1.

OTH/003: Uncertainty quantification of time-average quantities of chaotic systems using sensitivity-enhanced polynomial chaos expansion

*[1]Papadakis, George; [2]Kantarakias, Kyriakos

[1]Dept of Aeronautics, Imperial College London, SW7 2AZ g.papadakis@ic.ac.uk, *Presenting Author

[2]Dept of Aeronautics, Imperial College London, SW7 2AZ

We consider the effect of multiple stochastic parameters on the time-average quantities of chaotic systems. We employ the recently proposed sensitivity-enhanced generalized polynomial chaos expansion, se-gPC [1] to quantify efficiently this effect. se-gPC is an extension of gPC expansion, enriched with the sensitivity of the time-averaged quantities with respect to the stochastic variables. To compute these sensitivities, the adjoint of the shadowing operator [2] is derived in the frequency domain. Coupling the adjoint operator with gPC provides an efficient uncertainty quantification algorithm, which, in its simplest form, has computational cost that is independent of the number of random variables. The method is applied to the Kuramoto-Sivashinsky equation and is found to produce results that match very well with Monte Carlo simulations. The efficiency of the proposed method significantly outperforms sparse-grid approaches, such as Smolyak quadrature. These properties make the method [3] suitable for application to other dynamical systems with many stochastic parameters.

	se-gPC $p=1$		se-gPC $p=2$		Monte Carlo	
QoI	mean	std	mean	std	mean	std
$\overline{J^{(1)}}$	0.0196	0.6286	0.0196	0.6395	0.0195	0.6370
$\overline{J^{(2)}}$	2.3478	0.5251	2.3505	0.5174	2.3552	0.5192

TABLE 1. Comparison between Monte Carlo simulations with 5000 samples and se-gPC for the Kuramoto-Sivashinsky equation.

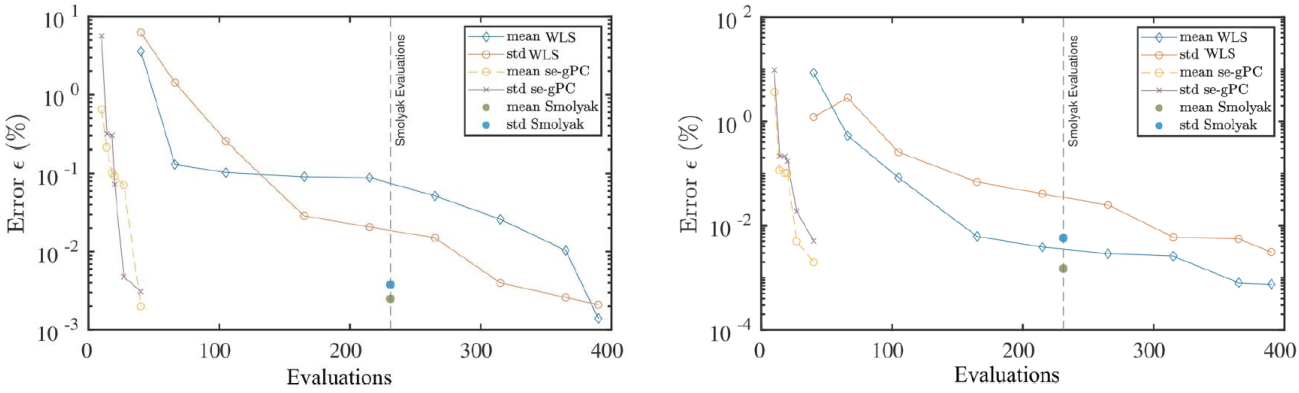

Figure 1. Convergence rate of mean and standard deviation against the number of evaluations for $\overline{J^{(1)}}$ (left) and for $\overline{J^{(2)}}$ (right).

[1] K. Kantarakias and G. Papadakis, 2023, J. Comp. Phys., vol. 491, 112377

[2] K. Kantarakias and G. Papadakis, 2023, J. Comp. Phys., vol. 474, 111757

[3] K. Kantarakias and G. Papadakis, 2024, Phys Rev E 109, 044208

OTH/004: Uncertainty quantification of the irregular flow past two side-by-side square cylinders using polynomial chaos

[1*]Namuroy, Claire; [2]Papadakis, George

[1]University of Cambridge, Department of Engineering, Trumpington Street, Cambridge CB2 1PZ (cmn46@cam.ac.uk).

[2]Imperial College London, Department of Aeronautics, Exhibition Road, London, SW7 2AZ (g.papadakis@imperial.ac.uk).

We consider the flow past a pair of identical square cylinders that are vertically separated by a gap equal to their diameter. At low Reynolds numbers, the wake behind the cylinders exhibits a rich set of chaotic flow dynamics driven by nonlinear interactions between the vortex shedding activity and the flow through the gap between the cylinders. In this study, the influence of the freestream Reynolds number on the statistics of the lift and drag coefficients and the velocity field is quantified. Starting from Direct Numerical Simulations (DNS) in the range $100 < Re_\infty < 200$, the uncertainties of the quantities of interest are computed very efficiently using non-intrusive polynomial chaos (PC). In a later stage, we perform Proper Orthogonal Decompositions (POD) of the velocity field to extract the dominant coherent structures in the wake. PC techniques are subsequently applied to construct sensitivity maps of the POD modes and their coefficients. Our analysis suggests that while the Reynolds number has a moderate effect on the underlying physical mechanisms, it regulates the degree of interaction between coherent structures. Over a narrow band of Reynolds numbers, the vortex shedding is found to synchronise with the gap flow, resulting in the emergence of periodic wake flow with sharp increases in the lift and drag coefficients. The results provide insight into the regions of the flow that are most sensitive to changes in Re_∞, which can be used to inform applications in flow control. They also demonstrate PC model's capability to capture the stochastic range of the quantities of interest with a low computational overhead.

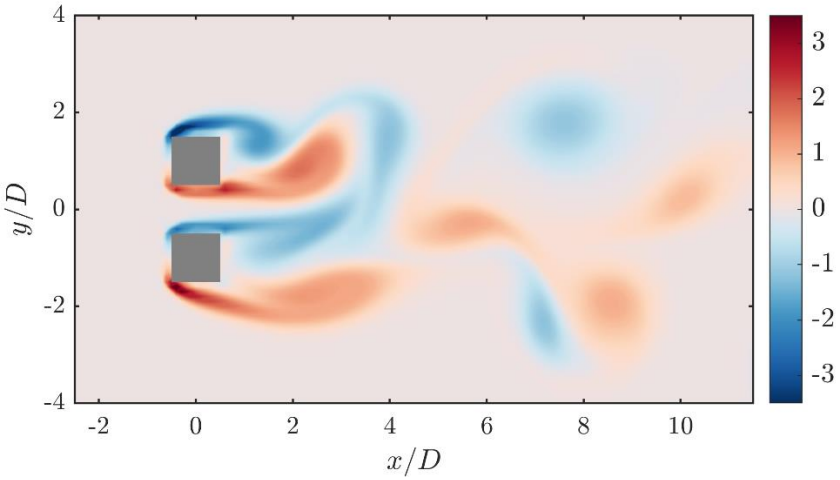

Figure 1. Contour plot of the instantaneous vorticity field at $Re_\infty = 139$. The cylinders are represented by grey squares of size $D \times D$.

OTH/005: Magnetohydrodynamic flow in circular and rectangular ducts

[1*] Puthan, Pranav; [1]Eardley-Brunt, Rupert ; [1]Politis, Gerasimos; [1]Dubas, Aleksander

[1]United Kingdom Atomic Energy Authority, Culham, Abington, OX14 3DB , *Presenting Author (pranav.naduvakkate@ukaea.uk)

The design of liquid metal blankets for nuclear fusion requires a thorough understanding of liquid metal behaviour under strong magnetic fields and thermal stresses. Several of the most prominent and extensively studied blanket concepts—such as the Water-Cooled Lead Lithium (WCLL), Helium-Cooled Lead Lithium (HCLL), and Dual-Cooled Lead Lithium (DCLL) designs—rely fundamentally on liquid metal technology for efficient heat extraction and tritium breeding. We conduct magnetohydrodynamic (MHD) flow simulations of liquid metals in ducts with circular and rectangular cross sections. Each case uses a geometry consistent with established experimental studies, enabling validation of the numerical results against published data. A steady magnetic field is applied perpendicular to the main direction of fluid flow, representing a common configuration in fusion blanket channels. The simulations capture detailed profiles of velocity and pressure under high Hartmann numbers, which quantify the relative strength of electromagnetic forces to viscous forces in MHD flows. We pay particular attention to flow behaviour in the Hartmann layers-thin boundary layers that form adjacent to walls perpendicular to the magnetic field and side layers, which develop along the walls parallel to the field. These boundary layers play a critical role in shaping the overall flow profile and pressure drop characteristics. To evaluate the accuracy of the numerical model, we extract velocity and pressure distributions along several key directions and locations within the flow domain. The results show excellent agreement with theoretical expectations, particularly in the development of flat core velocity profiles and steep gradients near the Hartmann and side walls. These simulations represent an initial set of results within a broader UKAEA verification and validation (V&V) strategy aimed at establishing confidence in numerical modelling of liquid metal flows relevant to fusion applications. The cases presented here are selected for their relevance to canonical MHD benchmark problems, forming a foundational step toward more complex geometries and transient conditions encountered in blanket systems. Future work will expand on this foundation by incorporating additional physical effects and comparing against a wider range of experimental data.

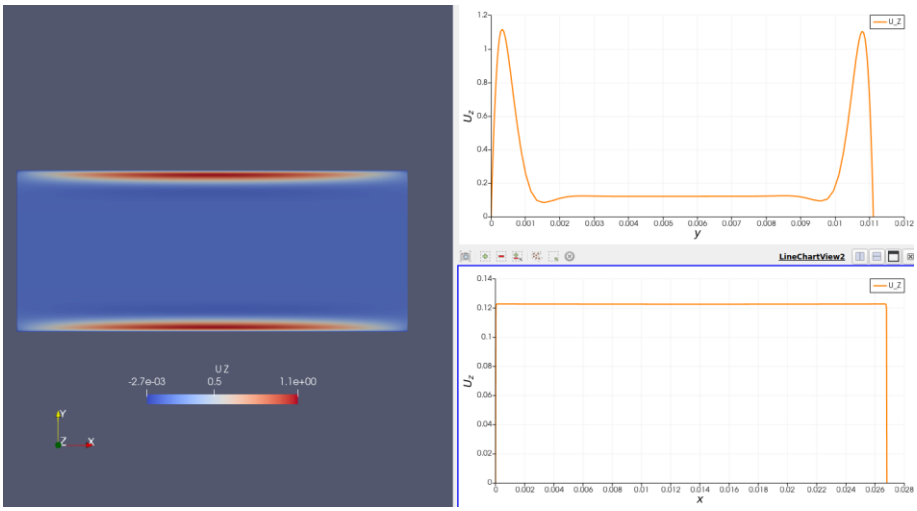

Qualitative representation of flow contours: Velocity profiles at the Hartmann layer (bottom) and the side boundary layer (top) at outlet of the rectangular domain

OTH/006: A general free-boundary lubrication framework for modelling dynamic capillary flows and application to the coflow system

[1*]Richards, Megan; [2]Pegler, Samuel

[1]EPSRC Centre for Doctoral Training in Fluid Dynamics, University of Leeds, Leeds LS2 9JT, UK, scmkr@leeds.ac.uk. [2]School of Mathematics, University of Leeds, Leeds LS2 9JT, UK, S.Pegler@leeds.ac.uk. *Presenting Author

Two-phase capillary flows in channels and pipes form a fundamental problem in fluid mechanics with widespread applications in physical, biological and microfluidic systems. We show that dynamic time-dependent phenomena in such systems can be described within a theoretical framework based on free-boundary lubrication theory combined with nonlinear representation of the interfacial curvature. The framework allows complex time-dependent capillary phenomena to be analysed using a relatively simple nonlinear hyperdiffusion equation with a moving boundary. Here, we propose the time-dependent framework and demonstrate its application to coflow, where two fluids (one viscous, the other inviscid) are injected concurrently into a channel.

The model predicts an oscillatory growth and pinch-off of the inviscid phase, producing a train of bubbles at a frequency, size and spatial pattern controlled by the capillary number C and flux ratio Q. We map a regime diagram over the C-Q parameter space, partitioned based on the formation of long (Taylor) bubbles versus smaller, approximately circular (non-Taylor) bubbles. An asymptotic theory of the former regime is developed, yielding an explicit theoretical prediction for the pinch-off frequency. The result is based on identifying a quasi-static regime of the necking region that is coupled via matching to an advancing dynamic contact line along the bubble film. The analysis thus reveals a link between the necking dynamics controlling confined bubble pinch-off and the time-dependent spreading dynamics of classical droplets. We propose the time-dependent nonlinear-curvature framework as a means to study dynamic capillary phenomena, providing a complement to experimental and full-Stokes simulation.

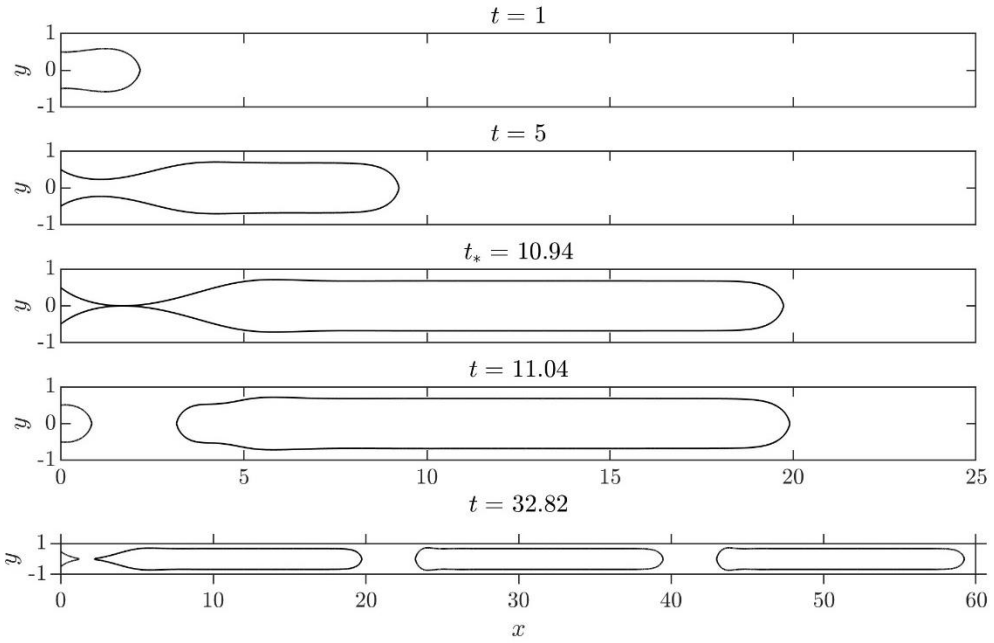

Figure 1. Time-dependent numerical solutions to the generalised lubrication model with nonlinear curvature, showing the formation of a Taylor bubble at t=10.94. The bubble then progresses through the channel as a closed bubble. Three detached bubbles are shown in the final plot to demonstrate the regular frequency of bubble formation.

OTH/008: Flame structure and NOx emissions of hydrogen LEan Azimuthal Flames (LEAF)

[1*]Pandey, Khushboo; [2]Malé, Quentin; [2]Noiray, Nicolas

[1]Institute for Multiscale Thermofluids, School of Engineering,

University of Edinburgh, EH9 3FD, UK, kpandey@ed.ac.uk

[2]CAPS Laboratory, Department of Mechanical and Process Engineering,

ETH Zurich, Zurich 8092, Switzerland. *Presenting Author

Reducing the carbon footprint and emissions of the power and transport sector is crucial for meeting the net-zero emission target by 2050. Hence, there is a pressing need to develop new sustainable combustion concepts and integrate the usage of carbon-free fuels such as hydrogen. Recently, the Lean Azimuthal Flame (LEAF) concept has demonstrated soot-free and ultra-low NOx emissions for Jet-A1[1] and hydrogen[2] operations. The LEAF concept involves the injection of multiple fuel jets in the presence of a whirling airflow, resulting in a toroidal reaction zone where the hot combustion products of each fuel jet provide a vitiated environment to one another, leading to their continuous and sequential combustion. The present work details the investigations of full hydrogen LEAF operations. The experiments are carried out for hydrogen thermal powers between 10 and 30 kW and the global equivalence ratios between 0.75 and 1.00. OH-Planar Laser-Induced Fluorescence is carried out

to identify the hydrogen flame characteristics, and exhaust gas sampling is performed at the burner exhaust. The experimental results show a dual-flame structure with variation in the ratio of air injected from the top and bottom manifolds of the LEAF burner. The exhaust emissions and the NOx formation pathways are elucidated using Large Eddy Simulations.

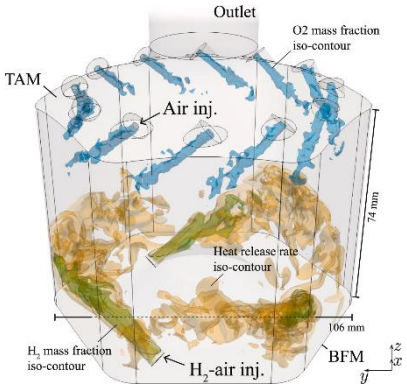

Figure 1. LEAF burner depicting the air and the fuel supply from the Top Air Manifold (TAM) and the Bottom Fuel Manifold (BFM). In the present study only the fuel ports from the BFM are utilised for Hydrogen injection. (Malé et al. 2024).

1. Miniero, L., Pandey, K., De Falco, G., D'Anna, A., and Noiray, N., "Soot-free and low-NO combustion of Jet A-1 in a lean azimuthal flame (LEAF) combustor with hydrogen injection," Proceedings of the Combustion Institute, Vol. 39, No. 4, 2023, pp. 4309–4318.
2. Malé, Q., Pandey, K., and Noiray, N., "The LEAF concept operated with hydrogen: Flame topology and NOx formation," Proceedings of the Combustion Institute, Vol. 40, No. 1-4, 2024, pp. 105278.

OTH/009: Role of Gravity and Surface Tension in Formation of Circular Hydraulic Jumps

[1*]Mallik, Arnab Kumar; [1]Bhagat, Rajesh Kumar[1]

[1]Department of Applied Mathematics and Theoretical Physics, University of Cambridge, UK

akm76@cam.ac.uk

The circular hydraulic jump (CHJ) is a common phenomenon, often seen when water from a tap impinges the surface of the kitchen sink and spreads outwards in a thin film before abruptly rising in height at a certain radius. This sudden rise in height is known as CHJ. Traditionally, this jump was thought to be created by gravity. However, Bhagat et al. (2018) questioned this view by showing that the location of the jump is independent of the orientation of the impinging surface. They analytically claimed that in the case of thin film flows, surface tension plays a dominant role over gravity, and the jump forms at the point where the local Weber number (We) ~ 1.

In this talk, I will present both experimental and numerical results across a wide range of conditions to test and build upon existing theories of the circular hydraulic jump. The parameters varied include flow rate (0.5–20 L/min), surface tension (0.2–0.072 N/m), viscosity ($10^{-6} - 99.3 \times 10^{-6}$), and gravity (0.5–9.8 m/s²). I will also examine the role of the contact line in the formation and positioning of the hydraulic jump. Finally, I will introduce a universal scaling relationship that captures both the experimental and theoretical trends (see Figure 1).

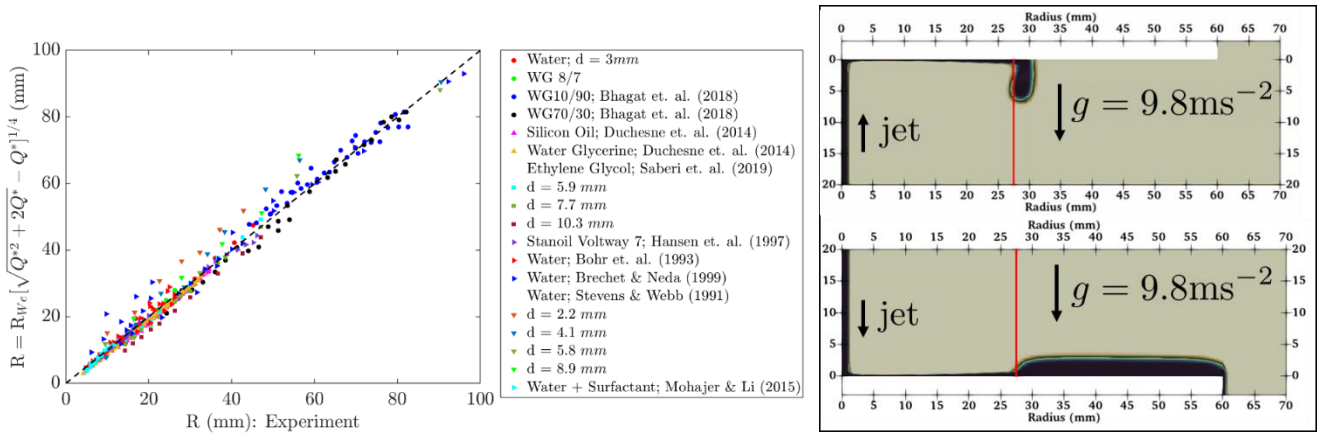

(a) (b)

Figure 1: (a) Shows the scaled radius (R) compared to the radius measured in experiments for different fluids. We compared our experimental results for water and a water–glycerine (8:7) mixture, WG 8/7, which is 6 times more viscous than water. The properties of the other fluids are given in Bhagat et al. (2020). The value of Q is estimated for different the flow rate (Q) and surface tension (γ). The γ is varied from 0.2 - 0.72 Nm^{-1}, Q from 0.5 - 20 LPM, yielding Q* between 0.2 and 1506. The predicted radius shows a good agreement with the measurement. (b) shows the result from simulation where the jump radius remains same when the jet hits the horizontal plate from bottom (against gravity) or top (in direction of gravity) and is in good agreement with the predicted radius highlighted by the red line.*

1. Bhagat, R.K., Jha, N.K., Linden, P.F. and Wilson, D.I., 2018. On the origin of the circular hydraulic jump in a thin liquid film. *Journal of Fluid Mechanics*, *851*, p.R5.
2. Bhagat, R.K., Wilson, D.I. and Linden, P.F., 2020. Experimental evidence for surface tension origin of the circular hydraulic jump. *arXiv preprint arXiv:2010.04107*.

OTH/010: Numerical Simulation of Colliding Non-Spherical Particles in Turbulent Channel Flow

[1*]Nolan, Connor; [2] Mortimer, Lee; [3] Jimack, Peter; [4] Fairweather, Michael.

[1*] Corresponding Author. EPSRC Centre for Doctoral Training in Future Fluid Dynamics, Faculty of Engineering and Physical Sciences, University of Leeds. Leeds LS2 9JT, United Kingdom. E-mail: mm18cn@leeds.ac.uk

[2] School of Chemical and Process Engineering, Faculty of Engineering and Physical Sciences, University of Leeds. Leeds LS2 9JT, United Kingdom. E-mail: l.f.mortimer@leeds.ac.uk

[4] School of Computer Science, Faculty of Engineering and Physical Sciences, University of Leeds. Leeds LS2 9JT, United Kingdom. E-mail: p.k.jimack@leeds.ac.uk

[4] School of Chemical and Process Engineering, Faculty of Engineering and Physical Sciences, University of Leeds. Leeds LS2 9JT, United Kingdom. E-mail: m.fairweather@leeds.ac.uk

Flows containing non-spherical particles in pipes and channels play a crucial role in many industrial, environmental and biological systems. Studying such flows is essential for gaining insight into particle transport, deposition and interaction dynamics, as well as for improving and optimizing related processes. Here we employ a high-fidelity direct numerical simulation of the fluid phase using the spectral element method-based code Nek5000 (Fischer et al., 2007), coupled with a Lagrangian particle tracker designed for non-spherical particles. The translational motion of the particles is determined by considering the effects of inertia, hydrodynamic lift, and drag (Ganser, 1993). Particle orientation is tracked over time using quaternions, with the rotational dynamics being governed by the Euler equations of motion, which account for external hydrodynamic torques acting on the non-spherical particles. Full four-way coupling between the fluid and the particles is in effect, accounting for the impact of fluid on the particle as well as the feedback of the particle motion on the fluid phase (Eaton, 2009). Inter-particle collisions are detected by representing ellipsoidal particles as a collection of overlapping fictitious spheres with varying radii. Collisions are resolved by identifying the sub-sphere pair with the maximum overlap and applying a hard-sphere collision response to that pair.

In this work we present some preliminary results from the model including validation of the translational and rotational dynamics of the Lagrangian particle tracker. In addition, we present results exploring the collision dynamics of non-spherical particles and how that varies with particle morphology and local flow conditions. We will explain how these results will be used in later work to augment the Lagrangian particle tracker with the addition of agglomeration.

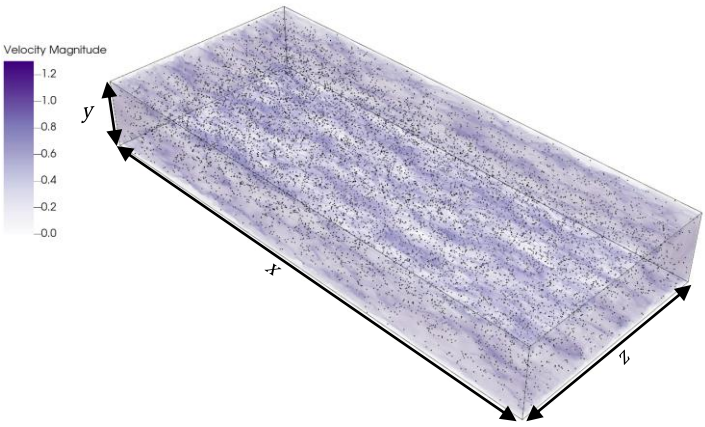

Figure 7: Snapshot of multiphase turbulent channel flow with 10,000 particles. Scale indicates fluid velocity magnitude non-dimensionalised by the bulk flow velocity.

Fischer, P., Lottes, J., & Tufo, H. (2007). Nek5000 (No. NEK5000). Argonne National Laboratory (ANL), Argonne, IL (United States).

Ganser, G. H. (1993). A rational approach to drag prediction of spherical and nonspherical particles. Powder Technology, 77(2), 143-152.

Eaton, J. K. (2009). Two-way coupled turbulence simulations of gas-particle flows using point-particle tracking. International Journal of Multiphase Flow, 35(9), 792-800.

OTH/011: The influence of Surface tension in thin-film planar hydraulic jumps

*[1]Bhagat, Rajesh Kumar; [1]Malik, Arnab

[1]Department of Applied Mathematics and Theoretical Physics, Wilberforce Road, Cambridge, CB3 0WA

Planar hydraulic jumps are commonly analysed using shallow-water theory, where the vertical momentum balance is primarily hydrostatic, and the horizontal momentum equation yields the well-known Froude number condition. This work investigates thin-film, planar hydraulic jumps in zero gravity by rescaling the full Navier–Stokes equations to incorporate deviatoric stresses arising from normal stress contributions at the free surface. Our theoretical analysis reveals that in this regime, the vertical momentum balance can become singular when the local Weber number approaches unity, leading to a hydraulic jump driven solely by surface tension.

Numerical simulations using OpenFOAM confirm the existence of two distinct jump mechanisms: one governed by gravity and the other by surface tension. The theoretical predictions show close agreement with simulation results. Figure 1 presents snapshots comparing two cases: (a) both gravity and surface tension are included; (b) surface tension (γ) is set to zero. The absence of surface tension markedly alters both the location and the mechanism of jump formation.

I will present results that reveal a previously unrecognised role of surface tension in hydraulic jumps, extending its influence beyond the classical Laplace pressure. The talk will focus on the theoretical framework for understanding these surface-tension-driven jumps in thin-film flows, supported by both experimental observations and a range of numerical simulations.

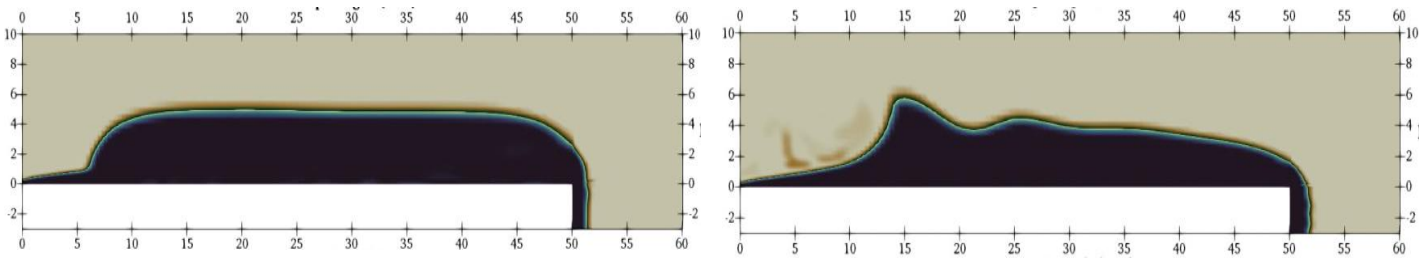

Figure 1. 1. Results from OpenFOAM simulations of thin-film planar hydraulic jumps: (a) with both gravity and surface tension; (b) with surface tension set to zero.

OTH/012: HYDRODYNAMIC SIMULATIONS OF TURBULENT CONVECTION IN STELLAR INTERIORS

[1*]Goodman, Kate; [2]Hirschi, Raphael; [3]Varma, Vishnu

[1]Astrophysics Research Centre, Lennard-Jones Laboratories, Keele University, Keele ST5 5BG, c.s.goodman@keele.ac.uk. [2]Keele University, r.hirschi@keele.ac.uk. [3]Keele University, v.r.vejayan@keele.ac.uk. *Presenting Author

The evolution and fate of massive stars are governed by complex, multiscale processes occurring deep within their interiors. Among these, turbulent convection and mixing across convective boundaries play a central role in the redistribution of energy and chemical species, influencing whether a star explodes as a supernova or collapses into a black hole. Traditional one-dimensional models of massive stars approximate these effects over the whole lifetime of the star, using simplified diffusion schemes which cannot capture the dynamic behaviour of convective boundaries. To address this, we use PROMPI, an Implicit Large Eddy Simulation (ILES) code, to model compressible, stratified convection with realistic nuclear energy generation. Our three-dimensional simulations of convective shells within massive stars explore convective boundary mixing (CBM), showing that turbulent entrainment scales with the bulk Richardson number. Due to the computational demands of these high-resolution, high Reynolds number flows, we can only simulate thousands of seconds compared to the millions of years that massive stars live. To bridge this gap, results from our 3D simulations are used to inform and improve the accuracy of 1D stellar models that can evolve massive stars over their full lifetimes. In particular, we use our results to enhance the treatment of convective mixing in 1D, allowing us to extend insights from turbulent flow regimes to the stellar models that can evolve until collapse. Our work highlights the relevance of astrophysical flows for studying buoyancy-driven turbulence, turbulent entrainment and mixing in compressible, stratified systems at high Reynolds number. By studying these extreme regimes, we contribute to a broader understanding of turbulence, boundary layer dynamics, and mixing in complex flow environments.

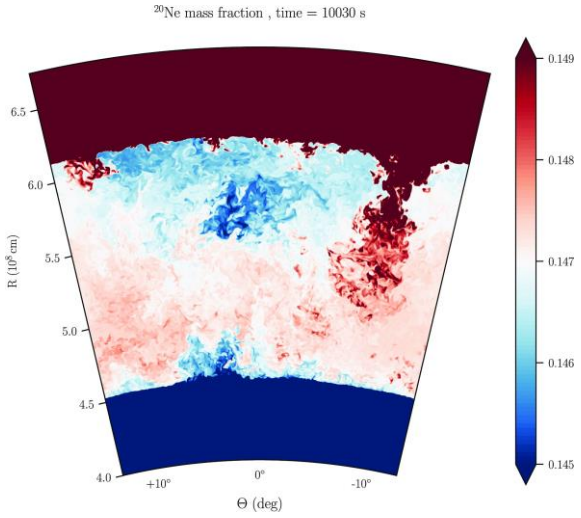

Figure 1. Cross-section of the neon mass fraction (values in colour scale) from a simulation of a neon burning shell within a massive star, from Rizzut et al., (2024). The frame shows entrainment of some neon-rich material from the upper stable region into the convective zone.

Rizzuti, F., Hirschi, R., Arnett, W.D., Georgy, C., Meakin, C., Murphy, A.S., Rauscher, T. and Varma, V., 2023. 3D stellar evolution: hydrodynamic simulations of a complete burning phase in a massive star. *Monthly Notices of the Royal Astronomical Society,* 523(2), pp.2317-2328.

OTH/013: THE IMPACT OF MAGNETIC FIELDS ON THE TURBULENT CONVECTION IN STARS

[1*]Varma, Vishnu; [2]Mueller, Bernhard

Keele University, v.r.vejayan@keele.ac.uk. [2]Monash University, bernhard.mueller@monash.edu.

Core-collapse supernovae (CCSNe) are some of the brightest, most energetic events in the universe, which are the result of the death of stars over 10 times the mass of the Sun. In order to model their explosions accurately, we need to have a diverse range of physics such as neutrino transport and neutrino interactions, general-relativistic gravity, detailed equations of state (EoS) of dense matter and detailed progenitor models. Recent studies have shown that the presence of magnetic fields can play an important role in driving these explosions, however, the role of magnetic fields have largely been ignored in the modelling of stars, leading to a substantial uncertainty in CCSN initial conditions. In this talk, I will present the first 3D magnetohydrodynamic (MHD) simulations of convection in the cores of massive stars, with (Varma & Mueller 2023) and without (Varma & Mueller 2021) the presence of rotation. We simulate the final minutes before the death of the star, starting from a weak seed magnetic field and allowing the fluid motions to naturally amplify and saturate the magnetic fields inside these convective shells which are heated by the nuclear fusion of Oxygen. Our results provide the first realistic estimates of the magnetic field strengths and geometries in the cores of massive stars. By comparing these MHD models to their purely hydrodynamic counterparts, we show how the feedback from these fields impacts the convective flow, angular momentum transport and subsequent nuclear burning in stars.

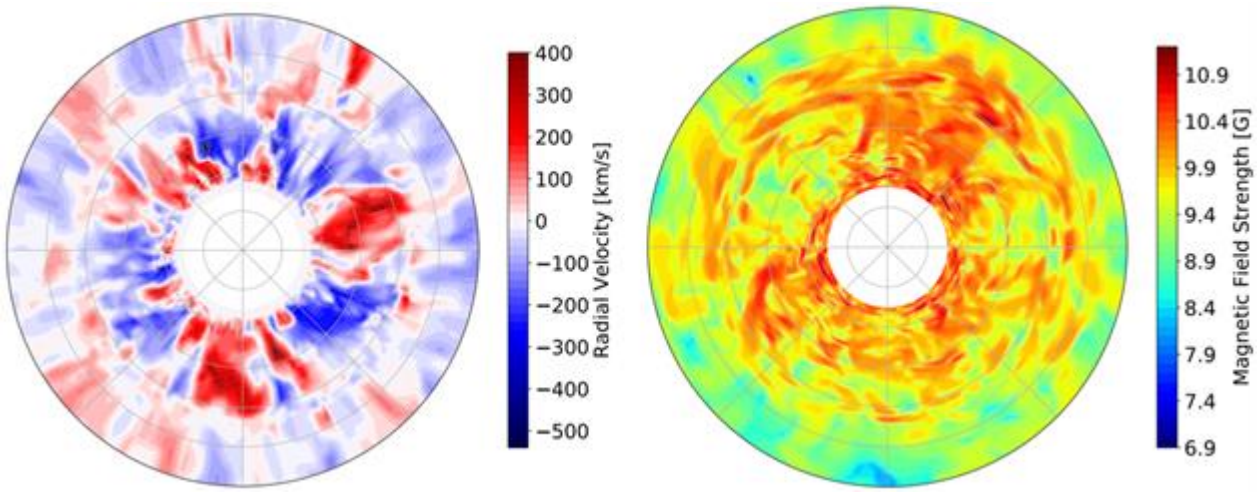

Figure 1. Image adapted from Varma & Mueller (2021), where we simulate a stellar convective shell undergoing the nuclear fusion of Oxygen.The left image shows an equatorial snapshot of radial velocity, and the right image shows the corresponding magnitude of the magnetic field strength (in log scale), which is amplified by the turbulent convective motions.

Varma V., Mueller B., 2021, MNRAS, 504, 636

Varma V., Mueller B., 2023, MNRAS, 526, 5249

OTH/015: Learning Turbulent Flows and RANS Models from Flow-MRI data using Bayesian Inference - Poster

[1]Namuroy, Claire; [2*]Kontogiannis, Alexandros; [3*]Juniper, Matthew P.

[1]Department of Engineering, University of Cambridge, Trumpington Street, Cambridge CB2 1PZ (cmn46@cam.ac.uk)

[2]Department of Engineering, University of Cambridge, Trumpington Street, Cambridge CB2 1PZ (ak2239@cam.ac.uk)

[3]Department of Engineering, University of Cambridge, Trumpington Street, Cambridge CB2 1PZ (mpj1001@cam.ac.uk)

*Presenting Author

Magnetic Resonance Imaging (Flow-MRI) is an experimental technique that provides 3-component measurements of the blood flow velocity in time and space. The method holds great potential in the assessment of cardiovascular diseases such as aortic stenosis and coarctation, which are known to induce turbulent motions characterized by sub-voxel length- and time-scales. Such turbulent structures cannot be measured directly owing to the coarse spatiotemporal resolution and low signal-to-noise ratios of Flow-MRI. In this study, we formulate an inverse Reynolds-averaged Navier-Stokes (RANS) problem for the mean flow given noisy velocimetry data. We employ adjoint-accelerated Bayesian inference, which we have recently applied to sparse and noisy Flow-MRI data [1,2], in order to assimilate experimental observations of a confined turbulent jet. We present results for two RANS models: (1) a 5-parameter algebraic model, and (2) a transport equation for turbulent kinetic energy (Prandtl's one-equation model [3]). For each model, we compute Maximum-A-Posteriori (MAP) estimates of the model parameters and their uncertainties using a quasi-Newton method. The proposed framework not only achieves accurate data reconstructions, it also enables the estimation of hidden flow quantities, such as wall shear stress and pressure, that are of clinical interest. The methodology can further be extended to more complicated turbulence models under the condition that they are differentiable. The results demonstrate the viability of the Bayesian framework in patient-specific cardiovascular modelling and present new opportunities for turbulence model selection.

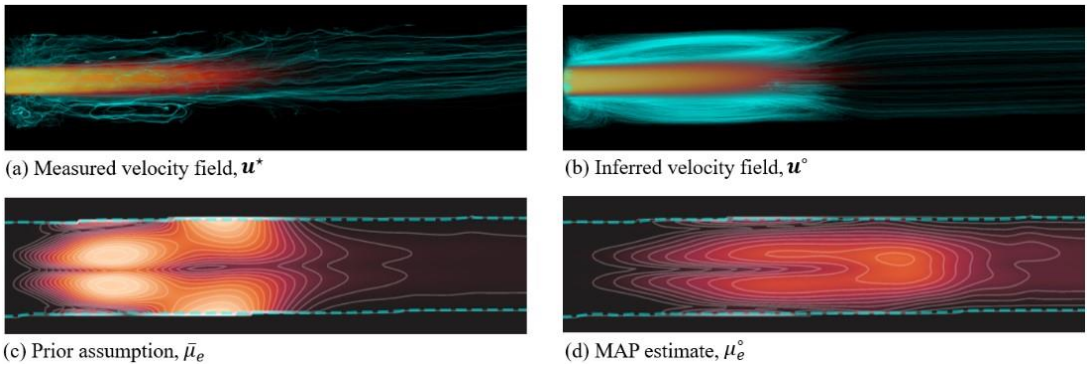

Figure 1. Noisy 3D flow-MRI data, $\boldsymbol{u}^{*}$ (figure 1a), and RANS model reconstruction, $\boldsymbol{u}^{\circ}$ (figure 1b), for a confined turbulent jet [4]. Figures 1a and 1b show velocity streamlines in cyan color and velocity magnitude in red color. The prior mean, $\bar{\mu}_e = \bar{\mu}_l + \bar{\mu}_t$, and inferred MAP estimate for the effective viscosity field, $\bar{\mu}_e^{\circ} = \bar{\mu}_l^{\circ} + \bar{\mu}_t^{\circ}$, are displayed in figures 1c and 1d respectively. A colourmap scale of [0,100cm/s] is used in all subfigures.

[1] Kontogiannis, A. et al. 2024, Bayesian inverse Navier–Stokes problems: joint flow field reconstruction and parameter learning. *Inverse Problems*. 41 (1), pp 015008.

[2] Kontogiannis, A. et al. 2025, Learning rheological parameters of non-Newtonian fluids from velocimetry data. *Journal of Fluid Mechanics*. 1011, pp R3.

[3] Wilcox, D. C. 2006, Turbulence Modeling for CFD (Third edition). pp 111-122.

[4] Kontogiannis, A. et al. 2024, Proceedings of the 2024 Summer Program. *Center for Turbulence Research*. pp 153-162.

OTH/016 - Interfacial Study of the Pore-scale Influence of Surfactants on Evaporation in a Porous Medium - *Poster*

[1*]Bello, Ayomikun; [1]Kharaghani, Abdolreza; [1]Tsotsas, Evangelos

[1]Institute of Process Engineering, Otto von Guericke University, Universitatsplatz 2, 39106 Magdeburg, Germany *Presenting Author

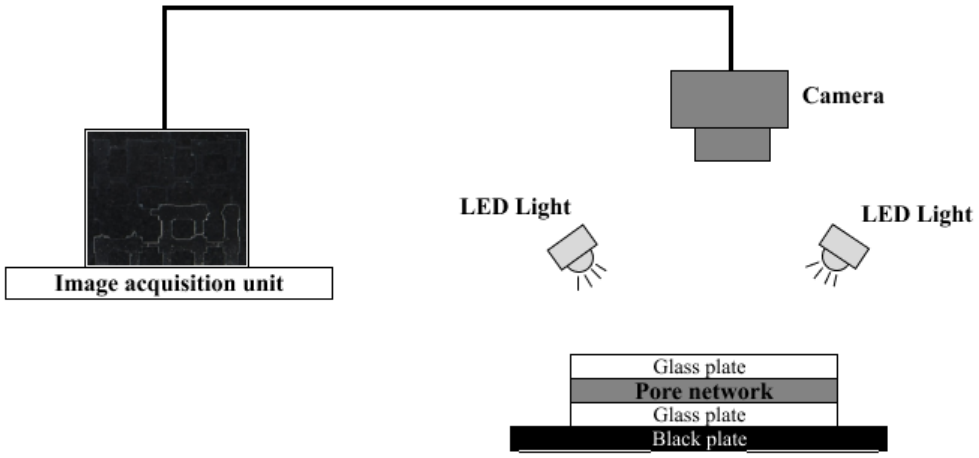

Controlling evaporation in porous media is crucial for applications ranging from soil remediation to fuel cell operation, yet the effects of surfactants at the pore scale in evaporation processes are still poorly understood. In this study, we experimentally investigate how varying concentrations of the anionic surfactant, sodium dodecyl sulfate (SDS), alter evaporation dynamics within a PDMS microfluidic pore network.

Our pore network consists of a 5×5 array of 1 mm square pores connected by throats whose widths span 0.14 - 0.94 mm. We performed evaporation experiments at four SDS concentrations: 0.10 wt.% (below CMC), 0.23 wt.% (at CMC), 0.30 wt.% and 0.50 wt.% (above CMC), as well as with pure water.

Our results reveal that below the CMC, moderate surface-tension reduction accelerates early-stage drainage but sustains thin corner films, thereby prolonging late-stage drying (395 min in total). At the CMC, minimum surface tension (~40 mN/m) and optimal wettability ($\theta \approx 70°$) promote cooperative merging of menisci, yielding rapid, uniform invasion and complete drying in 220 min, which is 47% faster than pure water. Above the CMC, micelle formation and Marangoni-driven interfacial stresses impede vapor escape, stabilize residual clusters.

These findings demonstrate that tuning surfactant concentration to the CMC maximizes evaporation efficiency by balancing capillary entry pressures and dynamic interfacial flows. Our pore-scale results bridge the gap between molecular-level surfactant behavior and macroscopic drying rates and this provides a basis for continuum-scale models that incorporate dynamic wetting transitions.